A critical review on ozone and co-species, generation and reaction mechanisms in plasma induced by dielectric barrier discharge technologies for wastewater remediation

Emile Salomon Massima Mouele [a,d,*,1], Jimoh O. Tijani [a], Kassim O. Badmus [a], Omoniyi Pereao [a], Omotola Babajide [a], Ojo O. Fatoba [a], Cheng Zhang [c], Tao Shao [c], Eduard Sosnin [b], Victor Tarasenko [b], Katri Laatikainen [d], Leslie F. Petrik [a,**]

[a] Environmental Nano Science Research Group, Department of Chemistry, University of the Western Cape, Bellville, Cape Town 7535, South Africa
[b] Institute of High Current Electronics, Russian Academy of Sciences, 2/3 Akademichesky Avenue, Tomsk 634055, Russia
[c] Institute of Electrical Engineering, Chinese Academy of Sciences, P.O. Box 2703, Beijing 100190, PR China
[d] Lappeenranta-Lahti University of Technology LUT, Department of Separation Science, P.O. Box 20, FI-53851 Lappeenranta, Finland

ARTICLE INFO

ABSTRACT

The development of cost-effective, feasible, and advanced wastewater treatment techniques remains critical to the availability and sustainability of scarce water resources. Advanced oxidation processes (AOPs) based on non-thermal plasma processes such as dielectric barrier discharges (DBDs) have recently been employed to combat biologically recalcitrant organic substances in water and wastewater streams. This is mostly due to their capability to generate in-situ UV light as well as numerous free radicals' reactive oxygen species (ROS) such as ozone (O_3), hydrogen peroxide (H_2O_2), atomic oxygen ($O^·$), ozone radical ion (O_3^-), hydroperoxyl radical (HO_2), and superoxide anion (O_2^-) amongst others. $OH^·$, O_3, and O_2^- react directly or indirectly with complex organic pollutants in aqueous solutions while H_2O_2, $O^·$, O_3^- and HO_2 mineralise organic toxins in water and in most cases act as the principal precursors for either $OH^·$, O_3, or O_2^- species during plasma treatment processes. This review primarily describes the principal reaction mechanism pathways of reactive oxygen species, and organic pollutants in DBD technologies. The pattern of RNS, methods for their quantification and the cause of their formation in DBD configurations have also been discussed. The outcomes of this review sustain that the optimisation of catalyst additives and critical parameters such as pH in DBD methods could efficiently promote the decomposition and mineralisation of water toxins. The review further highlights the superiority of double cylindrical DBD over single cylindrical and conventional DBD designs.

1. Introduction

From the time life began on planet Earth, oxygen (O_2) has been one of the most abundant and essential elements mostly used in photosynthesis and respiratory phenomena that sustain humans, plants, animals, and other living organisms' lives [1]. Conversely, oxygen generates poisonous metabolites known as reactive oxygen species (ROS) which also include reactive nitrogen species (RNS) [2]. These ROS could be advantageous or sometimes toxic to living organisms [3]. For instance, in signalling practices, the superoxide anion (O_2^-), or nitric oxide ($NO^·$), etc. play a crucial role as regulatory mediators [1]. The mediated responses of ROS shield the cells from oxidative stress and restore the redox process. On the contrary, the excessive production of ROS may induce endocrine cell damage (ECD). Besides these biomedical interactions, ROS have extensively been employed as non-toxic and environmentally friendly oxidants for surface cleaning, mostly in air and water purification [4]. Water is an unconditional vital source of survival not only for human consumption or household activities but for

---

industrial applications and sustainability of the surrounding ecosystems [5,6]. The proliferation of pollutants such as endocrine disrupting compounds (EDCs), pharmaceuticals and personal care products (PPCPs) and microbes, etc., in water streams has become a global distressing state of emergency for consumers, aquatic ecosystems and the environment that requires urgent remediation [7–9]. The establishments of effective recovery processes for drinking water and water reuse have become a worldwide contest in research. Several conventional separation methods such as sedimentation, flocculation, filtration, electrocoagulation, etc. have been employed for the removal of organic contaminants from water and wastewater [1,10–12]. Although, these procedures have been found effective in water purification, they produce a large amount of poisonous slurry that requires extended processing as biological digestion methods have been found futile in this regard. Likewise, Yang et al. [13]. sustained that pollutants, recalcitrance in water during conventional applications is probably due to their chemical stability, low biodegradability, and their resilience. Chemical oxidation processes including chlorination and ozonation have become known as complementary water treatment systems. Nevertheless, they have been found ineffective in the removal of total organic carbon (TOC) [14]. The remediation of industrial wastewater contaminated with dyes, pharmaceuticals, and personal care products has been widely studied [15–18]. In this regard, various treatment methods such as adsorption on activated carbon, ozonation, and reverse osmosis, ion exchange on synthetic adsorbent resins, flocculation, and decantation have been developed [19–21]. Yet, the elevated operational costs of these procedures and the complexity of the aromatic structures of chemicals often limit their application [21]. Advanced oxidation processes (AOPs) majorly producing powerful oxidants hydroxyl radicals (OH·) have been deemed as efficient methods for the decomposition of pollutants in water and wastewater and their conversion into harmless end-products with no need of post-treatment protocols [22,23]. Though, the extreme use of chemicals, UV loss, deterioration of catalyst supports, ozone leaks and AOPs overall costs constrain their use in water and wastewater treatment. Recently, advanced oxidation processes (AOPs) induced by non-thermal plasma processes through the production of non-selective hydroxyl radicals have been established [24,25]. For example, dielectric barrier discharges (DBDs) have recently been acknowledged as efficient non-thermal plasma AOPs that generate UV-light and numerous ROS including O_3, H_2O_2, OH., and RNS such as NO, NO_2, N_2O_5 amongst others which contribute to the decomposition and mineralisation of the targeted contaminants [26]. Hence, the oxidative potentials of ROS and their potent effects on organic pollutants and microorganisms have emerged as promising technologies for water purification [1,27–30]. Mouele et al. [1] reviewed the degradation of organic pollutants and microorganisms using dielectric barrier discharge systems. In their investigations, the authors discussed in detail the most common DBD configurations reported in the literature [31] claiming that double cylindrical DBD has not been widely used for water and wastewater treatment and could be a promising remediation technology. However, it can be pointed out that a comparison in terms of efficiency between single cylindrical DBD, double cylindrical DBD and planar DBDs was not provided in Mouele et al. [1]. Next, Mouele et al. [32] reviewed the quantification of ROS in DBD technologies and highlighted that the principal reactive species including O_3, could be measured in DBD configurations by indigo method, H_2O_2 by Eisenberg method using per titanyl sulphate, while OH can feasibly be quantified using terephthalic acid probe. Nonetheless, their study lacks information on the measurement of RNS, and the interruption of their formation in DBD configurations. Furthermore, Mouele et al. [33] reviewed the global occurrence of pharmaceuticals and their removal in aqueous media using DBD technologies. Their investigation indicates that various DBD configurations have been employed for the degradation of pharmaceuticals and their efficiency could be evaluated using their energy yield G_{50} (g/kW h) required to decompose half of the pollutant concentration as earlier suggested by Malik [34] and recently endorsed by Tang et al. [35] Still,

it can be observed that in these reviews, the expanded production of O_3 and its disintegration in the presence or absence of catalysts in DBD geometries were not detailed. Also, the reaction mechanisms between O_3 and co-species, and/with pollutants were not fully explored. Therefore, the main goal of this review is to assimilate the production mechanisms of ROS in DBD systems and their interaction mechanistic pathways with targeted pollutants in the presence or absence of catalyst. In addition, this assessment highlights the superior benefits of double cylindrical DBD over single cylindrical and normal DBDs. The production and quantification of RNS and their disruption in DBD configurations are also discussed. These aspects facilitate the understanding of ROS selectivity towards organic pollutants in DBD electrode geometries. This, in turn, offers researchers working on water and wastewater treatment by non-thermal plasma systems an insight into the type of chemical additives that should be incorporated in the reactor and clear ideas on which working parameters should be optimised to boost the production of non-selective OH free radicals that directly mineralise the contaminant into CO_2, H_2O and harmless inorganics (without any interference with aqueous additives). The review further suggests that double cylindrical dielectric barrier discharge (DCDBD) could be used as adequate integrative AOPs for the complete removal of refractory contaminants in water and wastewater treatment plants.

2. Historical background of free radicals

The concept of the free radical and its history began with Denham [36] who postulated that free radicals might be crucial in the aging process. A few years later Arnold et al. [37] demonstrated that the hydroxyl radical (OH•) may stimulate guanylate cyclase which may generate cyclic guanosine monophosphate (cGMP) referred to as "the second messenger". From that moment on, biologists discovered that free radicals are produced in most living systems and may be involved in several physiological functions. Hence, several expressions have been utilised to denote hydroxyl species. For instance, the interchangeable terms "free radical" has been widely used in the literature. Indeed, reactive species with an unpaired electron are conventionally illustrated with a superscript dot (•). Besides, the term "free" was literally used by chemists to differentiate the free "radical" R· and the bonded "radical" R· in (R·-X·). Halliwell [38] reported that a free radical was defined as an atomic or molecular species (such as oxygen or nitrogen) that may exist independently and may carry at least one unpaired electron in its valence electron shell. Therefore, two categories of free radicals including reactive oxygen species (ROS) and reactive nitrogen species (RNS) have been considered [39]. The unpaired electron in ROS or RNS free radicals produced in non-thermal plasma electrode geometries may confer selective or unselective reactive properties.

In recent decades, advanced oxidation processes (AOPs) have been established as principal methods to produce strong non-selective hydroxyl radicals (OH·) that have been employed in various applications including air purification, surface cleaning and water purification [39–41]. In terms of water treatment, OH· decomposes and mineralises water contaminants to H_2O, dissolved CO_2, and harmless inorganics [32, 33]. In this regard, the conversion of organic pollutants to non-toxic inorganic and organic remains does not require any separation and post-treatment processes. The main AOPs including UV disinfection (photolysis) and photolytic combinations such as UV/H_2O_2, UV/O_3, UV/H_2O_2/O_3 photocatalysis, supercritical water oxidation, electron-beam, wet air oxidation, water sonolysis and ultrasound cavitation, plasma technologies, electrochemical advanced oxidation processes (EAOPs), microwave, plasma-based AOPs reported in the literature, have been highlighted by Mouele et al. [1] and Saracino et al. [14]. Even if these practices use different approaches, they all focus on the production of robust but short-lived non-toxic and non-selective hydroxyl radicals (OH·) that degrade and mineralise water pollutants into amenable by-products. Li et al. [42] showed that OH can successfully be produced during supercritical oxidation of water and could

enhance the process of removing nitrogen-containing organics and ammonia as recently sustained by Wei et al. [43]. Next, the generation of OH in electrochemical advanced oxidation processes (ECAOPs) was documented by Oturan and Brillas [44] and Sirés et al. [45], and further reinforced by Jing et al. [46]. On the other hand, Badmus et al. [47] successfully determined the concentration of OH generated in a sonicator using a terephthalic acid chemical probe. Furthermore, the production of OH in an ultrasonic-microwave system was proved by Liu et al. [48] during rapid synthesis of spindle-like Ag/ZnO nanomaterials featuring enhanced photocatalytic and antibacterial properties. Ghatak [22] emphasised/reported that various AOPs technologies producing OH have been employed widely in water treatment facilities for the remediation of bio recalcitrant substances to prevent their escape to the environment during discharge processes. The authors further clarified that the majority of AOPs do not only produce OH·, but related oxidative and reducing species such as atomic oxygen (O·), atomic hydrogen (H·), and/or solvated electrons which are also produced. These later radicals boost the efficiency of chemical processes that are often referred to as advanced redox methods. However, excessive use of chemicals, corrosion of the catalyst supports, wasted UV, ozone escape, and the cost associated with AOPs often restrict their application for the decontamination of water and wastewater effluents. Beyond these aspects, plasma technologies that are often viewed as sources of UV radiations, high energetic electrons, various free radicals, ions, and neutral species have emerged as potent AOPs in recent decades. The principal categories of plasma processes include thermal plasma and non-thermal plasmas that depend on temperature effects [49]. Non-thermal plasma operated at room temperature is often more solicited than thermal plasma that requires high temperature [33]. The supremacies of dielectric barrier discharges (DBDs) over other types of non-thermal plasma have been reviewed by Mouele et al. [1] and Mouele et al. [33]. The efficiency of DBDs depends on reactor configurations. Double cylindrical DBD (DCDBD) with only 1 eV generates energetic electrons, UV radiation and large amounts of reactive species mostly OH radicals supplemented by long-lived species such as O_3 and H_2O_2 [1,33]. The advantages of DCDBD system are the fact that the high voltage electrode is protected at least by one dielectric material, the abundance of high energy electrons, also the fact that no chemical additives are needed, allowing effective dissociation of feed gas leading to several successive reaction chains that consequently yield abundant reactive species such as O_3, O·, H_2O_2, OH·, HO_2, etc., forming a chemical cocktail that efficiently enhances the removal of refractory water pollutants. So, for the past years, dielectric barrier discharges (DBDs) showing impeccable physical and chemical properties, have become part of the most explored plasma technologies for water and wastewater purification. Finally, the applications of the radical OH vary from air purification mostly in the deactivation of viruses and bacteria, to the elimination of noxious gases such as carbon monoxide, formaldehyde and ammonia. Alternatively, the neutralisation of allergens and odours through indoor spaces is also common.

3. Ozone a primary oxidant, its origin, properties, and applications in various fields

The discovery of ozone began in the 19th century with Van Marum, a Dutch chemist who for the first-time discovered ozone gas through its toxic smell during electrifier experiments [50,51]. At that time, the discovered gas was still known as decennia. Only in 1840, after Schönbein repeated the same experiment carried out by Van Marum when the same characteristic smell was noticed, the identified gas was named ozone that stands for ozein, the Greek term for scent. In addition to this, Schönbein remains the first scientist to investigate the effects of ozone on organic matter. Afterward, the first ozone producer was invented by Siemens [50,52] in Germany (Berlin). This resulted in multiple examinations towards the use of ozone as a disinfectant agent and its disinfection mechanisms. For instance, Marius Paul Otto, a French chemist was the first scientist to initiate an enterprise specialised

in the installation of ozone production systems [53]. In this regard, an earlier technical-scale application of ozone was established in 1893, in Oudshoorn (Netherlands) and was fully examined by French scientists [50,51,53] and similarly, in 1906, a similar ozone installation was mounted in Nice. Since this later installation was continuously used for water purification, Nice became the centre of ozone production for drinking water treatment. At the time of World War, I, the number of ozone installations increased worldwide. For example, in 1916 about 49 ozone installations were developed in Europe, and 29 were specifically located in France [50]. After that, the multiplication of ozone installations faded because of toxic gas enquiry and this led to the discovery of chlorine as an alternative disinfectant. In this way, chlorine was considered as an appropriate substitute for ozone as it did not show critical limitations such as low yield of generation like in the case of ozone. After World War II the number of ozone installations started to increase again. Even then, the use of chlorine for water purification was still dominant over that of ozone. However, around 1973, trihalomethanes (THMs) were detected as harmful disinfection by-products of the chlorine disinfection process, and thus, scientists started searching for new purifiers [50]. Besides the detection of THMs as disinfection by-products, scientists also experienced difficulties in removing organic micropollutants in surface waters. Moreover, this class of pollutants was found to be oxidised faster by ozone than chlorine and its derivatives. Ozone was also found capable of deactivating microorganisms such as cryptosporidium that are resistant to sterilisers. Based on these benefits, ozone has been readmitted as a potent oxidant and its previously encountered limitations were ignored. Besides its advantages, ozone may also exhibit some drawbacks mainly related to its toxicity. Indeed, the breathing of a high concentration of ozone may result in health effects. Mucous membrane irritation and headaches are the most common symptoms often noticed after prolonged exposure to ozone. For instance, exposure to a concentration of more than 50 ppm for 30 min might be disastrous [54]. Likewise, apart from the decrease in lung capacity and lung diseases, the lasting effects of ozone exposure are still undetermined [54,55]. To preclude the health threats, a maximum concentration of 0,06 ppm of inhaled ozone has been established. This represents the maximum concentration of ozone that a human can be exposed to for about 30 min [54]. Based on this value, ozone concentration in each system should be controlled. With its scent threshold of about 0,02 ppm, ozone could only be sensed by its distinct smell near or above the maximum admitted concentration [54]. Despites being used as an excellent oxidant in water purification [56–58], O_3 has widely been used in various fields such as biomedical applications including bacteria and virus inactivation [59], treatment of foot ulcers in patients with diabetes [60], ozonation of oils as antimicrobial systems in topical applications [61] among others. Ozone has extensively been used as a mediator in depolymerisation and solvolysis processes [62] and in food preservation [63–65] only name a few. Nevertheless, catalytic systems and non-thermal plasma technologies have been identified as the most common sources of ozone and have gained a wide application for environmental remediations [66–72]. Therefore, this current review focuses only on ozone generated in non-thermal plasma induced by DBD and its application for water and wastewater treatment.

4. Non-thermal plasma

Unlike other types of plasma atmospheric non-thermal plasma (ANTP) occurs at the temperature range of 300–50,000 K. According to Thagard [73], ANTP is characterised by its electron temperature (T_e) which is much higher than the initial temperature (T_i) but is in turn approximately equal to gas temperature (T_g) that lies between 300 and 1000 K (Te ≫ Ti > Tg ≈ $300·10^3$ K) and a corresponding ionisation energy range of 1–10 eV [1]. Besides, ANTPs are also featured by their electron density (n_e) estimated to about 10^9–10^{15} m^{-3} ($10^{10} \leq n_e \leq 10^{15}$ m^{-3}). For decades, electrical discharges (EDs) such as corona discharges (CD), dielectric barrier discharges (DBD), atmospheric pressure plasma

jet (APPJ), and micro hollow cathode discharges (MHCD) have been considered as the major types of ANTPs regardless of their characteristic properties and applications [74]. These discharge processes have emerged in recent years as effective methods for water decontamination. Therefore, water purification efficiency may depend on the type of ED configuration. The most common non-thermal plasma (NTP) configurations discussed in the literature [1,4,32,75] have been summarised in Section 4.1. Apart from electrode geometry, the electron density in EDs previously mentioned might play a crucial role in water treatment [76, 77]. Although various AOPs have been widely used for effective removal of water organic pollutants, the incomplete degradation of pollutants leading to toxic intermediates can result in greater detrimental effects than from parent compounds; hence alternatives for total oxidation of targeted contaminants are highly sought. Non-thermal plasma (NTP) configurations have been utilised in various sectors for wastewater decontamination. For instance, NTP induced by corona discharge has been utilised for the removal of pharmaceutical toxins from water and wastewater and improved removal percentages between 87% and 99.99% have been reported [78–82]. However, it can be remarked that in these corona discharge configurations the high voltage electrode (HV) is directly submerged in the effluents being remediated and could be depleted by aqueous oxidative species. Conversely, glow discharge plasma has been used for various purposes including sterilisation and surface decontamination [83] and food packaging [84], screening of contaminants in foodstuff [85], fabrication, modification, and treatment of nanomaterials with enhanced properties [86–88]. The reports indicate that these technologies are feasible, cost-effective, and appropriate for the cleansing of medical tools. Alternatively, air discharge plasma jet has been utilised for the treatment of textile wastewater [89,90] and in mass spectrometry analysis for direct detection of compounds from surfaces and complex matrices [91]. The outcomes of these investigations highlighted that about 70% degradation of targeted pollutants was achieved while their total removal required prolonged treatment time. This behaviour was noticed at low pH and was attributed to the recalcitrant behaviour of the degradation intermediate by-products in an acidic environment.

Furthermore, dielectric barrier discharge configurations have been used for the decomposition of pharmaceutical contaminants and improved removal efficiencies between 73.7% and 99.9% have been recorded [92–96]. In these cases, the analyses of the treated effluents showed that pharmaceutical pollutants were oxidised into the dissolved CO_2, and harmless inorganics. Although corona discharge electrode arrangement has been shown efficient for the remediation of polluted waters, direct exposure of the high voltage (HV) electrode to the solution being treated could result in undesired corrosion and hence the discontinuation of the treatment process and extended contamination of the treated effluent. Contrariwise, glow discharge and plasma jet have demonstrated an attractive capacity for surface cleansing, water, and wastewater purification to some level. Yet, the scalability of these electrode geometries to semi or industrial units for the treatment of thousands of litres of polluted water could be expensive and challenging. Despite the abundance of O_3 and co-species generated in DBD technologies, the prominence of DBDs over other configurations relies mainly on the abundance of high energy electrons freely circulating the dielectric barrier tube at minimal energy of 1 eV. Its feasibility at room temperature, scalability, and flexibility renders DBD potentially one of the most applicable treatment techniques for water and wastewater purification. These advantages of DBDs have therefore attracted worldwide attention for their use in water and wastewater treatment. Moreover, Nehra et al. [74] established a comprehensive comparison between CD, DBD, APPJ, and micro hollow cathode discharge (MHCD) processes. Nehra et al. [74] found that most physical and chemical properties of DBD configurations were superior especially in electron energy and density, break down voltage, scalability, and flexibility. This, therefore, makes DBD one of the most efficient, affordable, feasible, and environmentally safe plasma water treatment techniques. Furthermore,

the DBDs treatment method encapsulates several electrode configurations that may depend not only on the electron density and other properties but on the operational ease at ambient conditions [97]. Nevertheless, the generally known DBD geometries have already been reported [1,98]. The single/double planar dielectric barrier discharges have been employed as effective ozone generator water treatment methods and significant toxin degradation efficiencies have been achieved [76]. Likewise, single cylindrical DBD configurations consisting of one dielectric barrier have been used separately as efficient plasma water treatment techniques, in which higher removal efficiencies were also attained [99,100]. However, the double cylindrical dielectric barrier discharge (DCDBD) configuration made of two dielectric layers has not been widely explored for water purification.

4.1. Description of dielectric barrier discharge configurations

Dielectric barrier discharge (DBD) also referred to as a silent electrical discharge is characterised by thermodynamic properties and is a source of non-equilibrium atmospheric plasma. Various terminologies including, silent discharge, barrier discharge, normal pressure glow discharge, arc-discharge, display discharge and ozonizer discharge have been established to illustrate DBD plasma process [97]. The common DBD designs studied in the literature comprise of the anode (positive) and cathode (negative) probes. The anode also termed as high voltage electrode is enveloped by one or more dielectric barriers mainly quartz, ceramic or pyrex frequently used as insulators [1]. The insulator barriers are utilised to split the anode from the feed gas (single dielectric) or between two electrodes to create the gas discharge zone (double dielectric). The main purpose of non-thermal plasma induced by DBD is to continuously produce ozone gas that is promptly disseminated in the contaminated water being remediated or to the surface being cleaned up [97]. In conventional DBD configurations, both high voltage and cathode electrodes interact with the feed gas and plasma. This often stimulates electrode etching and leads to erosion during the plasma discharge procedure [74]. On the contrary, the presence of dielectric barrier insulators around the anode in innovative DBD electrode arrangements, reduces the possibility of electrode etching and corrosion and further strengthens the electric and magnetic fields, therefore enhancing the even dissemination of high energy electrons around the dielectric layers surrounding the anode [32]. In Lopez [101] and Valinčius et al. [197], it was reported that the discharge zone/ air gap (the region between dielectric barriers) could range from a few to several millimetres. In DBD electrode geometries, the dielectric barrier layers spread the charges carried by microdischarge (microplasma) over the whole surface of the anode electrode. Konelschatz et al. [102] underlined that the operational conditions in non-thermal plasma are straightforward as compared to low-pressure discharges, pulsed high-pressure corona discharges and electron beam. The common DBD electrode configurations reviewed by Kogelschatz [103] include single or double planar and single/double cylindrical dielectric-barrier discharges as shown in Fig. 1.

Although the upscaling of DBD configurations has been challenging, the DBD electrode geometries displayed in Fig. 1 have been utilised for water and wastewater remediation [33]. Despite the increasing use of DBD technologies in water treatment, the configuration shown in Fig. 1 (e), referred to as double cylindrical dielectric barrier discharge (DCDBD) has restrictively been applied for the removal of organic pollutants from water and wastewater. Hence this review suggests that the physical and chemical properties of plasma produced in DCDBD can be explored further for water treatment.

4.2. Ozone generation in non-thermal plasma

Literature stipulates that ozone is often generated in situ due to its short lifetime. Corona-discharge and UV-light processes have been considered as the two main systems of producing ozone. However, based
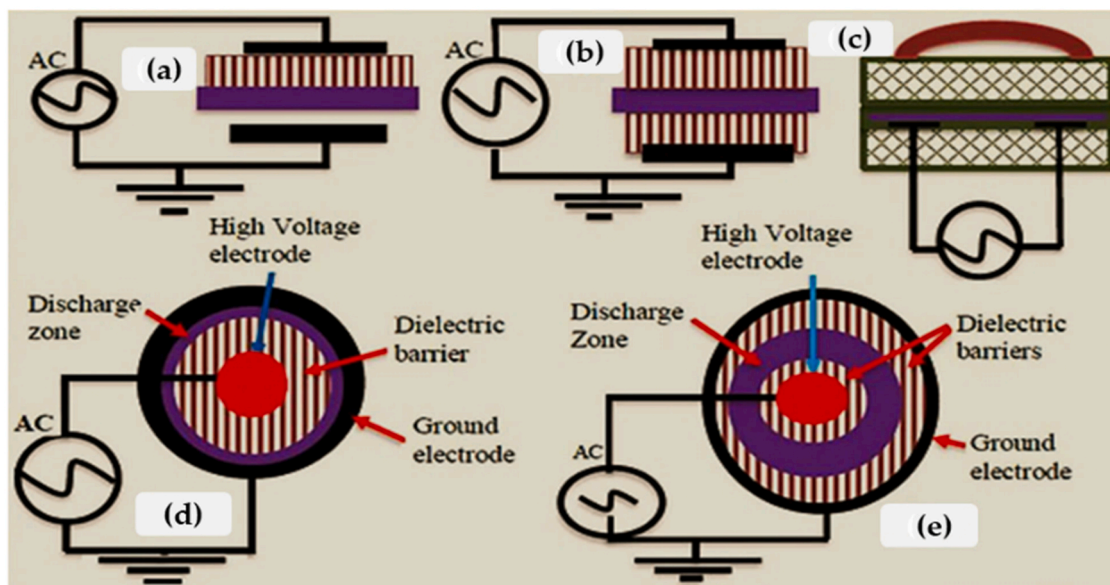
Fig. 1. Most common dielectric barrier discharge systems used in water and wastewater treatment; a = single planar DBD, b and c = Double planar DBD; d and e = single and double cylindrical DBD [32,100].

on the higher ozone production, the sustainability of the generation system, and the reasonable cost of the production unit, generating ozone by corona-discharge mode is more advantageous than UV-light systems that are preferred when only minute concentrations of ozone are needed [104,105]. In electrical discharges based on plasma generation such as corona, dielectric barrier discharges, etc., the common gases used are often oxygen or normal air. In these discharge systems, ozone is produced by the dissociation of the oxygen molecule into atomic oxygen radicals. These later recombine with oxygen molecules to produce ozone. In ozone production systems, dielectric materials are often used to monitor the flow of charged particles while water solutions are often used to cool electrodes [106] as shown in Fig. 2.

The main factors that might impede ozone production include the humidity and purity of the feed gas, oxygen concentration in the inlet gas, cooling water temperature, and electrical parameters. Therefore, for the generation of a significant amount of ozone, these parameters should be optimised. The ozone generated is further decomposed to yield more atomic oxygen radicals which, by side reactions, might result in the formation of other free radicals such as H_2O_2, $O_2^{\cdot-}$, and $OH^{\cdot}$ which may contribute largely to the decontamination of water effluents [107]. The decomposition of ozone leading to various free radicals is usually

accelerated by the addition of catalysts, while the principle and reaction mechanisms of the catalytic decomposition of ozone have been succinctly discussed in the following sections of this paper. Furthermore, the rapid decomposition of ozone, often indicated by its short lifetime, is due to its instability. Consequently, the life span of ozone in water appears to be shorter than in air. Literature sustains that the rapid decay of ozone mostly occurs in drinking water conditions where the pH value lies between 6 and 8.5 and is often a result of side interaction with OH radicals. In this way, systems in which OH radicals dominate are usually referred to as advanced oxidation processes (AOP). Moreover, the predominance of OH radicals in ordinary water is usually identified by the drastic decrease of ozone concentration [104]. So, the lifetime of ozone (often in seconds or minutes) may depend on the type of water quality. For instance, Hoigné [108] reported that in wastewater contaminated with sulphite, nitrite, olefinic aliphatic hydrocarbons, phenols, polyaromatic hydrocarbons, organic amines and sulphides, the estimated lifetime of ozone at a concentration of 0.5 mg/l is within less than 10 s. In addition, the author recalled that in wastewater containing chlorosubstituted olefins (chlorinated solvents), benzene, saturated hydrocarbons, or tetrachloroethylene, it can require days for ozone to initiate their significant oxidation. Furthermore, Hoigné [108] endorsed that in
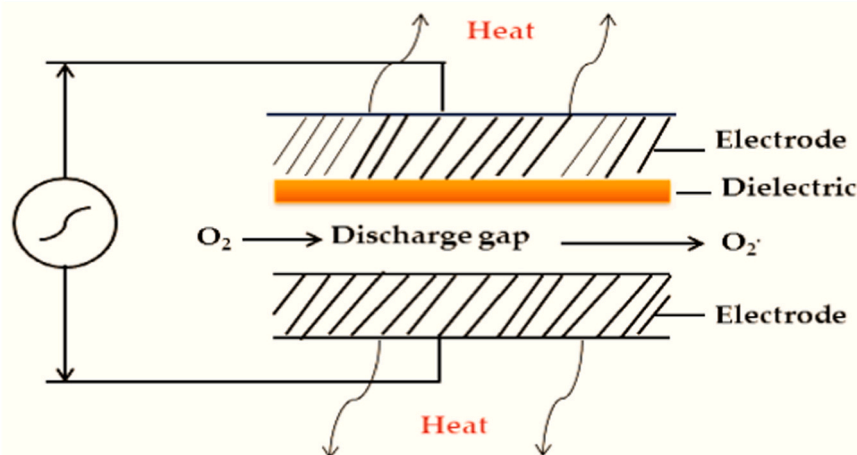

Fig. 2. Principal schematic of non-thermal plasma generator [74,75].

standard drinking water, the lifetime of ozone could vary from 1 to 20 min. Therefore, catalyst additives and solution pH are a critical parameters that should be carefully monitored during remediation of water effluents.

4.3. Catalytic ozonation process for water and wastewater remediation

Catalytic ozonation is an efficient advanced oxidation procedure for wastewater purification that mostly involves the use of nano/catalysts such as Ti, Mn, Fe, Ni, Co, Zn, Cr, Ag zero valent metals or in the form of oxides and nanocomposites or suspended on metal supports (e. g. meshes and membranes) [109,110]. Catalytic ozonation in the presence of nano-catalysts or ordinary catalyst are mainly induced by oxidation-reduction processes [111]. Various authors endorsed that from the reaction mechanisms and kinetics trends, followed by possible interaction of nano-catalysts, it could be inferred that nano-catalysts such as MgO, SiO$_2$, TiO$_2$, ZnO, Mn^{2+}, and MgO-ZnO/carbon nanocomposites are employed to promote ozonation method for the demolition of wastewater pollutants [112–119]. Numerous studies focusing on the removal of organic pollutants from water and wastewater using the combination of catalysts and ozone have been conducted [120–123]. In these investigations, the mechanisms of catalytic ozonation process have been of great interest. During remediation of contaminated water by catalyst-ozone systems the rate of pollutant decomposition directly depends on ozone reaction, indirectly dependent on the interactions of OH and the catalysts used. Indeed, the assimilation of reaction mechanisms of catalyst and ozone, ozone and pollutants or catalyst-ozone-pollutant is crucial to define the synergic potential of targeted catalysts and pollutants. Consequently, Guo et al. [120] and Khuntia et al. [121] sustained that the decomposition of pollutants may follow two distinct mechanisms including homogeneous and heterogeneous catalytic ozonation.

4.3.1. Homogeneous nano-catalytic ozonation

The homogeneous nano-catalytic ozonation is usually initiated by the nano-metals such as nano-Ag^{2+}, Fe^{2+}, Mn^{2+}, Co^{2+}, and Zn^{2+} that are often used as nanocatalysts during treatment of water and wastewater [124,125]. The mechanisms of homogeneous catalytic ozonation involves the decomposition of ozone leading to the production of powerful OH oxidants [126]. In this regard, the efficiency, and the rate of homogeneous catalytic ozonation systems may also depend on the direct production of O$_3$ and OH$^.$ oxidants via interactions of nano-metals. According to Dang et al. [110], the main reaction mechanisms involved in this process could be illustrated in Eqs. (1) and (2) as follows:

$$\text{Contaminant} + O_3 \rightarrow \text{by-products} \qquad (1)$$

$$\text{Contaminant} + OH \rightarrow \text{by-product} \qquad (2)$$

Hence the rate and kinetics of homogeneous catalytic ozonation could summarised according to Eqs. (3) and (4).

$$-\frac{dCp}{dt} = \text{Cp}\left(k_1 CO_3 + k_2 COH\right) \qquad (3)$$

$$-\ln\frac{Cp}{Cp,0} = \text{Cp}\,(k_1 C_{O3} + k_2 C_{OH})t \qquad (4)$$
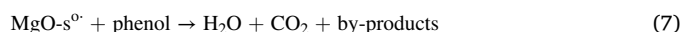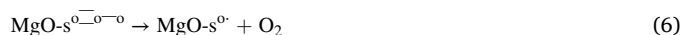
where Cp, C$_{O3}$ and C$_{OH}$ are the concentrations of pollutants, O$_3$ and OH$^.$, respectively. On the other hand, k$_1$ represents the kinetic constant of direct reaction of O$_3$ with the pollutants (k$_{O3}$/pollutant), while k$_2$ is the kinetic constants of reaction of OH$^.$ with the pollutant (k$_{OH}$/pollutant). These mechanisms were recently reviewed and clarified by Li et al. [127] and Malik et al. [128].

To recall, the homogeneous catalytic ozonation process is often initiated to improve the decomposition of water pollutants [129]. However, Guo et al. [120] highlighted that the lack of control of
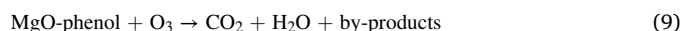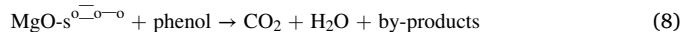
nano-ions or ions in solution could lead to secondary pollution and might become problematic.

### 4.3.2. Heterogeneous nano-catalytic ozonation

To enhance the decomposition of O$_3$ leading to the production of OH$^.$ and to assimilate the regeneration process of the catalysts used during water and wastewater remediation, the comprehension of heterogeneous nano-catalytic ozonation mechanisms is a crucial step. Kasprzyk-Hordern et al. [130] and Zhao et al. [131] conveyed that heterogeneous nano-catalytic ozonation could be summarised in three distinctive scenarios presented below. The first scenario involves the chemisorption of ozone onto catalyst surface resulting in the generation active species such as OH$^.$ and O$_2$, that interact with non-chemisorbed organic molecules and agrees with Moussavi et al. [132]. The second process refers to the associative or dissociative chemisorption of organic molecules onto the catalyst surface and interaction with dissolved ozone or aqueous gases [133]. The last step involves the chemisorption of O$_3$ and pollutant and their interaction. The effectiveness of heterogeneous catalytic ozonation for wastewater remediation may depend on various factors including the selected pollutants, catalysts, their surface characteristics, and the operational experimental conditions [134]. A typical example of heterogeneous catalytic ozonation occurring at the surface of nano-MgO during the degradation of phenol has been reported in Dang et al. [110]. The radical type of catalytic oxidation occurring at the surface of the catalyst is expressed in Eqs. (5)–(7) as follows:

$$\text{MgO-s} + O_3 \rightarrow \text{MgO-s}^{o\overline{}o\overline{}o} \qquad (5)$$

$$\text{MgO-s}^{o\overline{}o\overline{}o} \rightarrow \text{MgO-s}^{o\cdot} + O_2 \qquad (6)$$

$$\text{MgO-s}^{o\cdot} + \text{phenol} \rightarrow H_2O + CO_2 + \text{by-products} \qquad (7)$$

In addition, the direct oxidation of phenol by catalyst-O$_3$ molecules is highlighted as shown in Eqs. (8) and (9)

$$\text{MgO-s}^{o\overline{}o\overline{}o} + \text{phenol} \rightarrow CO_2 + H_2O + \text{by-products} \qquad (8)$$

$$\text{MgO-phenol} + O_3 \rightarrow CO_2 + H_2O + \text{by-products} \qquad (9)$$

Furthermore, the direct oxidation of phenol by O$_3$ molecules in the bulk solution is shown in Eq. (10).

$$O_3 + \text{phenol} \rightarrow CO_2 + H_2O + \text{by-products} \qquad (10)$$
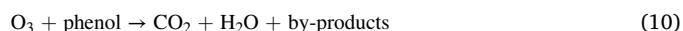
In case the contaminant is adsorbed onto the surface of the catalyst, Khuntia et al. [121] and Sable et al. [135] reported that the rate of adsorption could be approximated according to Eq. (11).

$$-\frac{dCp}{dt} = k_3 C_p C_{cat} \qquad (11)$$

where C$_p$ and C$_{cat}$ represent the pollutant and catalyst concentrations, correspondingly. Various studies involving the catalytic-ozonation for the removal or organic contaminants from wastewater have been conducted [136–139]. However, it should be emphasised that for powder catalysts used in catalytic-ozonation processes, post-treatment separation is often involved and could be a cost related limitation to some extent. Alternatively, some researchers have suggested that suspension/immobilisation of the catalysts on appropriate supports could be promising to boost the degradation of pollutants in catalytic ozonation during water and wastewater treatment [11,12,100]. In this case, the study published by Pana et al. [140] could be useful to overcome any corrosion constraint that might be encountered during the remediation process.

4.4. Effect of pH on catalytic ozonation

Various authors [141–143] conveyed that the solution pH is an extremely sensitive parameter in chemical reactions such as ozonation and catalytic ozonation methods. Its alteration can result in strong

modification of solution chemistry and decomposition efficiencies/-rates. Therefore, its optimisation at an early stage of these treatment processes is mandatory [138]. Depending on the catalyst used and their properties, model pollutants and their solution pKa values, Amat et al. [144]; Barik and Gogate [145] and Barik and Gogate [146] emphasised that optimal removal of contaminants can happen either in acidic or basic conditions. In this regard, Sanz et al. [147] and Martins et al. [148] endorsed that wastewater consisting of pollutants of acidic nature such as alkylsulfonic acids could optimally remediated at low acidic pH. While Ma et al. [141] and Boczkaj et al. [149] sustained that improved removal efficiencies could be achieved during ozonation treatment of wastewater in basic conditions having a high density of hydroxyl radicals. In addition, Buffle et al. [142] and Patil et al. [138] supported that the variation of pH can impact on the properties of the catalysts surface, mineralisation of contaminant, reactivity of ozone or production of free radicals. Nevertheless, numerous investigations have demonstrated that the reaction rate of ozone on selected pollutants could be significant in acidic and alkaline pH media [147,148,150–153]. Indeed, the decomposition of ozone is favoured in basic pH because of the presence of hydroxyl ions and often results in improved efficacy. Likewise, Martins et al. [148] stated that catalytic ozonation can be improved in acidic conditions because of the enhanced adsorption and subsequent surface interactions recalling that surface reactions are impeded in basic media because of electrostatic repulsions. Furthermore, in complex mixed effluents, the occurrence of scavenging ions at different pH can significantly obstruct the generation and reactivity of reactive species. Similar trends on the impact of pH during ozonation and catalytic ozonation have been outlined by Alinejad et al. [134]. It can be highlighted that solution pH is a complicated factor that deeply depends on the nature of the pollutants and hence the composition of wastewater. Hence, water temperature and pH, concentrations of dissolved matter and UV light and catalyst dose have been considered as factors that influence the decomposition of ozone in aqueous media [107]. The development of adequate non-thermal plasma technologies based on dielectric barrier discharge has attracted attention in the past decades. The drive of using DBD systems focuses on finding an effective configuration in which O_3 and related oxygen species could be abundantly produced at low cost and environmentally safe experimental conditions. For instance, Mouele et al. [1] reported that a double cylindrical dielectric barrier discharge plasma configuration could still be explored to produce ozone and co-oxidants for the detoxification of polluted water.

4.5. General description of single and double cylindrical dielectric barrier discharge configurations

Dielectric barrier discharge configurations aim at the generation of various molecular and radical species such as O_3, H_2O_2, $O^·$, $O_2^{·-}$, OH, etc., electrons, and UV photons that directly or indirectly decompose hazardous compounds. The priority of DBDs is the production of the non-selective hydroxyl radical that is an exceptionally effective oxidant, with an oxidising potential of 2.8 V higher than that of ozone 2.07 V [154]. The OH radical is the most dominant oxidative species that non-selectively attacks recalcitrant contaminants and converts them into dissolved CO_2, H_2O, and harmless substances. Among the most common DBD electrode configurations earlier reviewed in Section 4.1 single and double cylindrical dielectric-barrier discharges (SCDBD and DCDBD) have been used in wastewater recovery [98,154]. Therefore, the current review focuses on SCDBD and DCDBD systems as effective methods for the treatment of contaminated water/wastewater. These configurations consist of one or more insulating layers often referred to as a dielectric barrier between/around metal electrodes and discharge gap(s). The presence of more dielectric boundaries in DBD configurations intensifies the existence of electric and magnetic fields to ensure the even distribution of highly energised electrons around the dielectric materials even though the upscaling of these configurations has always been challenging. A typical schematic comparison of single and double cylindrical DBDs is presented in Fig. 3.

In Fig. 3a, the following scenarios can be encountered:

Scenario 1: The feed gas (air) bubbled in the system is directly in contact with the effluent being treated. In this case, the air components (N_2 and O_2) dispersed in the liquid might not immediately reach the high energy electrons around the dielectric barrier to induce air dissociation that leads to the formation of gaseous species. So, the fact that the dielectric barrier is in contact with the pollutant being remediated, might decrease the abundance of high energy electrons as these latter become randomly dispersed and solvated and could be involved in parallel slow reactions occurring in the solution. This consequently decelerates the dissociation of the feed gas and declines the density of gaseous and secondary aqueous species and could therefore retard the treatment process.

Scenario 2: The feed gas (air) is often passed through direct contact with the high voltage electrode (HV) in the dielectric barrier tube [100]. This could result in electrode deterioration after long periods of experimental runs.

Scenario 3: If the electrolyte is introduced into the inner dielectric tube, this could amplify the intensity of UV generated [155]. However, this might result in scenario 1 as the dissociation of feed gas dispersed in the water might become a slow process and could decelerate the production of active species.

Scenario 4: If the electrolyte and the feed gas are fed into the inner tube of the electrolyte and both are in contact with HV, this could therefore result in scenarios 1 and 2.

On the other hand, in Fig. 3(b) the common scenario susceptible to occur in the DCDBD system can be highlighted as follows:

Scenario 1: The feed gas is passed through between the first and second dielectric layers. The presence of electric and magnetic fields in the plasma zone (the region between the first and second dielectric layers) in Fig. 3b ensures free circulation of high energy electrons around the surface of the inner (first dielectric) tube that largely participates in the dissociation of the feed gas (air in this case) and effectively contributes to the abundant production of gaseous species mainly O_3, N*, and others in the air gap. These in return, are directly circulated and dispersed into the polluted water and further induce the generation of secondary species such as H_2O_2 and $OH^·$ radicals in the water being treated. These hence boost the density of both gaseous and aqueous species that enhance the degradation of targeted pollutants. During these scenarios, the HV is protected by the inner dielectric tube.

Scenario 2: The introduction of the electrolyte solution in the inner dielectric tube improves the UV intensity and accelerates the dissociation of air gas which increases the amount of gaseous and liquid species. These consequently improve the decomposition of selected contaminants.

Therefore, the addition of a second dielectric barrier in DBD configuration (Fig. 3b) allows the focus of a magnetic field that facilitates the bending motion of gaseous elements around the first dielectric tube, while the electric field facilitates their acceleration in the plasma zone. This validates the superiority of double cylindrical DBD configuration over the single cylindrical DBD electrode geometry. Hence double cylindrical DBD configuration can still be explored for the remediation of recalcitrant organic pollutants in water and wastewater. The differences between single and double cylindrical describes in this text were summarised and is presented in Table 1.

4.5.1. Degradation of organic pollutants by single dielectric barrier discharge

Single cylindrical dielectric barrier discharge (SCDBD) has been used for the remediation of organic pollutants in water and wastewater. For instance, Mok et al. [156] investigated the decomposition of orange II (O. II) azo dye using SCDBD reactor that generates UV light and reactive species mainly ozone that effectively destroyed the model pollutant O.II dye. Their study conducted at the working parameters displayed in Table 2 showed that the removal efficiency of O. II with SCDBD alone
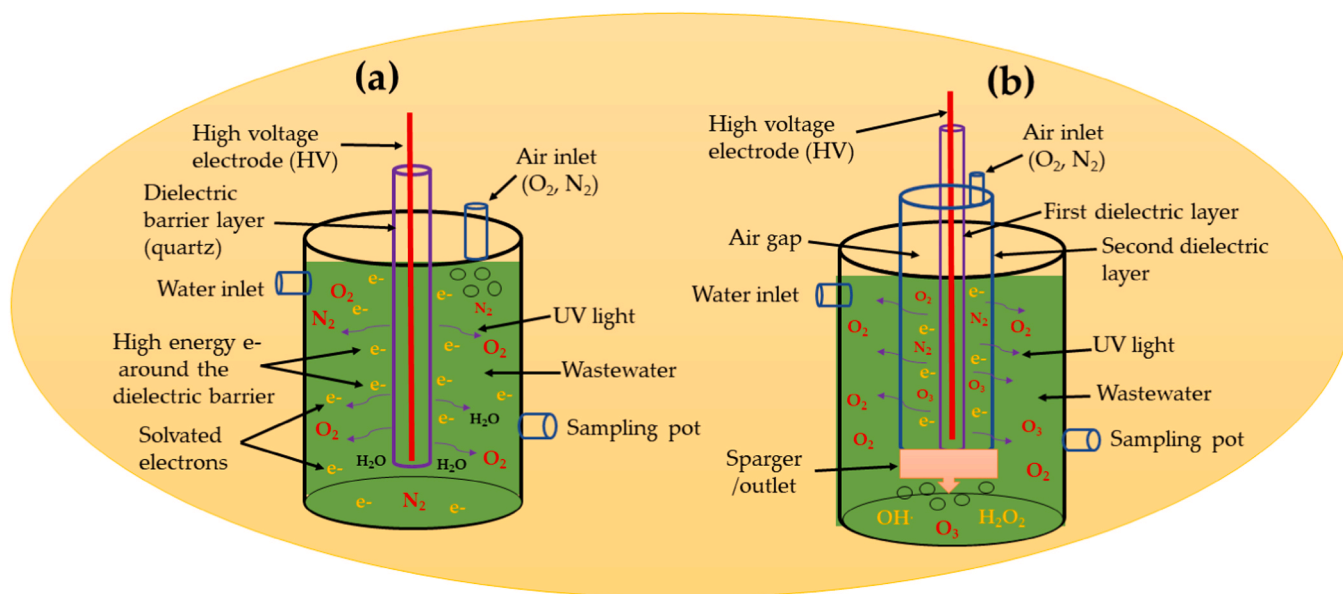
Fig. 3. (a) Photograph of the UV light produced in a single dielectric barrier discharge with the aqueous electrolyte solution (plus 1.5 mm silver rod in an electrolyte solution), and (b) silver rod in an electrolyte in the inner tube compartment of the double cylindrical DBD [155].

Table 1
Summary of the difference between single and double cylindrical DBDs.

Properties/benefits	Single cylindrical DBD	Double cylindrical DBD	Ref.
Number of dielectric barriers	1	2 or more	
High energy electrons distribution & diffusion	Low abundance, randomly distributed and dispersed in liquid	High abundance, highly distributed and effectively dispersed in polluted water	[74]
High voltage electrode corrosion protection	Exposed to feed gas and may result in corrosion that may limit its usability	Well protected from feed gas and polluted water and can be used in prolonged experimental runs	[1]
Electrical and magnetic fields strength	Could be weak around the dielectric barrier due to polluted water surrounding	Strong between the first and second dielectric barriers leading to effective acceleration and bending of gaseous free radicals	[98, 103]
Feed gas dissociation & diffusion	Directly and randomly diffused in solution and may retard its contact with high energetic electrons, hence decelerating the formation of active species	Well dissociated to gaseous active species and efficiently diffused in solution	[6]
Introduction of electrolyte solution in the inner dielectric barrier	Electrolyte might intensify UV radiation generation but the diffusion of flow gas in electrolyte might limit the production of active species and retard the decontamination process	This intensifies the circulation of high energy electrons around the inner dielectric, improves the dissociation of feed gas and amplifies the production of UV radiation and active species, and hence accelerate the depollution of water effluents	[11, 12, 32, 33, 90]

was up to 90% after 60 min of plasma experiment. However, addition of powder TiO_2 catalyst in the system enhanced the efficacy of UV radiation and hence the degradation efficiency of O.II to 99.9% after 20 min of plasma exposure though the degradation intermediate by-products showed recalcitrance behaviour during oxidation process with SCDBD alone. The authors showed that dye initial concentration influences its removal and better TOC removal was achieved with pure O_2 feed gas than in air-SCDBD system. Conversely, Kim et al. [100] conducted the treatment of wastewater simulated by various antibiotics including lincomycin, ciprofloxacin, enrofloxacin, chlortetracycline, oxytetracycline, sulfathiazole, sulfamethoxazole, sulfamethazine, and trimethoprim using SCDBD configuration at experimental conditions recorded in Table 2. During their investigations, the impact of pollutant initial concentration, feed gas (air, O_2) and discharge power on the removal efficiency of antibiotics were discussed. Their results indicate that the degradation of antibiotics depended on the energy yield, though different degradability were observed. Their report sustains that at an initial concentration of 5 mg L^{-1}, the energy required to degrade 60% of antibiotics was in the range of 0.26–1.49 kJ mg L^{-1} and 0.39–2.06 kJ mg L^{-1} for pollutants with degradation efficiency of 90%. The authors further claimed that the SCDBD configuration used in their study is a promising technology for wastewater remediation. Comparably, Tichonovas et al. [157] studied the plasma oxidation of 13 industrial textile dyes using a pilot single cylindrical dielectric barrier discharge (SCDBD) at experimental factors reported in Table 2. The results of their study demonstrated that when the discharged power was varied from 3 to 33 W, the concentration of ozone fluctuated between 0.19 mg/s and 0.46 mg/s with a corresponding energy in the range of 18.7–866 kJ/g. In addition, the authors showed that the decomposition of 10 out of 13 dyes reached 95% after 5 min of the start of the plasma experiment and the main degradation by-products comprised of amines and amides, carboxylic acids, and nitrates and the treated effluent had a toxicity of near-zero values. Their investigation further claimed that the SCDBD reactor used in their research is a competitive technology that effectively remedies recalcitrant dye simulated textile wastewater. A similar investigation carried out by Reddy et al. [158] who assessed the degradation of the aqueous pesticide endosulfan in an aqueous single cylindrical dielectric barrier discharge reactor at the experimental conditions shown in Table 2. Their report highlights that the degradation percentage of endosulfan reached 65% after 30 min of plasma time

Table 2
Energy yield G_{50} of conventional DBDs, single/double cylindrical DBD (SCDBD and DCDBD) configurations used for the degradation of organic pollutants.

Type/name of pollutant	Initial concentration (mol/L)	Solution pH	Type of DBD configuration	Power (kW)	Reaction time (min)	Degradation efficiency (%)	Rate constant Kr (min^{-1})	Half-life (min)	Energy Yield (G_{50}) (g/ kW h)	Ref.
Pentoxifylline	3.59×10^{-4}	NA	DBD with falling liquid film	0.001	60	100	$1 4.2 \times 10^{-2}$	16.5	0.6055	[165]
Carbamazepine	8.46×10^{-5}	NA	Ex situ DBD system	0.012	60	90	3.8×10^{-2}	18.23	0.0045	[166]
Sulfadiazine antibiotics	3.99×10^{-5}	9	Water falling film DBD	0.15	30	87	6.8×10^{-2}	10.19	0.0003	[77]
Oxacillin	2.49×10^{-4}	NA	DBD with falling liquid film	0.002	30	100	3.83×10^{-1}	1.81	2.761	[166]
Carbamazepine	9.98×10^{-5}	NA	DBD rotating drum reactor	0.75	60	94	4.68×10^{-2}	14.81	0.0010	[167]
Amoxicillin	2.7×10^{-4}	NA	DBD rotating drum reactor	0.75	10	100	3.32×10^{-1}	2.08	0.0316	[167]
Atrazine	1.39×10^{-7}	5.06	Atmospheric pulsed DBD	0.0017	45	61	2.09×10^{-1}	3.31	0.0002	[168]
Azo dye Orange II	7.14×10^{-5}	5.3	SCDBD	0.0168	60	99.9	1.15×10^{-1}	6	0.06	[156]
Endosulfan pesticide	3.68×10^{-5}	NA	SCDBD	0.0026	30	65	2.1×10^{-2}	33	0.08	[158]
13 industrial textile dyes	2.25×10^{-5}	7–8	DCDBD	0.033	5	95	5.89×10^{-1}	1.63	0.18	[157]
Veterinary antibiotics	1.04×10^{-5}	NA	SCDBD	0.0089	30	90	7.3×10^{-2}	9.5	0.03	[100]
Various micropollutants	6.70×10^{-4}	NA	SCDBD	0.04–0.09	30	90–99.5	7.3×10^{-2}–1.76×10^{-1}	13.19–5.47	0.30–0.50	[159]
3 micropollutants	3.37×10^{-6}	NA	SCDBD	0.0397	20	99.8	3.10×10^{-1}	3.10	0.004	[160]
Alachlor pesticide	3.70×10^{-6}	NA	SCDBD	0.04	30	90	7.3×10^{-2}	13.19	0.0005	[161]
Tetracycline antibiotic	4.50×10^{-5}	NA	DCDBD	NA	5	82	3.03×10^{-1}	3.17	0.0002	[164]
Sulfadiazine antibiotic	3.99×10^{-5}	9.10	DCDBD	0.100	30	99.99	3.07×10^{-1}	2.14	0.0016	[77]
Diclofenac	3.37×10^{-5}	6.15	DCDBD	0.050	10	99.99	9.21×10^{-1}	1.04	0.0096	[162]
Methylene Blue dye	3.10×10^{-5}	2.5	DCDBD	0.060	12	99.99	7.67×10^{-1}	1.25	0.098	[90]
Bisphenol-A	4.38×10^{-5}	3	DCDBD	0.125	80	67.90	9.0×10^{-3}	107	0.0009	[11]
2-nitrophenol	7.20×10^{-5}	3	DCDBD	0.125	60	58.60	5.7×10^{-3}	168	0.0003	[12]
Methyl orange dye	3.05×10^{-4}	3	DCDBD	0.117	18	99.90	3.83×10^{-1}	2.51	0.034	[163]

on stream. Likewise, the decomposition of endosulfan followed a first-order kinetic trend and its rate of degradation depended on the initial concentration and input power. The study further conveyed that the addition of cerium oxide catalysts in the plasma reactor improved the mineralisation of recalcitrant endosulfan. Another study focusing on the degradation of various micropollutants (atrazine, alachlor, diuron, dichlorvos and pentachlorophenol, carbamazepine and 1, 7-α-ethinylestradiol, and bisphenol A) using a continuous flow pulsed single dielectric barrier discharge (DBD) configuration with falling water film was conducted by Wardenier et al. [159]. During their assessment, the effect of multiple parameters including the type of feed gases and their flow rates, discharged power and energy efficiency on the removal of pollutants were examined. At optimum conditions specified in Table 2, the degradation percentages of micropollutants were in the range of 90–99.5% with a corresponding energy range of 2.42–4.25 kW h/m^3 achieved after 30 min of time on stream. The authors further asserted that the SCDBD reactor used in their study is a promising AOP that can be used for the efficient remediation of industrial wastewater. The extended use of SCDBD plasma configurations in the degradation of micropollutants including atrazine (ATZ) and alachlor (ALA), bisphenol A (BPA) and 1,7-a-ethinylestradiol (EE2) has been reported in the literature [160,161]. From these investigations, it can be observed that the degradation of organic pollutants with SCDBD alone resulted in reasonable removal efficiencies but somehow the degradation by-products of targeted pollutants showed resistance behaviour. However, the addition of catalysts improved the removal processes and boosted the mineralisation of recalcitrant degradation intermediate by-products.

4.5.2. Degradation of organic pollutants by double cylindrical dielectric barrier discharge

Rong et al. [77] studied the degradation of diclofenac (DF) using a double cylindrical dielectric barrier discharge (DCDBD) reactor at the applied conditions shown in Table 2. In their study, the authors assessed the impact of various working parameters on the removal of DF. The outcomes show that at concentration 10 mg/L of pH 6.15, and a discharge power of 50 W, diclofenac was totally removed (99.9%) within 10 min of time on stream. Rong and colleagues showed that the supplement of Fe^{2+} in the DCDBD system boosted the decomposition of DF toxin. The authors showed that O_3 and OH· were the major reactive species involved in the decomposition of DF that resulted in 5 degradation intermediate by-products whose mineralisation was futile due to the recalcitrance of their aromatic rings. Nevertheless, DF and its degradation intermediates were fully detoxified. These results indicate that in DCDBD systems producing both O_3 and OH·, the by-products resulting from the interaction of OH with DF might appear to be converted to H_2O, dissolved CO_2, and simpler inorganics. The reaction of O_3 with unsaturated pollutants such as DF results in more bulky and stable intermediates whose total conversion might require prolonged treatment time. Soon after, Rong et al. [162] examined the decomposition of sulfadiazine antibiotic using the same DCDBD reactor. They showed that at a discharge power of 100 W, 99.9% removal of 3.99×10^{-5} mol/L sulfadiazine (10 mg/L) was reached at pH 9.10 within 30 min time on stream. The degradation of sulfadiazine resulted in eight degradation intermediate by-products that were successfully transformed to H_2O and CO_2. Double cylindrical DBD was also used by Tijani et al. [11] for the degradation of 2-nitrophenol (2-NP) pollutant simulated wastewater at conditions indicated in Table 2. The results showed that after 120 min time of stream, about 58.8% removal of 2-NP was achieved in acidic conditions at pH 3 and nine degradation intermediates by-products were detected and were further transformed to dissolved CO_2 and H_2O. The 64% removal achieved in this study inferred that 2-NP and its degradation by-products were recalcitrant but afterward got totally decomposed. Likewise, Tijani et al. [12] used the same DCDBD configuration to decompose bisphenol-A (BP-A) at the corresponding conditions recorded in Table 2. The outcomes showed that 67.9% of BPA removal was

reached within 80 min of experiment. In total six recalcitrant degradation intermediates were identified which further were transformed to H_2O and CO_2. Moreover, Tao et al. [163] investigated the decomposition of methyl orange using a DCDBD reactor at the applied conditions indicated in Table 2. Their outcomes showed that at a discharge power of 117 W about 99.9 of O.II removal was achieved at pH 3 within 18 min time on stream. Unfortunately, their report does not highlight any information about O.II degradation intermediate by-products. Extended assessment of the efficiency of DCDBD configuration was performed by Mouele et al. [90] for the degradation of Methylene Blue (MB) dye at experimental conditions shown in Table 2. Their results demonstrated that with a discharge power of 60 W, 3.10×10^{-5} mol/L (40 mg/L) MB was totally degraded at pH 2.5 within 12 min time on stream. The authors reported that the decay of MB resulted in four degradation intermediate by-products that were fully converted into H_2O, CO_2, and harmless inorganics. Thus, this review proposes that DCDBD could be an effective treatment method for the remediation of contaminated waters. Nevertheless, a short and succinct comparison between conventional, single, and double cylindrical DBD configurations in terms of their efficiency during the removal of water pollutants has been summarised and presented in Table 2. Their energy yield (G_{50}) was approximated according to Malik [34] and Tang et al. [164]. The outcomes recorded in Table 2 show that complete removal of pollutants with single cylindrical dielectric barrier discharges (SCDBD) was achieved within 60 min and the half-life ($t_{1/2}$) required to decompose half of pollutant concentration was less than or equal to 33 min ($t_{1/2} \leq 33$ min) with a corresponding energy yield G_{50} in the range of 0.0005–0.50 g/kW h. On the other hand, the total degradation of pollutants with double cylindrical dielectric barrier discharge (DCDBDB) configurations was reached within 30 min of plasma exposure except for Tetracycline antibiotic, Bisphenol-A and 2-nitrophenol that showed strong resistance and reduced degradation percentages of 82%, 67.90% and 58.6%, respectively due to the recalcitrance of their degradation by-products that required extended times to reach complete conversion to H_2O, dissolved CO_2 and harmless inorganics. It is worthwhile to recall that Tijani et al. [11,12] highlighted that 2-nitrophenol, Bisphenol-A and antibiotic such as Tetracycline are often listed as compounds of emerging concern because of their tenacity to be totally decomposed. Likewise, the minimal removal percentages obtained for the recovery of these three compounds could be because, the DCDBD configurations used were open systems which might have favoured the escape of O_3 and related gaseous species that could majorly enhance the removal process if recirculated. Apart from Bisphenol-A and 2-nitrophenol whose half-lives 107 and 168 min were required to degrade half of their initial concentrations, correspondingly, the data presented in Table 2 indicate that the decomposition of half of pollutant concentrations happened within 3 min of plasma run ($t_{1/2} \leq 3$ min) with corresponding energy yield (G_{50}) range of 0.0016–0.098 g/kW h. These results together sustain the superiority of DCDBD configurations over SCDBD electrode geometries. Furthermore, since all G_{50} calculated in Table 2 are less than 50%, this indicates that DBD technologies are energy efficient treatment protocols for the recovery of polluted water.

4.6. Dielectric barrier discharge working scheme: benefits of double dielectric barrier discharge configuration

Double cylindrical dielectric barrier discharge (DCDBD) electrode geometry presents benefits over other DBD geometries. Its dominance is based on several aspects such as high electron density, even distribution of electrons around the inner tube (first dielectric material), minimum anode corrosion, and good stability. Similar advantages of this configuration were explored by [6,162] during the degradation of dyes and pharmaceutical water contaminants. DBD involves the generation of non-selective hydroxyl radicals as a promising tool for effective degradation and mineralisation of target pollutants in water and wastewater [169,170]. Apart from the production of OH radicals, the DBD system

also generates UV light, O_3, and H_2O_2 and their combination in aqueous media allows water and wastewater treatment without the addition of chemicals. Even though various DBD configurations have been employed in the decomposition of pharmaceuticals in aquatic media [32,77,165,166,170], their efficiency may depend on their electrode geometries. A typical DBD reactor described by Mouele [6] presented in Fig. 4 consists of the inner and outer quartz dielectric barriers/tubes and the region between the two tubes is often referred to as the air gap or discharge zone. The two tubes are sealed at the top of the outer part of the reactor.

At the bottom of the airgap, the second barrier is sealed onto a porous sparging outlet. The inner tube diameter is often around 1 mm and that of the outer tube is about 7 mm. The DBD reactor (23–25 cm) long is with an inlet and outlet for air circulation and an air gap of about 2 mm. The simulated wastewater placed in the reactor is considered as the ground electrode and earthed to complete the circuit. The air compressor with a controllable flow rate (using an airflow metre) is connected to the gas inlet. The feed gas fed from the inlet freely circulates through the airgap or plasma zone and is uniformly spread as bubbles into the simulated wastewater via the porous sparging material to achieve maximum oxidation of the pollutant. The set voltage, airflow, pollutant volume, and other parameters are either varied or kept constant for optimisation purposes. A power supply set at a voltage delivering a certain amount of current is directly connected to a high voltage electrode that is immersed in an electrolyte solution placed in the inner tube of the reactor. The interaction between the highly energised electrons around the inner tube and air gas (N_2 and O_2) or pure oxygen (O_2) induced the formation of UV light and various exciting unstable species such as N^*, $O^.$, O_3, etc. in the plasma zone. The generated species in the air gap follow an avalanche of chemical reactions and are directly circulated into the polluted water, where secondary species such as H_2O_2, $OH^.$, etc. are subsequently produced. From the diagram presented in Fig. 4, the flow of about 1 eV current through the anode electrode is a source of high energy electrons that are evenly distributed around the first dielectric barrier governed by the electric and magnetic fields. So, the interaction of the highly energised electrons with feed gas such as

air, oxygen, nitrogen, etc. in the plasma zone (b) is the driving force responsible for the generation of UV radiation, shock waves, and various types of reactive oxygen species (ROS). The primarily generated species in zone (b) are then circulated by continuous gas flow into the bulk solution where other species are subsequently formed. Beforehand, the dissociation of air gas described by Massima [6] and Magureanu et al. [165,166,171] in the region (b) occurs in four distinctive reactions among which excitation (Eq. (12)), dissociation (Eq. (13)), ionisation (Eqs. (13)–(16)) and electron capture (Eqs. (17) and (18)) occurs. M represents the third collision substrate such as O_2, N_2, etc.

$$e^{-*} + N_2 \rightarrow N_2^* + e^- \tag{12}$$

$$e^{-*} + N_2 \rightarrow N^. + N^. + e^- \tag{13}$$

$$e^{-*} + O_2 \rightarrow O^. + O^. + e^- \tag{14}$$

$$e^{-*} + H_2O \rightarrow OH^. + H^. + e^- \tag{15}$$

$$e^{-*} + O_2 \rightarrow O_2^+ + 2e^- \tag{16}$$

$$e^{-*} + N_2 \rightarrow N_2^* + e^- \tag{17}$$

$$e^{-*} + O_2 + M \rightarrow O_2^- + M \tag{18}$$

Consequently, various reactive oxygen species such as H_2O_2, $O^.$, O_2^-, $HO^.$, HO_2, H_3O^+, OH^-, H_2O, etc. are produced in the DCDBD configuration. The principal chemical reactions for their subsequent production as earlier discussed by Locke et al. [172] and Panicker [173] are presented in Eqs. (19)–(33)

$$2H_2O \rightarrow H_3O + e^-_{eq} + OH \tag{19}$$

$$H_2O \rightarrow OH^. + H \tag{20}$$

$$H_3O^+ + OH^- \rightarrow 2H_2O \tag{21}$$

$$H^. + O_2 \rightarrow HO_2 \tag{22}$$

$$H^. + H_2O_2 \rightarrow H_2O + OH \tag{23}$$

Fig. 4. Different reaction zones encountered in the DCDBD system. (a) High voltage electrode, (b) air gap/plasma zone, (c) ROS formed in plasma discharge zone, (d) sparger, (e–g) ROS discharged in polluted water, (h) magnetic stirrer [62].

$$OH^- + H_2O_2 \rightarrow H_2O + HO_2^{\S} \qquad (24)$$

$$OH^- + H^- \rightarrow H_2O \qquad (25)$$

$$e_{eq}^- + OH^- \rightarrow OH^- \qquad (26)$$

$$e_{eq}^- + H^- + H_2O \rightarrow OH^- + H_2 \qquad (27)$$

$$e_{eq}^- + H_2O_2 \rightarrow OH^- + OH^- \qquad (28)$$

$$2\ OH^- \rightarrow H_2O_2 \qquad (29)$$

$$2\ HO_2 \rightarrow H_2O_2 + O_2 \qquad (30)$$

$$H^- + HO_2 \rightarrow H_2O_2 \qquad (31)$$

$$2H^- \rightarrow H_2 \qquad (32)$$

$$HO_2^- + OH^- \rightarrow H_2O + O_2 \qquad (33)$$

During the formation process of reactive oxygen and nitrogen-based species (ROS) in DCDBD, free radicals take up electrons from neighbouring atoms or molecules and several new chemically active species, such as H_2O_2, $O^\bullet$, $OH^\bullet$, $HO_2^\bullet$, O_3^*, N_2^*, e^-, O_2^-, O^-, O_2^+, etc. are formed. The dislocated electrons in newly generated entities tend to return to their initial states and the process becomes uninterrupted. This consequently gives rise to reaction chains of the formation of reactive oxygen-based species as shown in Fig. 5. To avoid confusion, the RNS formed in DCDBD system as previously claimed, have been presented and discussed in a separated section in Fig. 5.

Similarly, reactive nitrogen-based species (RNS) presented in Fig. 5 are also produced in atmospheric non-thermal plasma geometries mainly DCDBD following the same scenario as shown in Fig. 4. Electrical discharges based on non-thermal plasma processes are sources of several reaction chains leading to the formation of ROS in Fig. 4. The principal goal of these avalanche reactions is the generation of the most powerful and non-selective hydroxyl radicals that destroy any type of contaminant and micro-organisms [1]. In addition to this, the multiple ROS produced in DCDBD and other DBD configurations is often characterised by their different oxidation potentials. Hence their effects on target pollutants may be completely different. For instance, ozone with an oxidation potential of 2.07 V selectively reacts with unsaturated compounds. Based on these particularities, the most common ROS produced in DCDBDs, their densities, oxidation potential, and half-life have been reviewed and are shown in Table 3.

Table 3
Chemical properties of common oxidants in non-thermal plasma configurations [169].

Reactive oxygen species	Oxidation potential (V)	Density (cm^{-3})	Half-life (s)	Ref.
$OH^\bullet$	2.80	10^{15}–10^{17}	10^{-9}	[174]
$O^\bullet$	2.42	10^{14}–10^{16}	10^{-6}	[174]
O_3	2.07	10^{15}–10^{17}	1.2×10^3	[175]
H_2O_2	1.78	10^{14}–10^{16}	60	[174, 175]
$HO_2^\bullet$	1.70	NA	NA	[174]
O_2^-	1.44	10^{10}–10^{12}	10^{-6}	[174, 175]
Nitric oxide (NO)	NA	10^{13}–10^{14}	NA	[175]

The various physical and chemical properties summarised in previous paragraphs showed that DBDs are sources of powerful chemical oxidant mixtures that directly or indirectly mineralise organic contaminants in polluted water bodies. During advanced oxidation processes, based on ozonation, Fenton or photo Fenton reactions, etc. O_3, UV, and H_2O_2 are often used separately or in combination. This often requires the purchase of UV lamps, ozonisers, and liquid H_2O_2, and other necessary equipment which could be costly, energy demanding, or maybe time consuming to operate. In contrast, with only 1 eV, DCDBD configuration solely produces UV–vis light and multiple selective and non-selective oxidising agents that destroy contaminants [1]. This, therefore, gives DCDBD an advantage in eliminating toxins from polluted water. Most established water treatment techniques do not successfully remove water pollutants, but they generate carcinogenic by-products that are often more toxic than the parent pollutants [11]. Consequently, this has rendered the most developed treatment methods inefficient. So, the determination of the reaction mechanisms or degradation steps of ROS on organic pollutants might be crucial in understanding the chemistry of the oxidative agents when reacting with contaminants. These in turn may guide researchers in choosing the type of treatment of each targeted pollutant and hence having a lucid comprehension of the expected by-products. So far filtration and adsorption processes have failed to remove these contaminants from the water being treated. Hence oxidative methods that may directly break down the remaining recalcitrant pollutants should be applied. Double cylindrical dielectric barrier discharge (DCDBD) technology described in this manuscript presents
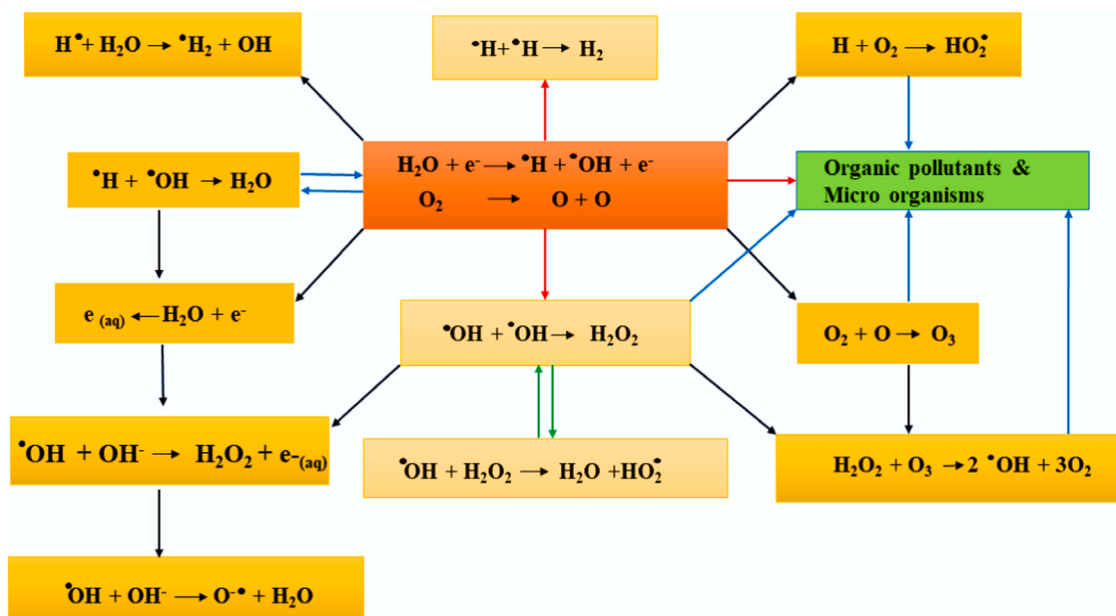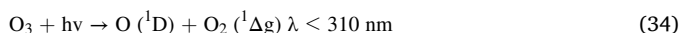

Fig. 5. Generation of reactive oxygen species in atmospheric DBD plasma configurations [2,74,102].

various physical and chemical benefits and may be considered as an alternative, efficient method that can be utilised to destroy aqueous pollutants into dissolved CO_2, H_2O, and harmless by-products [1]. This does not mean that DCBD would purify water from the raw state to the final step; rather DCDBD could be employed as an integrative technology to treat secondary or tertiary water effluents. Furthermore, from the numerous publications focusing on the use of non-thermal plasma for water treatment, literature presents little information on descriptive reaction effects/mechanisms of ROS produced in non-thermal configurations on organic contaminants and micro-organisms. Therefore, this review also highlights in greater detail, the reactive mechanisms of the common ROS produced in DBDs on organic contaminants and micro-organisms. The formation mechanisms of ROS previously described in Figs. 4 and 5 show that O_3 and its derivatives are produced in DBD reactors via a series of chemical reactions. However, more mechanisms could still be discovered depending on the DBD systems/configurations and perhaps additives used to enhance the generation of ROS. In this regard, it could be challenging to discuss the production of ROS mechanisms in a DBD plasma system without highlighting their reaction mechanisms with targeted contaminants. Furthermore, since the physical and chemical properties of the DBD system appear as chemical cocktails, it would be challenging to state the production route of each ROS in DBD solely, rather their production occurs in consecutive chains of reactions.

4.7. Reactivity of ozone and its impact on persistent organic compounds in aqueous dielectric barrier discharges

Various studies [176,177] have shown that ozone with an oxidation potential of $E_0 = 2.08$ V is a strong oxidiser agent and its oxidation reaction yields hydrogen peroxide. Likewise, Lide [178] showed that at normal conditions of temperature and pressure, ozone has a very low solubility. Moreover, Atkinson [179] showed that when exposed to UV radiations at $\lambda = 310$ nm, ozone decomposes to a singlet oxygen atom and singlet oxygen molecules according to Eq. (34). Moreover, the highly reactive singlet oxygen atom with a lifetime of 4.4 μs in aqueous media reacts with water to produce hydroxyl radicals as shown in Eq. (35) [180]. The generated OH radicals may recombine to form H_2O_2 as presented in Eq. (36) [1].

$$O_3 + h\nu \rightarrow O\,(^1D) + O_2\,(^1\Delta g)\ \lambda \leq 310\ \text{nm} \tag{34}$$

$$O\,(^1D) + H_2O\,(g) \rightarrow 2OH \tag{35}$$

$$O\,(^1D) + H_2O\,(l) \rightarrow H_2O_2 \tag{36}$$

At normal conditions of temperature and pressure and in an acidic environment, ozone behaves as an electrophilic substance and reacts with organic molecules [181]. Gurol [181] postulated that this is probably due to the positive charge carried by the oxygen atom in the resonance structures of ozone as presented in Fig. 6.

An extended property of ozone is that ozone can be converted into oxygen by hydroxyl radicals according to Eqs. (37) and (38).

$$O_3 + OH^{\cdot} \rightarrow O_2 + HO_2^{\cdot} \tag{37}$$

$$HO_2^{\cdot} + O_3 \rightarrow OH^{\cdot} + 2O_2 \tag{38}$$

Furthermore, the reactivity of ozone is often classified into two categories mainly, direct, and indirect reaction mechanisms [183].
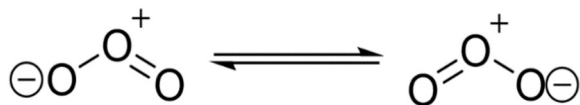
4.7.1. Direct and cycloaddition reactions of ozone reactions in DBD configurations

The Lewis ozone molecular structure presented in Fig. 7 shows a resonance structure with the two oxygen atoms carrying lone pairs of electrons making ozone a polar molecule. Hence, the Lewis model of the ozone molecule exhibits two dipole moments both oriented towards the central oxygen atom. Based on its resonance structure, it has been reported that ozone can act as a 1, 3-dipole, an electrophilic agent, and as a nucleophilic agent during aqueous chemical reactions with organic pollutants [49,183–185]. These interactions have been summarised as shown below.

The 1, 3 dipole structure of ozone has been demonstrated to undergo dipolar cycloaddition reaction with unsaturated compounds yielding ozonide compounds as shown in Fig. 7.

This is often referred to as the Criegee mechanism [182,183,185, 186]. Moreover, the literature supports that in aqueous media, the ozonide structure more likely disintegrates into an aldehyde, a ketone, or a zwitterion [76,100,183]. These can further be converted into hydrogen peroxide and carboxyl compounds [186]. The direct cycloaddition attack of ozone on organic pollutants in aqueous media has already been highlighted by a few authors. For example, Rivera-Utrilla et al. [187] studied the degradation of naphthalene sulphonic acids by oxidation with ozone in the aqueous phase. The authors showed that the abatement of naphthalene sulphonic acids was induced by 1, 3 cycloaddition reaction of ozone. Similar studies were conducted by von Gunten [51] and Yargeau et al. [188] who successively investigated the ozonation of drinking water and the impact of operating conditions on the decomposition of antibiotics during the ozonation process, respectively. Even though, non-thermal plasma technologies have recently been used for the removal of organic pollutants from water and wastewater [161,189–192], the direct oxidative degradation of pharmaceuticals by dielectric barrier discharge technologies is an emerging research field that can still be explored for water and wastewater decontamination. The few studies conducted in this regard show that DBD technologies are effective in the conversion of pharmaceutical toxins into more amenable intermediate degradation by-products [28–30,193–195]. Among the various ROS produced in DBDs systems ozone and OH radicals have been identified as the major oxidants that largely participate in the deactivation of pharmaceutical toxins as described in Fig. 2. For instance, Liu et al. [76] investigated the removal of carbamazepine from water by dielectric barrier discharge. The results of their study showed that upon the cycloaddition reaction of ozone with carbamazepine (CBZ) various degradation by-products were obtained. On the other hand, Kim et al. [100] performed the degradation of veterinary antibiotics by dielectric barrier discharge plasma; the authors specified that the direct attack of ozone on the aromatic rings in the antibiotic molecules was initiated by 1, 3-dipole addition reaction of ozone as shown in Fig. 8.

Alekseeva [196] and Dantas et al. [197] supported that the cycloaddition oxidation of aromatic rings can sometimes involve/induce the hydroxylation process that often leads to the formation of hydroxyl compounds as shown in Fig. 9.

Munter et al. [198] and Pintar et al. [199] reported later that the hydroxyl molecules formed are further altered to small entities such as aldehydes and carboxylic acids that often resist oxidation. The authors
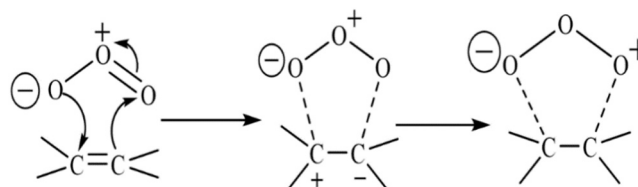
Fig. 6. Ozone resonance structures; the positively charged oxygen is electrophile [182].
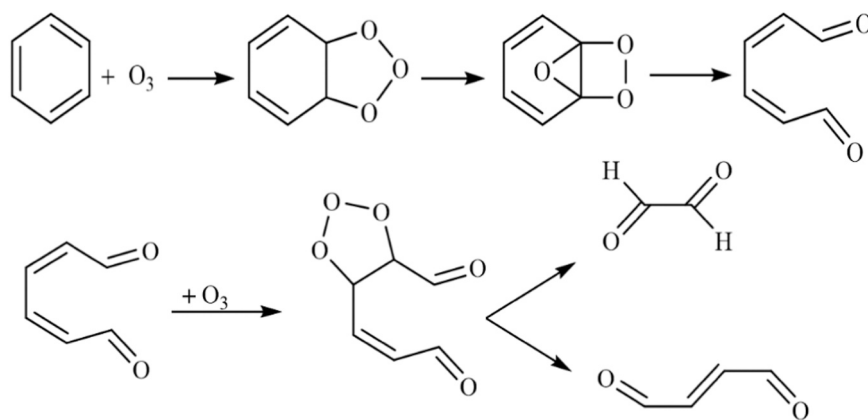
Fig. 7. Dipolar cycloaddition [184].

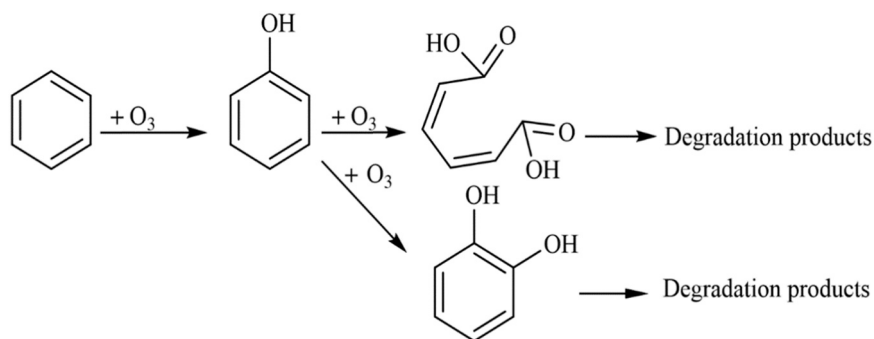**Fig. 8.** Degradation pathways of antibiotics in the DBD system [100].

Fig. 9. Hydroxylation of aromatic molecules during 1, 3-dipole reaction of ozone in DBD configuration [100].

found that the total mineralisation of hydroxylated fragments by hydroxyl radicals into dissolved H_2O, CO_2, and simpler intermediates is a slow process. Based on these observations, they concluded that the decomposition of pharmaceuticals, mainly antibiotics, could be characterised by a fast disintegration of their bulky organic frameworks followed by slow oxidation stages. This was also supported by Kim et al. [100] who investigated the degradation of veterinary antibiotics by dielectric barrier discharge and whose degradation mechanistic pathways in the DBD system are presented in Figs. 8 and 9. Although the resultant carbonyl by-products could be aldehyde or ketones, the toxicity effect of these metabolites that represent a critical parameter during water and wastewater treatment was not discussed. Besides the cycloaddition reaction discussed above, ozone can also react as either an electrophile or a nucleophile [49,184].

4.7.2. Electrophilic reactions of ozone in DBDs

In aqueous media, electrophilic reactions take place between ozone and compounds with high electron density, principally aqueous aromatic mixtures [183]. For instance, substituted aromatic molecules by electron donors OH and NH_2 groups display significant electron density on carbonic molecules at ortho and para positions [200]. Therefore, in these positions, ozone is readily active to substituted aromatic compounds. A typical illustration of ozonation of aromatic compounds is the
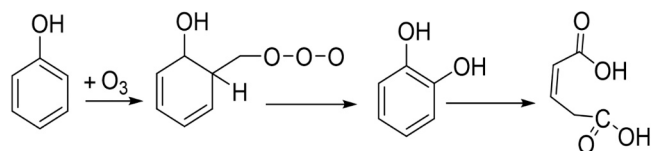
Fig. 10. The reaction between phenol and ozone [201].

reaction of phenol with ozone that occurs rapidly as shown in Fig. 10.

This was also sustained by Rong et al. [162] and Chen et al. [202] who consecutively studied the degradation of sulfadiazine antibiotics by water falling film dielectric barrier discharge and the synergistic degradation performance and mechanism of 17b-estradiol by dielectric barrier discharge non-thermal plasma combined with Pt–TiO_2. The results of their studies showed that through electrophilic reactions occurring in DBDs, both sulfadiazine and 17b-estradiol were successfully oxidised to their corresponding carboxylic acids and further to H_2O, CO_2, and harmless substances. Moreover, Tang et al. [190] studied the removal of oxytetracycline (OTC) antibiotic in water using a gas phase dielectric barrier discharge (GPDBD) plasma reactor. During their investigation, the authors found that the applied voltage is one of the factors that affect the production of the principal reactive species in the DBD reactor. They proved that the concentration of O_3, H_2O_2 and OH in GPDBD system increased with an increase of the applied voltage and successfully improved the degradation of OTC model pollutant. This was in accordance with previous investigations [203–205]. In addition, Tang et al. [190] demonstrated that at a prolonged treatment time, the concentrations of both O_3 and H_2O_2 were superior in deionized water than in OTC wastewater when exposed to plasma treatment. This signified that both O_3 and H_2O_2 were used up during the plasma treatment process and were accountable for the demolition of OTC in GPDBD configuration. The electrophilic attack of ozone reinforced by OH reaction completely converted OTC to H_2O, dissolved CO_2, and simpler inorganics. Furthermore, Xin et al. [67] examined the role of ozone and hydroxyl radical during the removal of bromoamine acid (BAA) in dye wastewater by gas-liquid plasma system. In their study, the authors successfully quantified O_3, H_2O_2 by indigo colorimetric method and Ti^{4+} colorimetric method, respectively as recommended in previous publications [206,207]. The results of Xin et al. [67] showed that the presence of BAA in DBD reactor resulted in a decrease of ozone concentration but

an improved of H_2O_2 production. This implied that dissolved ozone contributed to the abatement of BAA in aqueous solution. However, the authors claimed that $OH^.$ originating mainly from H_2O_2 participated at 60% in the decomposition of BAA while O_3 only contributed 20% towards the detoxification of BAA pollutants. The electrophilic attack of ozone on BAA contaminant followed by OH mediation principally resulted in small entities consisting of epoxides, alcohols, and carboxylic acids. These studies clearly showed that O_3 is one of the reactive oxygen species produced in DBD configurations. Its electrophilic reaction with organic pollutants directly converts/oxidises them into amenable degradation intermediates by-products.

4.7.3. Nucleophilic reactions of ozone in DBD system

In aqueous dielectric barrier discharge technologies, the nucleophilic reaction of ozone occurs in organic compounds with an electron deficiency, mainly those containing electron withdrawing groups such as —COOH and —NO_2. This consequently lowers the rate of reaction of ozone with electron deficient molecules [100,181]. Consequently, it could be inferred that ozone selectively reacts with organic compounds in DBD systems. On the one hand, its reaction is faster with compounds containing electron donor groups and much quicker with unsaturated aromatics [49]. In this regard, Rong et al. [162] studied the degradation of aqueous diclofenac (DF) using a dielectric barrier discharge system. During plasmas discharge experiment, several active species including $HO^.$, $O^.$ and $H^.$, and molecular species such as H_2O_2 and O_3 were produced in the DBB actuator. Likewise, the authors showed that O_3 was the major species that initiated the decomposition of DF. In this regard, the nucleophilic interaction of O_3 produced in the DBD reactor with the amino group on DF led to the formation of aminyl radical that was further converted to more stable intermediates. A comparable study on the nucleophilic reaction of ozone during the degradation of bisphenol-A (BPA) by dielectric barrier discharge alone and in combination with polyethylene glycol stabilised nano zero valent iron (PEG-nZVI) catalysts was carried out by Tijani et al. [11]. Their results revealed that complete removal (99.99%) of BPA was achieved with DBD/PEG-nZVI system compared to 67.9% BPA removal reached with DBD alone. The authors showed that in both DBD/PEG-nZVI and DBD alone systems, the decay of BPA was mainly initiated by ozone through an epoxidation process followed by ring opening and elimination of various groups such as —CO_2. Apart from these, the authors noticed that the oligomerisation of recalcitrant degradation intermediate by-products of BPA resulted in the formation of bigger molecules that required extended time to reach total mineralisation. Similar studies focusing on the nucleophilic reaction of ozone during degradation of organic pollutants in AOPs have been reported [208–211]. A similar activity of ozone has been observed during its reaction with ionised and dissociated organic materials compared to neutral or non-dissociated particulates where the ozone reaction rate is relatively low [212]. Furthermore, during the treatment of drinking water, the speed of reaction of ozone with various inorganics, ionised and dissociated inorganic components are extremely high [212]. Likewise, during oxidation of inorganic compounds, the electron transfer remains the driving process through which one of the oxygen atoms in the ozone molecule is transferred to the inorganic compounds. Hence, the oxidation of ozone with organic compounds is selective and partial while inorganic substances are quickly and completely oxidised by ozone.

4.7.4. Indirect reactions of ozone in dielectric barrier discharges

Depending on various factors such as temperature, pH, and the chemical composition of water, both direct and indirect oxidation reactions usually occur during the ozonation process [100]. However, indirect oxidation is often governed by side chain reactions during which ozone reacts with dissolved oxygen and aqueous metabolites giving rise to new active species such as OH radicals that unselectively

contribute to the mineralisation of organic pollutants [185]. Indeed, indirect reactions during the ozonation process are often complex. In this way, a single indirect reaction can be summarised in three steps among which initiation, radical chain- reaction, and termination. The initiation step is characterised by the decomposition/inhibition of ozone by the OH-molecule [185] as shown in Eq. (39).

$$O_3 + OH^- \rightarrow O_2^{\bullet-} + HO_2^{\bullet} \ (pKa = 4.8) \tag{39}$$
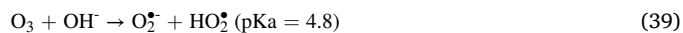
Likewise, the hydroxyl peroxide radical formed in Eq. (27) has a pK_a value of 4.8 above which it forms superoxide radical as shown in Eq. (40).

$$HO_2^{\bullet} \rightarrow O_2^{\bullet-} + H^+ \ (pK_a = 4.8) \tag{40}$$

In the radical chain reaction, the generated superoxide anion interacts with O_3 yielding OH-radicals which further react with O_3 as shown in Eqs. (41)–(44).

$$O_3 + O_2^{\bullet-} + \rightarrow O_3^{\bullet-} + O_2 \tag{41}$$

$$O_3^{\bullet-} + H^+ \rightarrow HO_3^{\bullet} \ (pH < \approx 8) \tag{42}$$

$$OH^{\bullet} + O_3 \rightarrow HO_4^{\bullet} \tag{43}$$

$$HO_4^{\bullet} \rightarrow O_2 + HO_2^{\bullet} \tag{44}$$

Consequently, the $HO_2^{\bullet}$ radicals formed in Eq. (33) often react all over again (propagation reaction step) leading to a reaction-chain initiated by the so-called promoters such as humic acid (HCO_3^-/CO_3^{2-}) and Aryl-R (PO_3^{4-}) that are known as substances that convert OH-radicals to superoxide radicals as presented. Otherwise, the disintegration of ozone (O_3) in dielectric barrier discharge configurations, yielding secondary species potent for the mineralisation of water pollutants has been widely outlined in the literature. Mikheyev et al. [213] examined the production of ozone and oxygen atoms in a dielectric barrier discharge in pure oxygen and O_2/CH_4 mixtures. From the experimental modelling scenarios studied in the DBD system, the authors showed that the vibrationally excited and unstable ozone produced in the bulk solution disintegrated following chains of interactions with co-species such as atomic oxygen and hydrogen (O and H) and hydroxyl radical (OH) resulting in the formation of secondary oxidants including perhydroxyl radical (HO_2) and OH and molecular O_2 according to Eqs. (45)–(48).

$$O_3 + O \rightarrow O_2 + O_2 \tag{45}$$

$$H + O_3 \rightarrow OH + O_2 \tag{46}$$

$$OH + O_3 \rightarrow HO_2 + O_2 \tag{47}$$

$$HO_2 + O_3 \rightarrow OH + O_2 + O_2 \tag{48}$$

In addition, Tang et al. [164] investigated the degradation of tetracycline (TC) antibiotic in dielectric barrier discharge system followed by addition of sodium percarbonate (SPC) as ROS promotor. Their study demonstrated that addition of small amount of SPC in the DBD reactor increased the production of reactive species, mainly hydroxyl and superoxide radicals that significantly contributed to the elimination of TC. Their outcomes indicated that the concentration of H_2O_2 (44.0 μmol/L) detected in the SPC + DBD synergy system surpassed the 38.1 μmol/L H_2O_2 measured in the DBD system alone. Alternatively, the authors reported that the concentration of O_3 2.1 mg/L quantified in DBD alone was higher than 1.8 mg/L O_3 measured in the synergic DBD + SPC system. Their results implied that the decrease of O_3 concentration in the synergic DBD + SPC system promoted the formation of H_2O_2. This was attributed to the O_3 disintegration to related matters such as $OH^.$ and O_2^- through a cascade of reactions shown in Eqs. (49)–(56).

$$O_3 + h\nu \rightarrow O_2 + O^{\bullet} \tag{49}$$

$$O_3 + H_2O + hv \rightarrow 2OH\cdot + 2O\cdot \tag{50}$$

$$O_3 + OH^- \rightarrow HO_2^- + 2O \tag{51}$$

$$O_3 + OH^- \rightarrow HO_2^- + O_2 \tag{52}$$

$$HO_2^- + O_3 \rightarrow OH\cdot + O_2 + O_2^- \tag{53}$$

$$O\cdot + H_2O \rightarrow 2OH\cdot \tag{54}$$

$$HO_2^- + H^+ \rightarrow H_2O_2 \tag{55}$$

$$O\cdot + H_2O \rightarrow H_2O_2 \tag{56}$$

Therefore, the study by Tang et al. [164] concluded that the hydrolysis of SPC in DBD configuration could substantially boost the generation of H_2O_2 that is the major source of $OH\cdot$; while the mechanistic chains of ozone destruction result in the production of O_2^- in the bulk solution which together accelerated the direct and indirect oxidation of TC in the DBD + SPC coupling approach. Furthermore, the destruction of O_3 to various ROS such as $^1O_2$ and O_2^- that play a crucial role in the direct inactivation of simulated S. Typhimurium bacterial wastewater in the DBD system was reported by Baek et al. [214]. In their research, the authors showed that the formation of $^1O_2$ and $O_2^{\cdot-}$ via decomposition of O_3 followed an avalanche of reactions shown in Eqs. (57)–(59).

$$O_3 + HO^- \rightarrow HO_2^- + O_2^{-} \tag{57}$$

$$HO_2^- + HO_2^- \rightarrow {}^1O_2 + H_2O_2 \tag{58}$$

$$HO_2^- + O_2^{\cdot-} + H^+ \rightarrow {}^1O_2 + H_2O_2 \tag{59}$$

Several investigations involving the disintegration of ozone in plasma systems leading to the production of secondary species for wastewater remediation have been widely reported [215–219]. From these reaction mechanistic trends, it can be inferred that the indirect reactions of O_3 in DBD geometries significantly participate in the decontamination of polluted water. For typical selected contaminants that O_3 cannot decompose directly, its disintegration to secondary species is crucial for the effective removal process.

4.7.5. Ozonation of water and wastewater at elevated pH values in DBD systems

For decades, ozone has been known as a potent oxidant that strongly reacts with various organic contaminants containing functional groups such as C=C, C=N, N=N. However, its reaction with functional groups such as C—C, C—O, O—H of single bonded compounds is very low [220]. Likewise, Staehelin and Hoigne [221] indicated that the reaction of ozone at elevated pH values is unselective. Hence, reacts with all organic and inorganic aqueous species. This was supported by Munter [222] who stated that increasing solution pH might increase the decomposition rate of ozone which often dissociates into superoxide anions radicals (O_2^-) and hydroxyperoxyl radicals (HO_2). In turn, the O_2^- generated reacts with O_3 to produce the ozonide anion O_3^- which further decays to $OH\cdot$ radicals in such a way that three ozone molecules produce two HO· radicals as shown in Eq. (60).

$$3O_3 + HO^- + H^+ \rightarrow 2HO\cdot + 4O_2 \tag{60}$$

The produced hydroxyl radicals have been proved non-selective and more potent oxidisers than ozone. This was verified by Munter [222] who showed that the hydroxyl radical rate constant is usually 10^6–10^9 times higher than the corresponding reaction rate constants of molecular ozone. Besides the decomposition processes of ozone in DBDs previously highlighted, ozone actively reacts with aqueous H_2O_2 to generate HO· radicals in a way that two molecules of ozone yield two hydroxyl radicals [183] as presented in Eq. (61).

$$2O_3 + H_2O_2 \rightarrow 2HO\cdot + 3O_2 \tag{61}$$

Hence, the generation of both ozone and OH· and their oxidative character in DBD aqueous configurations may relatively boost the degradation of the targeted contaminants.

4.7.6. Reactivity of ozone radical ion in DBDs

Even though the OH· radicals have been known as the strongest oxygen-based species, Buxton et al. [174] and Bratsch [223] showed that the ozone radical (O_3^-) with a standard reduction potential of $E_0 = 3.3$ V principally results from the interaction of oxygen radicals and molecular oxygen as shown in Eqs. (62) and (63). These authors stated that O_3^- could be a potent oxidant in acidic media.

$$O^- + O_2 \rightarrow O_3^- \tag{62}$$

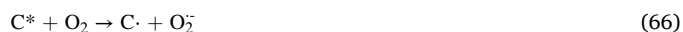$$O_3^- + 2H^+ + e^- \rightarrow O_2 \text{ (g)} + H_2O, E_0 = 3.3 \text{ V} \tag{63}$$
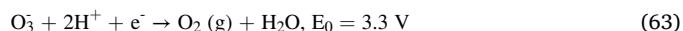
In addition to this, the generated ozone anion may oxidise water molecules to yield hydroxyl radical, a hydroxide anion, and oxygen as shown in Eq. (64).

$$O_3^- + H_2O \rightarrow OH + OH^- + O_2 \tag{64}$$

4.7.7. Interaction of catalyst with ozone in DBDs technologies

The photo-oxidation process is often characterised by the excitation of an electron from the valence (C) to the excited state (C*) by UV radiation (photon) as shown in Eq. (10). Furthermore, Legrini et al. [224] showed that the excited organic molecule may react with molecular oxygen to yield radical ions and cations that often recombine either by hydrolysis or homolysis to form new radicals that further react with oxygen and hence producing oxygenated substrates as shown in Eqs. (65)–(68).

$$C + hv \rightarrow C^* \tag{65}$$

$$C^* + O_2 \rightarrow C\cdot + O_2^- \tag{66}$$

$$R\text{-}X + hv \rightarrow R\cdot + X\cdot \tag{67}$$

$$R\cdot + O_2 \rightarrow RO_2 \tag{68}$$

In addition to this, Legrini et al. [224] highlighted that the quantum yield of the process, the photon rate at the wavelength of excitation, and the concentration of dissolved molecular oxygen may be the dependent factors of the oxidation process. Conversely, the authors claimed that complete mineralisation of the targeted pollutant could be achieved by a combination of photolysis with oxidising species such as H_2O_2, O_3, and/or semiconductors, particularly titanium dioxide as a catalyst. Since O_3 and H_2O_2 are produced in DBD systems, the addition of semiconductors photocatalysis may significantly improve the destruction of water contaminants. Consequently, the mechanistic pathways associated with the catalyst surface in decomposing the ozone in DBD technologies should be clarified.

4.7.7.1. Photocatalytic principle, mechanisms, and its integration with ozone in DBD configurations

Most semi-conductor photocatalysts such as TiO_2, ZnO, MgO deriving from transition metals have different properties. For instance, often characterised in rutile, anatase or amorphous phase to some extent and their band gap varies in different ranges [225]. For instance, the band gap of TiO_2 catalysts is usually encountered between 3.0 eV and 3.2 eV [226]. When a photon with energy exceeding this gap ($\lambda < 388$ nm) strikes the catalysts, electrons are excited and promoted from the valence band (V_b) of the catalyst to its conduction (C_b) leaving behind positive holes referred to as the electron-hole pairs ($e^- – h^+$) on the V_b as indicated in the schematic diagram shown in Fig. 11 earlier
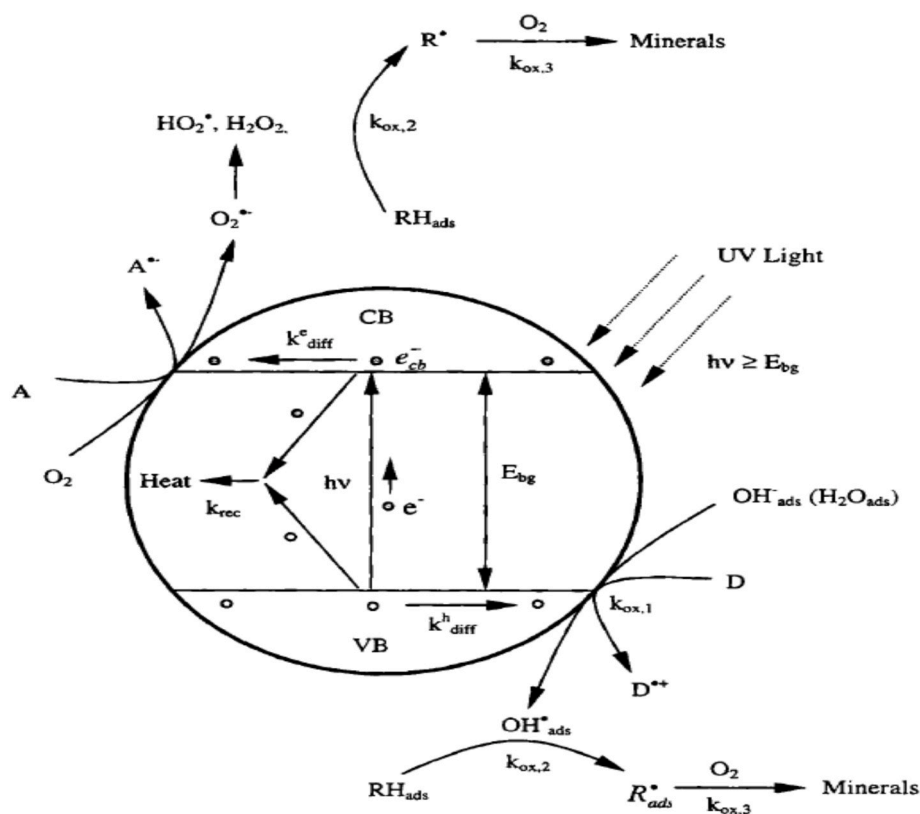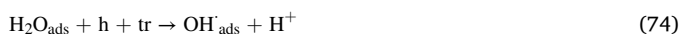
Fig. 11. Photocatalysis principle of spherical TiO$_2$ particle for the formation of electron–hole pair and reactions pathways in the production of ROS Chen et al. [227].

discussed by Chen et al. [227] and reinforced by Mouele et al. [228]. In the work by Gilmour [226], it was reported that the excited electrons, depending on their excitation energy/wavelength converge back to their original states and interact with positive holes releasing heat or could be trapped; else they mostly migrate to the surface of the catalyst and become solvated, and hence involved in series of oxidation and reduction reactions exhibited in Eqs. (69)–(72), where e$_{tr}$ indicates the trapped charge.

$$TiO_2 + hv \rightarrow e^-_{cb} + h^+_{vb} \tag{69}$$

$$e^-_{cb} + h^+_{vb} \rightarrow heat \tag{70}$$

$$E_{cb} \rightarrow e^-_{tr} \tag{71}$$

$$h^+_{vb} \rightarrow h^+_{tr} \tag{72}$$

At steady state, Lafi and Al-Qodah [229] reported that the number of electrons and positive holes moving to the surface becomes equal, this consequently renders the catalyst electrostatically stable. In this regard, the authors endorsed that the mineralisation of the contaminant happens either by oxidation reaction with the surface trapped holes, or by oxidation with hydroxyl radicals (OH$\cdot$), or with surface adsorbed water molecule and hydroxide ions that contribute to the generation of $\cdot$OH as shown in Eqs. (73)–(80), where ads stand for the adsorbed species.

$$D_{ads} + h^+_{tr} \rightarrow D + ads \tag{73}$$

$$H_2O_{ads} + h + tr \rightarrow OH\cdot_{ads} + H^+ \tag{74}$$

$$OH_{ads} + h + tr \rightarrow OH\cdot_{ads} \tag{75}$$

$$(O_2)_{ads} + e^- \rightarrow O_2^{\cdot -} \tag{76}$$

$$H+ + O_2^- \rightarrow HO_2^{\cdot} \tag{77}$$

$$2HO_2^{\cdot} \rightarrow H_2O_2 + O_2 \tag{78}$$

$$H_2O_2 + O_2^{\cdot -} \rightarrow OH\cdot + O_2 + OH^- \tag{79}$$

$$H_2O_2 + e^- \rightarrow OH\cdot + OH^- \tag{80}$$

From this sequence of Equations, Gilmour [226] underlined that because the surface holes take part in oxidation reactions, the charge equilibrium in the treatment system must be preserved. Consequently, dissolved oxygen could be used as electron scavenger so that it gets adsorbed onto the catalyst surface and reduced by the surface trapped electrons. Even though ozone may be produced via the association reaction of O$_2$ and O (Eq. (81)) or by other chemical routes, its interaction with the catalyst in the schematic in Fig. 11 may follow the same principle and mechanisms as those earlier described in Section 4.3.2 that are also expected to occur in processes detailed in Fig. 11.

$$O_2 + O \rightarrow O_3 \text{ association} \tag{81}$$

These result in various reactions and hence in the formation of diverse molecular and ionic species such as H$_2$O$_2$ that promote the production of OH$\cdot$, the powerful non-selective oxidant that mineralises the selected pollutants. The variety of ROS generated during photocatalysis have been extensively used for the removal of organic contaminants from water and wastewater [230–232]. Mouele et al. [1,32, 90] demonstrated that ozone is abundantly produced in DBD configurations reviewed in this text, and its formation and disintegration contributed to the generation of OH$\cdot$. So, both catalytic ozonation process earlier described in this paper and the photocatalytic principle illustrated in Fig. 11 are adequate procedures that synergically converge toward the production of OH radicals and related active species in DBD configurations for the successfully destruction of targeted pollutants. Though measuring the intensity of the UV radiation produced in DBD actuators has been one of the major challenges, incorporation of catalysts in DBD configurations inducing either catalytic ozonation or both photocatalysis and catalytic ozonation is a breakthrough in boosting the efficacy of DBD advanced treatment technologies. From this point of view, the combination of DBD systems with catalysts has been found an

effective route to enhance the concentration of reactive species, and hence the efficiency of DBD configurations for efficient degradation of water contaminants [233–237].

4.7.8. Removal of water contaminants by catalyst incorporated in DBD configurations

Based on the selective reactivity of ozone, some compounds such as atrazine may react poorly with ozone. Literature showed that oxidation of such substances could be accelerated by the incorporation of catalyst materials into the contaminated solutions [11,202,238]. In this way, numerous homogeneous catalysis including zinc and copper sulphates, silver nitrate, chromium trioxide, and heterogeneous catalysts such as Ru/CeO_2, MnO_2, TiO_2/Al_2O_3, and Pt/Al_2O_3 have been used [239–241]. The studies showed that both homogeneous and hetero photocatalysts in DBDs could expand the decomposition efficiency of diverse organic compounds in the presence of ozone in DBD aqueous media. Similarly, in case agglomeration of by-products occurs during the degradation of organic contaminants in DBD configurations, it has been advised that reasonable amounts of non-toxic catalysts could be incorporated to enhance the removal process [141,155,202]. For instance, Zhang et al. [242] studied the degradation of acetaminophen (APAP) by DBD combined with reduced graphene oxide (rGO) and P25-TiO_2. The authors found that the addition of rGO in the DBD system boosted the removal percentage of APAP from 50% to 92% after 18 min of plasma irradiation compared to solely plasma or plasma combined with P25-TiO_2. The results of the study conducted by Zhang et al. [242] also showed that the degradation of APAP was induced by two reactive species including O_3 and OH$^.$. Likewise, the decomposition of APAP with each oxidant followed a separate pathway but both routes resulted in simpler linear aliphatic and unsaturated degradation by-products even if their complete mineralisation into the water and dissolved CO_2 was not mentioned. Apart from this, the reaction mechanism of O_3 and OH reactions with APAP were not defined. A similar study was carried out by Aziz et al. [243] who successfully investigated the degradation of two non-steroidal anti-inflammatory drugs (NSAIDs) diclofenac (DCF) and ibuprofen (IBP) by the ozonation process and by other three aqueous systems including, photocatalytic ozonation, photocatalytic oxidation and non-thermal dielectric barrier discharge (DBD). Aziz and co-workers showed that the addition of Fe^{2+} to the DBD run in an argon atmospheric aqueous media improved the degradation efficiency of the NSAIDs due to the Fenton reaction. Nevertheless, the best mineralisation efficiency assessed by TOC removal was achieved by photocatalytic ozonation in a DBD/Ar/O_2 atmospheric plasma system. Besides, Xin et al. [244] investigated the degradation of triclosan (TCS) in an aqueous solution by dielectric barrier discharge combined with activated carbon fibres (ACFs). The results of their study showed that 85% of TCS removal was achieved with DBD alone and 93% with DBD combined with ACFs after 120 min of plasma treatment. Likewise, the mineralisation of TCS (12%) reached at pH 6.26 was improved to 24% at pH 3.5. Furthermore, the decomposition of TCS mainly induced by the direct reaction of OH led to numerous aromatic degradation intermediates which by ring opening pathway were oxidised to carboxylic acids that were mineralised to H_2O, dissolved CO_2, and harmless inorganics. Furthermore, Wang et al. [245] studied the degradation of triclocarban (TCC) in aqueous solution by dielectric barrier discharge (DBD) plasma combined with TiO_2 coated activated carbon fibres (TiO_2/ACFs) catalysts. The outcomes of their experiments showed that the incorporation of TiO_2/ACFs into the DBD reactor increased TCC degradation efficiency by 12% compared to the single DBD actuator. On the other hand, the study highlighted that after 30 min of plasma reaction, the combined DBD/TiO_2/ACFs system lessened the toxicity of TCC from 64% to 32%. Wang et al. [245] showed that the degradation of TCC principally induced by O_3 and OH$^.$, probably by epoxidation and direct attack, resulted in various substituted nitro halides and alcohol degradation intermediates that were further mineralised into H_2O and CO_2. Even though Mouele et al. [90] showed that

during DCDBD run, the initial pH (acidic or basic) decreased with an increase of treatment time, Beltran et al. [240] and Xin et al. [244] pointed out that addition of catalysts in DBD reactors could also lower solution pH to more acidic media. This consequently may not only improve the degradation efficiency of compounds such as pharmaceuticals but enhance the removal of their total organic carbon (TOC) as well. In addition, Tijani et al. [12] studied the degradation of 2-nitrophenol (2-NP) by air DCDBD alone and in combination with TiO_2 supported on stainless steel mesh. In their report, the authors showed that high removal of 2-NP was achieved in acidic conditions at pH 3. Likewise, during DCDBD experiment without catalyst, all initial solution pH set at acidic or basic values decreased with increase of treatment time and fell below 6. A similar trend was observed when supported TiO_2 catalyst was incorporated DCDBD reactor. These indicate that addition of catalysts in air DBD systems does not impact on the solution pH, however, different observations could be rated when other gases such as pure oxygen (O_2), argon (Ar) or helium (He) are used as feed gases. Therefore, solution pH should carefully be optimised to achieve maximum decomposition of targeted pollutants. Several studies focusing on the removal of organic pollutants using DBDs configurations alone or in combination with catalysts have been conducted [246–250]. These investigations showed that the removal efficiency of contaminants by DBD combined with a catalyst was enhanced as compared to that of DBD alone. Nevertheless, they claimed that the type and the dose of catalysts being added should be controlled because at saturated state, they can impact on the degradation efficiency of targeted pollutants. Moreover, they argued that the operational costs of DBD and DBD assisted catalytic degradation processes should also be investigated. Considering the energy yield factor, Ansari et al. [250] outlined that the energy yield of DBD/catalysts was higher than that of DBD alone. This implied that the integration of catalysts in DBD configurations is a promising route that could result in economical, sustainable, and environmentally benign treatment protocols.

4.7.9. Extended reactions of ozone in DBD configurations

Glaze [175] and Munter [222] reported that the rate of production of free reactive species in aqueous solutions could considerably be improved by combining UV light and ozone/hydrogen peroxide (UV/O_3, UV/H_2O_2) or by the combination of both (UV/O_3/H_2O_2). This is because the adsorption of UV radiation by ozone at a wavelength of 254 nm results in the formation of hydrogen peroxide as an intermediate, which further decomposes to hydrogen peroxide radicals as shown in Eqs. (82) and (83), respectively.

$$O_3 + hv \rightarrow O_2 + O(^1D) \tag{82}$$

$$O(^1D) + H_2O \rightarrow H_2O_2 \rightarrow 2HO\cdot \tag{83}$$

In turn, H_2O_2 is cleaved off into OH$^.$ radicals as shown in Eq. (45). The authors also mentioned that in pH dependent circumstances, aqueous H_2O_2 solution and HO_2^- may also absorb UV radiation at 254 nm to form a hydroxyl radical as shown in Eqs. (84)–(86), correspondingly.

$$H_2O_2 + hv \rightarrow 2HO\cdot \tag{84}$$

$$H_2O_2 \leftrightarrow HO_2^- + H^+ \tag{85}$$

$$HO_2^- + hv \rightarrow +HO\cdot + O\cdot^- \tag{86}$$

During the plasma discharge process, apart from solvated electrons and Pandit [220] specified that the mixture of UV/O_3/H_2O_2 may strongly oxidise and attack recalcitrant pollutants in DBD configurations. The interaction of ozone with organic pollutants could be direct or indirect depending on the neutral or alkaline pH conditions. In an acidic medium, ozone reacts directly as an electrophile with aromatic and unsaturated alkenes leading to the formation of ozonide intermediates

which by ring cleavage result in the formation of zwitterion, aldehyde, or a ketone [187]. In turn, the zwitterion is hydrolysed to hydroxyalkyl hydroperoxide in an aqueous solution as shown in Fig. 12.

Likewise, Baily [251] showed that the hydroxyalkyl hydroperoxide may decay to yield aldehyde or a ketone by the elimination of hydrogen peroxide, alternatively rearrangement to carboxylic acids may take place depending on the substituents. On the other hand, the reaction of O_3 with olefins often leads to epoxides/peroxidation which further by hydrolysis may result in reduced chains of aliphatic compounds after a certain period. These hydrolysed by-products may seem harmless; however, a prolonged treatment time could lead to either their recombination that results in agglomerated bulky new substances that might be more dangerous than the starting materials, or to their complete mineralisation [100,167,239]. Therefore, the toxicity of the resulting by-products requires serious investigation.

Furthermore, water and wastewater contain both microorganisms and harmful contaminants [1]. From a hygienic point of view, these impurities are harmful to people causing diseases, irritations, and eczema, hence the necessity for their removal by disinfection or oxidation processes [251–256]. For several years, ozone has been used as a principal disinfectant for the removal of water contaminants [102]. The disinfection process refers to the purification of water streams to the extent that the aqueous impurities become inactive to consumers including humans, animals, and plants that come to contact with the water. Ozone, having a high oxidation potential of 2.07 V has been found potent to oxidise cell components of the bacterial cell wall [102]. The cell oxidation process is often initiated by penetration. After ozone enters the cell, components such as enzymes, proteins, DNA, RNA are immediately oxidised. So, after the cell membrane has been damaged, it falls apart and the process is known as lysis [223,257]. Thus, the common steps encountered during disinfection of bacteria by ozone include 1) penetration of a bacterial cell, 2) via attachment of ozone molecule on the bacterial cell wall, 3) ozone penetrates the cell wall and causes corrosion, 4) cell destruction (lysis) takes place [223,257]. These consequently show that ozone with numerous other active species produced in DBD systems can be effectively employed for the treatment of polluted water.

4.8. Hydroxyl radical and its reactivity towards persistent organic compounds in DBD reactors

Among the various oxidisers generated in AOPs as previously highlighted, OH radicals with a reduction potential of E = 2.80 V appear to be the most powerful non-selective species, predominantly produced in acidic conditions. Hydroxyl radicals being the most powerful and non-

selective free radical is often the final product aimed at in most AOPs. Based on their high reactivity and an oxidation rate constant of 10^8–10^{11} $M^{-1}\,s^{-1}$, the lifetime of OH radicals in aqueous media is often estimated in the range of 1–2 ns, corresponding to a diffusion radius of about 20 Å [174,258]. Hydroxyl radicals interact with various organic compounds that are mineralised into CO_2, water, and harmless organic and inorganic end products [222]. In non-thermal plasma (NTP) technologies induced by DBD, as in any other AOPs OH· radicals react with organic pollutants in four different ways. These include hydrogen abstraction, radical addition, electron transfer, and radical combination [182]. During hydrogen abstraction scenario in DBD systems, acidic H atoms are removed from the pollutant frame chain leading to the formation of water and unstable intermediates which by further chemical conversions are directly mineralised into dissolved CO_2, H_2O, and simpler entities. The radical addition involves the attachment of OH radical as a nucleophile on the pollutant. The last two reactions of OH radicals with organic pollutants implicate electron transfer and radical recombination. During these chemical interactions, OH radicals react either by hydrogen abstraction or deactivation of pollutants leading to bond cleavage and hence to the mineralisation of contaminants [182]. Although the OH radical reactions have been singly discussed in the next paragraphs, it is important to mention that the non-selectivity property of OH has given rise to the development of various AOPs which converge towards the production of huge amounts of OH radicals. Therefore, the efficiency of a typical AOP such as DBD would depend on the amount of OH produced. Atomic oxygen, with an oxidation potential of 2.4 V acts as a powerful oxidant in aqueous media and extensively participates in the production of O_3 and H_2O_2. Hydrogen peroxide with a reduction potential of 2.2 V appears as the recombination product of OH radicals and hence is one of the primary precursors of OH radicals in aqueous systems.

4.8.1. Hydrogen abstraction and radical addition reactions of OH in DBD configurations

During the hydrogen abstraction process, hydroxyl radicals often remove hydrogen from organic compounds resulting in the formation of radical organic compounds that can initiate a reaction chain in which the produced organic radicals interact with oxygen, generating peroxyl radicals that subsequently react with another organic substance and so forth as presented in Eq. (87).

$$R + HO\cdot \rightarrow R\cdot + H_2O \tag{87}$$

The abstraction of the hydrogen atom by the OH· radical from a saturated hydrocarbon chain, yielding radical sites was also highlighted
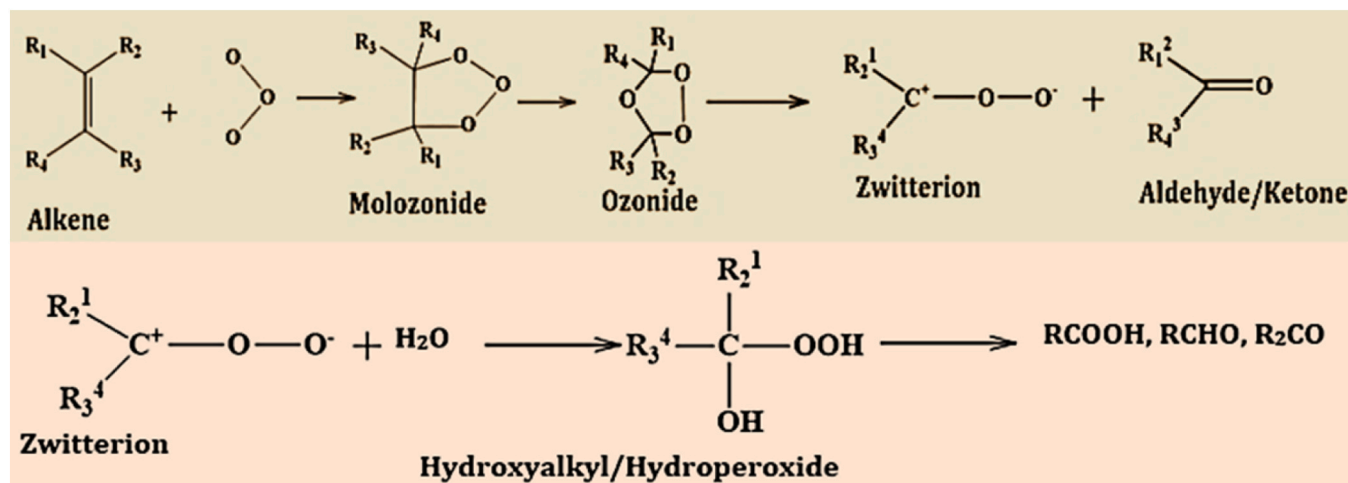

Fig. 12. The reaction of ozone with an unsaturated bond of an alkene or an aromatic compound [184].

by Hoeben [182]. According to the author, the radical sites created on the hydrocarbon framework after hydrogen abstraction, initiate oxygen attack. The interaction of oxygen on these sites leads to the formation of hydroperoxyl radicals and unsaturated compounds which further get cleaved by ozone as shown in Fig. 13.

In the radical addition reaction category, hydroxyl radicals react with unsaturated/aliphatic molecules to generate organic radical intermediates which further produce stable oxidised by-products by reaction with oxygen or ferrous iron as shown in Eq. (87a).

$$R + HO\cdot \rightarrow ROH \tag{87a}$$

For instance, Hoeben [182] stated that OH attack in unsaturated compounds focuses on regions governed by high electron density. In this regard, Pan and Schuchmann [257] and Von Sonntag [259] conveyed that the OH radicals add themselves to the double bonds of alkenes and aromatic molecules leading to the formation of hydroxycyclohexadienyl radicals. These later interact with molecular oxygen to yield endoperoxalkyl and endoperoxyl radicals. The endoperoxyl radicals in turn produce endoperoxides as shown in Fig. 14.

Since endoperoxides are unstable molecules, they likely undergo decomposition by ring- cleavage yielding unsaturated aliphatic hydrocarbons containing various functional groups such as aldehydes, carboxyls, carbonyls, or alkanols. Furthermore, the authors sustained that a slight amount of generated carbon monoxide formed during these reactions may get used up. Moreover, Hoeben [182] demonstrated that the hydroxyl radical and oxygen attack on alkene generate hydroxyalkylperoxyl radical intermediates. Hydroxyalkylperoxyl radicals were further proved to oligomerise (dimerise) hence forming tetraoxide metabolite. This in turn may decay in different routes, among which the fragmentation reaction that mostly produces carbonyl (aldehydes/ketones), α-hydroxyalkyl radicals, and oxygen. Von Sonntag [259] and Getoff [260] confirmed that the α-hydroxyalkyl radical reacts with molecular oxygen yielding an α-hydroxyalkylperoxyl radical which further produces an aldehyde or a ketone by the elimination of hydroperoxyl radicals as shown in Fig. 15.

4.8.2. Electron transfer reaction and radical combination reactions of OH in DBD systems

The electron transfer attack of OH in DBD systems is usually associated with the formation of ions with a greater valence. Indeed, the oxidation of a negative ion may produce an atom or a free radical. This case has been summarised in Eq. (88).

$$R^{n+} HO\cdot \rightarrow R^{n-1} + HO^- \tag{88}$$

Alternatively, the radical recombination reaction in DBD configurations is based on the combination of two OH radicals that may form a molecule such as a peroxide as presented in Eq. (89)

$$HO\cdot + HO\cdot \rightarrow H_2O_2 \tag{89}$$

Based on these different OH attacks, Ternes [261] confirmed that the

interactions of OH radicals with organic compounds in water commonly result in carbon dioxide and innocuous salts. Nevertheless, in the presence of dissolved oxygen, OH radical attacks repeatedly induce various oxidation reaction sequences whose complete mineralisation reaction mechanistic pathways have not been fully understood. For instance, chlorinated organic compounds in DBD actuators may primarily be oxidised into breakdown intermediates such as aldehydes and carboxylic acids which are further converted into carbon dioxide, water, and chlorine [222]. The extended hetero atoms such as nitrogen, phosphorous, and sulphur present in parent halogenated compounds are often removed or are directly converted to inorganic ionic species such as halides, nitrates, phosphates, and sulphates which consequently induce the reduction in solution pH. A typical case is shown in Fig. 16 where dichloromethane is oxidised by hydroxyl radicals and oxygen, producing carbon monoxide, carbon dioxide, and hydrogen chloride.

According to Von Sonntag [259] and Getoff [260], the carcinogenic phosgene is hydrolysed to carbon dioxide and hydrogen chloride. In the case of natural water, the formation of bicarbonate and carbonate that are known as OH· radical scavengers as presented in Eqs. (90) and (91) may significantly reduce the degradation efficiency of organic pollutants. The carbonate radical anion produced during the scavenging process is also an oxidising agent whose oxidation potential is less effective than that of OH· radicals [224].

$$HO\cdot + HCO_3^- \rightarrow H_2O + CO_3^{\cdot-} \tag{90}$$

$$HO\cdot + CO_3^{2-} \rightarrow HO^- + CO_3^{\cdot-} \tag{91}$$

Even though OH radicals non-selectively attack organic pollutants in DBD configurations, the reaction rate constant for the decomposition of chlorinated compounds is fast and predominates because of the presence of the double bond that is susceptible to hydroxyl attack. By comparison, oxidation of saturated compounds, mainly alkanes, is more difficult because their reaction rate with hydroxyl radicals is very low. Overall, the oxidation supremacy of OH· radicals give advanced oxidation processes the capability to completely decompose ozone and hydrogen peroxide refractory molecules.

4.8.3. Disinfection by OH-radicals in DBD technologies

As previously described, OH radicals are usually produced in aqueous media and largely contribute to the disinfection of various categories of microorganisms [176]. Unlike ozone, OH radicals are short-lived and non-selective reactive species that are often used up inside bacteria cell walls. These radicals have significant derivative effects toward disinfection resistant microorganisms. A typical example is the protozoa *Cryptosporidium parvum oocyst* that slowly reacts with ozone but is quickly decomposed by OH radicals. Based on this fact, it is believed that OH radicals considerably assist ozone in the disinfection process during advanced oxidation induced by DBDs. The disinfection properties of OH radicals towards microorganisms are only applicable to resistant protozoa and not to microorganisms that react quicker with ozone.
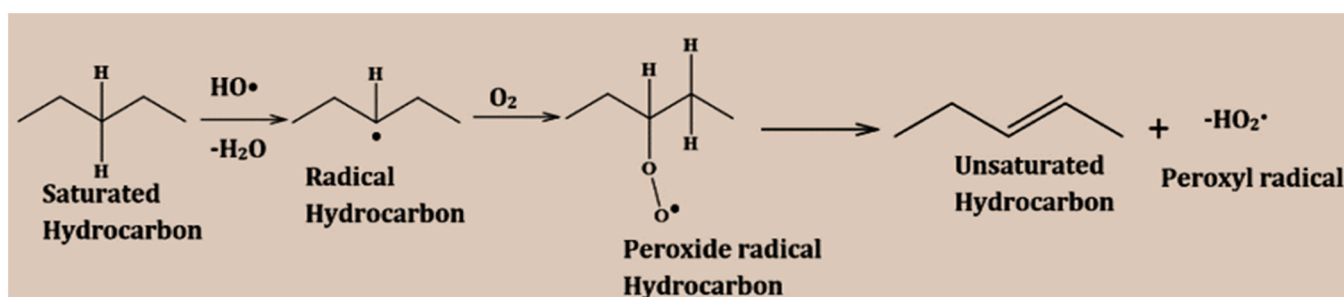

Fig. 13. Hydroxyl radical hydrogen abstraction from a saturated hydrocarbon chain followed by oxygen attack [182].
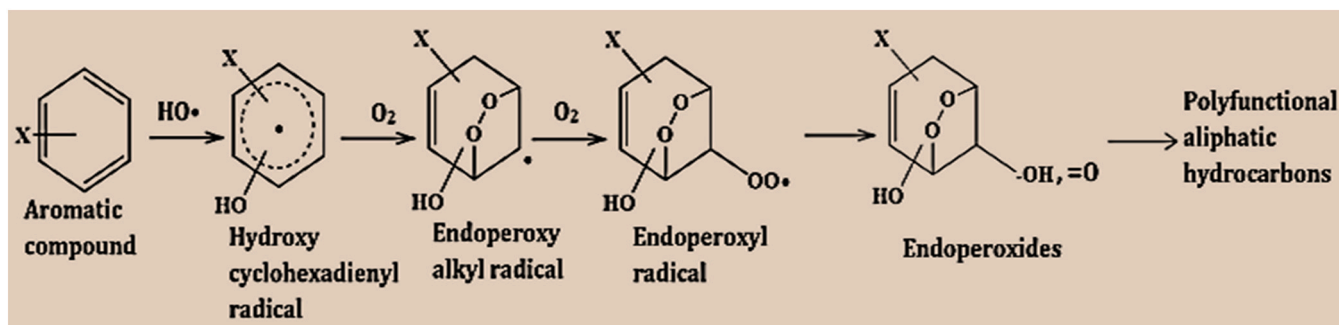
Fig. 14. Reactivity of hydroxyl radical and molecular oxygen on aromatic compounds yielding endoperoxides and polyfunctional unsaturated aliphatic hydrocarbons [184].
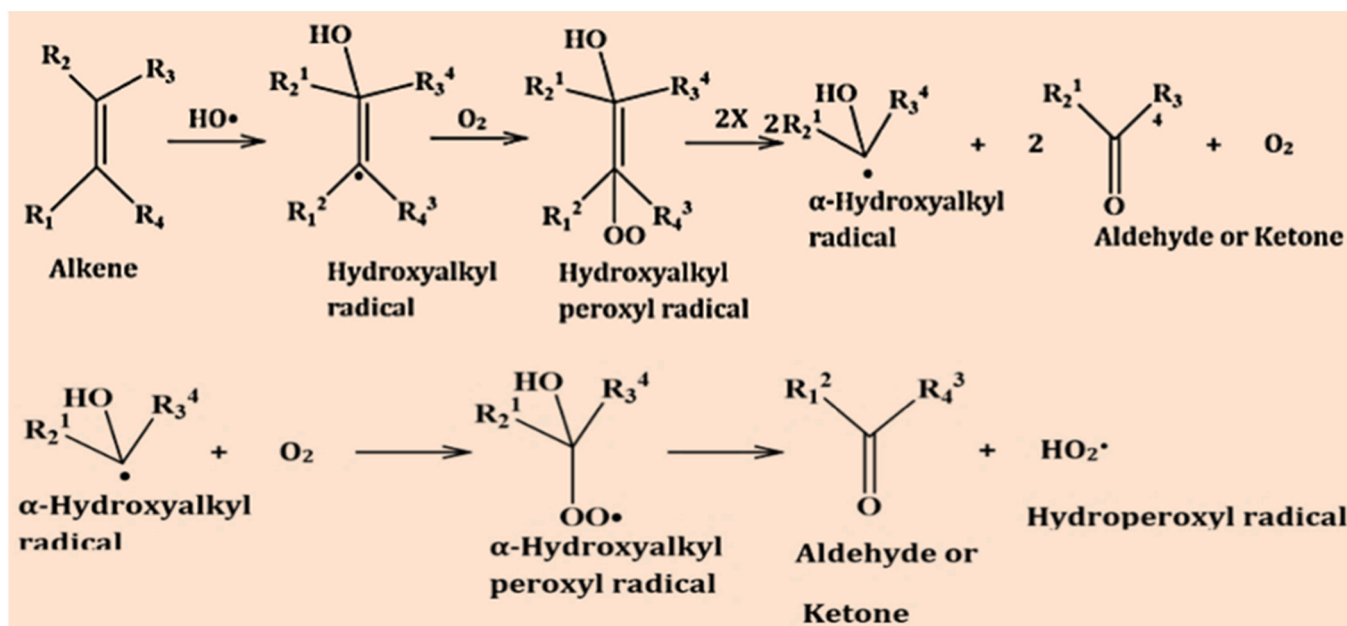

Fig. 15. Reaction attacks of a hydroxyl radical and oxygen on alkenes [182].
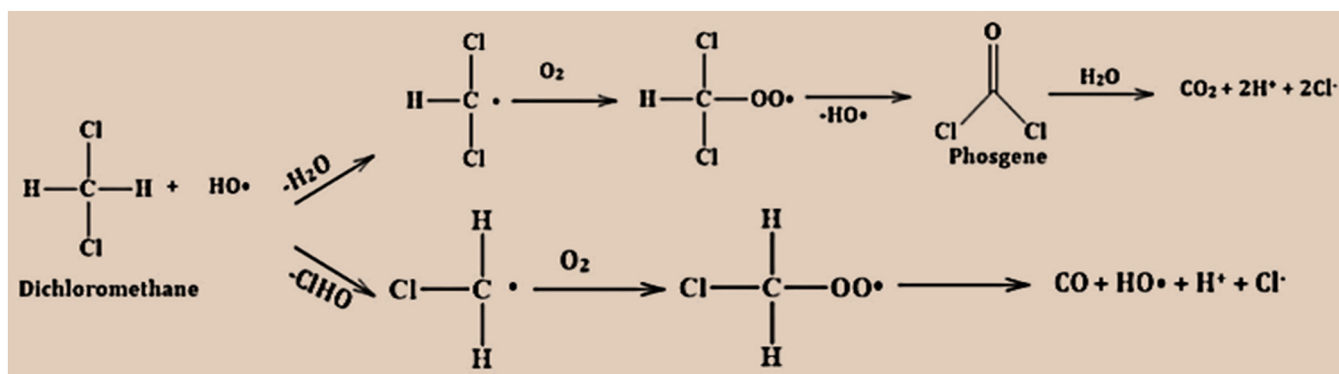

Fig. 16. Oxidation of dichloromethane by hydroxyl radicals and oxygen [182].

In summary of this section, ozone being one of the most utilised oxidants for water purification follows various reaction mechanisms or reaction pathways due to the existence of various reaction sites on organic pollutants. From the literature reviewed in this text, it could be remembered that the reaction of ozone towards microorganisms (bacteria and viruses) begins with the penetration of ozone into the cell membrane, followed by oxidation of cell components and its lysis. On the other hand, ozone reactions with organic pollutants via two categories which include direct and indirect reactions. Direct reactions occurring in acidic media begin with cycloaddition which is a process during which ozone interacts with olefins to yield epoxides. In acidic or basic conditions, epoxides may be broken down by cleavage leading to the formation of simpler by-products. The cycloaddition is followed by an electrophilic reaction during which ozone interacts with phenolic

compounds yielding various carbonyl substances such as aqueous carboxylic acids. Finally, the nucleophilic reaction appears as the third interaction of ozone with organic pollutants. In this step, ozone behaves as an electron provider and may react with compounds carrying electron withdrawing groups such as –COOH and – NO_2 resulting in short-chain organics and inorganics. Conversely, during the indirect reaction of ozone, three major interactions among which initiation, radical chain-reaction, and termination have been reported. In these three processes, O_3 behaves either as a precursor of various free radicals such as $OH^{\cdot}$, H_2O, $O_2^{\cdot-}$, etc. or O_3 gets decomposed via interaction with other chemical species such as H_2O, H_2O_2, etc. forming new radicals such as HO_2, $OH^{\cdot}$, $O_2^{\cdot-}$, $O^{\cdot}$, etc. that may directly or indirectly attack the targeted pollutants. Furthermore, ozone can be exposed to UV-light to induce photolysis, yielding new ROS. Ozone can also be combined with catalysts and UV light to initiate photocatalytic phenomena. Most of these combinations are referred to as advanced oxidation processes (AOPs) induced in DBD configurations. Since UV light and most free radicals are generated directly in DBD systems, therefore DBD configurations could be considered as effective integrative water treatment methods. Consequently, O_3 and co-oxidants such as H_2O_2, $OH^{\cdot}$, HO_2, O_2, etc., produced in DBD geometries, contribute directly or indirectly to the decomposition of pharmaceutical pollutants (PPs). Hence understanding their interaction mechanisms with PPs is mandatory.

4.9. Reactivity of hydrogen peroxide in DBD configurations

Hydrogen peroxide (H_2O_2), which is habitually considered as a recombination product of OH radicals, has an ineffective reactivity compared to that of its precursor OH radicals [177,178]. In acidic media, H_2O_2 has a reduction potential of $E_0 = 1.76$ V. Its photolysis decomposition (Eq. (94)) yields hydroxyl radicals whereby the dissociation of the OH—OH bond requires 213 ± 4 kJ/mol which is the same as 2.2 eV [178,182]. On the contrary, H_2O_2 may instantaneously oxidise and reduce itself; the decomposition of concentrated H_2O_2 into water and oxygen (Eq. (95)) is an exothermic reaction that releases up to 98.3 kJ/mol. In addition to this, Moeller [262] showed that H_2O_2 is a weak acid with a decomposition constant pKa = 11.75 as shown in Eq. (92).

$$H_2O_2 + H_2O \rightarrow H_3O^+ + HO_2 \tag{92}$$

Mouele et al. [90] investigated the production of H_2O_2 in a double cylindrical DBD reactor. The authors proved that the highest concentration 0.933 mol/L of H_2O_2 was achieved at pH 10.5 after 5 min of time on streamer However, the authors reported that within 60 min of plasma experiment in both acidic and basic conditions, H_2O_2 concentration fluctuated down to 0.613 mol/L and rose back to the primary amount. The observed variations were attributed either to the self-decay (Eq. (93)), photodecomposition to H^+, H_2O^-, and $OH^{\cdot}$ (Eqs. (93) and (94)), or H_2O_2 was involved in side reactions leading to the formation of various reactive oxygen species such as HO_2, OH^-, O_2^-, etc. as indicated in Eqs. (95)–(101).

$$H_2O_2 \rightarrow H^+ + H_2O^- \tag{93}$$

$$H_2O_2 + h\upsilon \rightarrow 2OH^{\cdot} \tag{94}$$

$$O_3 + H_2O_2 + OH^- \rightarrow OH + HO_2 + O_2 + OH^- \tag{95}$$

$$H_2O_2 + OH \rightarrow H_2O + HO_2 \tag{96}$$

$$H_2O_2 + H \rightarrow H_2O + OH \tag{97}$$

$$H_2O_2 + H^+ \rightarrow HO_2 + H_2 \tag{98}$$

$$H_2O_2 + O_2 \rightarrow 2HO_2 \tag{99}$$

$$H_2O_2 + O^- \rightarrow H_2O + O_2 \tag{100}$$

$$H_2O_2 + OH \rightarrow H_2O + H^+ + O_2^- \tag{101}$$
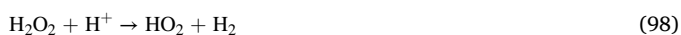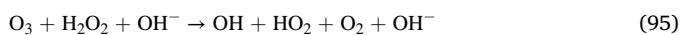
These chains of reactions demonstrate that H_2O_2 is one of the most important species produced in plasma technologies and plays a crucial role in generation of the secondary species. Most of these reactions have been summarised by Gupta [2] and supported by Ullmann [263] and Kirk and Othmer [264]. In a system with less OH^- scavengers, Gupta [2] and Sahni and Locke [265] conveyed that excess of H_2O_2 can scavenge OH radicals produced in the bulk solution according to Eqs. (102) and (103).

$$H_2O_2 + 2O_3 \rightarrow 2OH^- + 3O_2 \tag{102}$$

$$OH^- + H_2O_2 \rightarrow H_2O + HO_2 \tag{103}$$

Huang and Fang [266] highlighted that UV-radiation generated in DBD reactors can decompose H_2O_2 yielding $HO^{\cdot}$ as indicated in Eq. (104).

$$H_2O_2 + h\upsilon \rightarrow 2OH^- \tag{104}$$

In addition, the O_3 diffused in the bulk may react with accumulated H_2O_2 and further produce OH radicals (Eq. (105)); this reaction is often referred to as peroxonation process.

$$O_3 \text{ (aq)} + H_2O_2 \rightarrow O_2 \text{ (aq)} + OH^- + HO_2 \tag{105}$$

Mouele et al. [90] emphasised that, though H_2O_2 does not directly destroy targeted pollutants, it largely contributes to the generation of various reactive species.

4.10. Hydroperoxyl radical interactions in DBDs

The hydroperoxyl radical (HO_2) with a standard reduction potential of $E_0 = 1.44$ V in acidic media has been proved less effective than O_3, H_2O_2, and OH radicals but is slightly stronger than chlorine.

This weak free radical is usually formed via hydrogen atoms that derive directly from the decomposition of water molecules (Eq. (106)). Likewise, Patai [267] noted that in an alkaline environment, HO_2 occurs as the superoxide radical ion O_2^- as presented in Eq. (107). Also, literature supported that HO_2 auto reacts to generate H_2O_2 as shown in Eq. (108). Conversely, the decomposition constant of HO_2 is about pKa = 4.4 in an aqueous environment.

$$H_2O \rightarrow H + OH \tag{106}$$

$$HO_2 + OH^- \rightarrow O_2 + H_2O \tag{107}$$
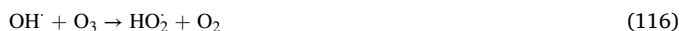
$$2HO_2^{\cdot} \rightarrow H_2O_2 + O_2 \tag{108}$$

Furthermore, the per-hydroxyl radical (HO_2) occurring as the superoxide radical (O_2^-) in alkaline media is a precursor of H_2O_2 which, by dissociation, generates OH radicals. Baek et al. [214] reported that the O_3 dissolved in the bulk is often unstable and may result in a sequence of reactions such as its interaction with hydroxide ion (OH^-) producing hydroperoxyl radical (HO_2) and super oxide ion (O_2^-) which majorly contribute to the generation of atomic oxygen ($^1O_2$) and H_2O_2 as shown in Eqs. (109)–(111).

$$O_3 + HO^- \rightarrow HO_2^- + O_2^- \tag{109}$$

$$HO_2^- + HO_2^- \rightarrow {}^1O_2 + H_2O_2 \tag{110}$$

$$HO_2^- + O_2^- + H^+ \rightarrow {}^1O_2 + H_2O_2 \tag{111}$$

Kovačević et al. [268] demonstrated that the interaction of atomic hydrogen with water molecule in the bulk initiate a series of reactions that lead to the formation of hydroperoxyl radicals whose recombination results in the production of co-species including hydroxyl radicals as shown in Eqs. (112)–(119). Nevertheless, the authors indicated that in acidic conditions (pH < 6), these processes might be slow but could accelerate when the solution pH is above 5. Likewise, Ma et al. [269] sustained that HO_2 can also be produced via the reaction of $OH^{\cdot}$ and O_3

in the bulk yielding various species through chains of reactions (Eqs. (112)–(119)).

$$H^. + OH_2 \rightarrow HO_2^. \tag{112}$$

$$HO_2^. + HO_2^. \rightarrow H_2O_2 + O_2 \tag{113}$$

$$O_3 + HO_2^- \rightarrow O_3^{.-} + HO_2^. \tag{114}$$

$$O_3^{.-} + H_2O \rightarrow OH^. + OH + O_2 \tag{115}$$

$$OH^. + O_3 \rightarrow HO_2^. + O_2 \tag{116}$$

$$HO_2^. + O_2^. \rightarrow HO_2^. + O_2 \tag{117}$$

$$O_3 + O_2^. \rightarrow 2OH^. + 2O_2 \tag{118}$$

$$3O_3 + OH^. + H^+ \rightarrow 2HO^. + 4O_2 \tag{119}$$

4.11. Reactivity of atomic oxygen in DBD configurations

Atomic oxygen (O$^.$), another powerful oxidant, is often produced by irradiation of O$_2$ with dissociation energy of 498.4 kJ/mol equivalent to 5.2 eV [216,270]. Lide [178] and Hoeben [182] claimed that in an acidic milieu, atomic oxygen is a powerful oxidant with an oxidation potential of $E_0 = 2.43$ V, higher than that of ozone. However, its instability makes its lifetime extremely short and often difficult to quantify. Conversely, Aziz et al. [216] and Moeller [262] reported that atomic oxygen in the gas phase contributes to the generation of ozone by reaction with molecular oxygen at an activation energy of Ea $= 16.7$ kJ/mol. Apart from this, Tang et al. [93] and Wang et al. [245] also highlighted that in aqueous solutions, atomic oxygen participates in the formation of OH$^.$ and H$_2$O$_2$ according to Eqs. (120)–(122) via oxidation of water molecules.

$$e^- + O_2 \rightarrow O^. + O^. + e^- \tag{120}$$

$$O^. + H_2O \rightarrow 2OH^. \tag{121}$$

$$O^. + H_2O \rightarrow H_2O_2 \tag{122}$$

Gupta [2] suggested that the reaction between dissolved O$_3$ and UV-radiation leads to the disintegration of ozone to atomic oxygen (O) and oxygen (O$_2$) (Eq. (123)) and H$_2$O$_2$ (Eq. (124)). The atomic oxygen further interacts with water molecules and yields OH radicals as previously shown in Eq. (120).

$$O_3 + h\nu \rightarrow O^. + O_2 \tag{123}$$

$$O_3 + h\nu + H_2O \rightarrow H_2O_2 + O_2 \tag{124}$$
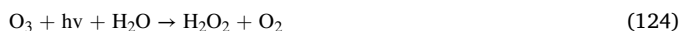
On the other hand, Massima [6] showed that solvated electrons can dissociate O$_2$ molecule to produce atomic oxygen (Eq. (125)) which in return converts water molecule to OH$^.$ (Eq. (121)) and reacts with dissolved oxygen to yield O$_3$ (Eq. (126)).

$$O_2 + e^- \rightarrow 2O \tag{125}$$

$$O^. + O_2 \rightarrow O_3 \tag{126}$$

4.12. Impact of superoxide anion in DBD technologies

The superoxide anion (O$_2^-$), another reactive oxygen species produced in DBD reactors with an oxidation potential of 1.44 V, has a short half-life of 10^{-6} s therefore, impedes its quantification in DBD systems. To the best of our knowledge, literature presents little information on the direct reaction of O$_2^-$ with organic contaminants. Giannakis [253] claimed that O$_2^-$ somehow shows antibacterial properties, but the mechanisms of its interaction with bacteria and viruses have not been

well elucidated. Nevertheless, in DBD protocols, the aqueous O$_2^-$ results from various reactions including the disintegration of HO$_2$ [271] as shown in Eqs. (127)–(132). The interaction of dissolved oxygen and highly energised/solvated electrons [272] majorly contributes to the production of OH radicals and other species via collision with H$_2$O molecules as disclosed in Eq. (60). This phenomenon has commonly been reported in other advanced oxidation processes [88,90], hence making O$_2^-$ one of the common OH radical precursors.

$$O_3 + OH \rightarrow HO_2^. + O_2 \tag{127}$$

$$O_3 + HO_2^. \rightarrow OH \, O_2^- + O_2 \tag{128}$$

$$HO_2^. + O_3 \rightarrow HO_2^. + O_3^- \tag{129}$$

$$HO_2\{Reciprocal\} \rightarrow O_2^- + H^+ \tag{130}$$

$$O_2^- + O_3 \rightarrow O_2 + O_3^- \tag{131}$$

$$H_2O_2 + O_2^- \rightarrow OH + OH^- + O_2 \tag{132}$$
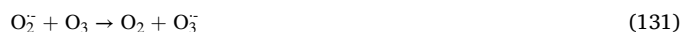
Gupta [2] supported that in aqueous media, solvated electrons (e$_{aq}^-$), atomic hydrogen (H$^.$) and super oxide radical anions (O$_2^-$) are the common reductive species generated underwater in non-thermal plasma discharges. In DBD aqueous media, the solvated energised electrons interact with dissolved oxygen resulting in the formation of super oxide ions (O$_2^-$). Alternatively, H$^.$ readily reacts with O$_2$ producing hydroperoxyl radicals (HO$_2$) that can alter to O$_2^-$ in neutral pH environment according to Eqs. (133)–(135).

$$e_{aq}^- + O_2 \rightarrow O_2^- \tag{133}$$

$$H^. + O_2 \rightarrow HO_2^- \tag{134}$$

$$HO_2^. \rightarrow O_2^- + H^+ \tag{135}$$

During the plasma discharge process, apart from solvated electrons and radical species such as OH$^.$, H$^.$ and O$^.$, molecular species including H$_2$, H$_2$O$_2$ and O$_3$ have been identified in the bulk solution [182]. The major reactions between these species that have been proved to occur near the plasma-water interface and in bulk water include the interaction of solvated electrons with H$_2$O$_2$ yielding hydroxyl radicals (OH$^.$) and hydroxide anion (OH$^-$) whose reaction further produces super oxide radical (O$_2^-$) (Eqs. (136) and (137)). The super oxide radical may react with H$_2$O$_2$ and O$_2$ producing multiple co-species as shown in Eqs. (138) and (139).

$$e_{aq}^- + H_2O_2 \rightarrow OH^. + OH- \tag{136}$$

$$2OH^. + 2OH^- \rightarrow O_2^- + 2H_2O \tag{137}$$

$$1/2O_2^- + H_2O_2 \rightarrow O_2^- + H_2O \tag{138}$$

$$O_2^- + 2O_2 \rightarrow 2O_3^- \tag{139}$$

4.13. Quantification of reactive oxygen species in dielectric barrier discharges

One of the most difficult tasks during wastewater remediation by plasma technologies is the determination of reactive oxygen species (ROS) in aqueous plasma discharge actuators, because of their inadequate selectivity and limited lifespan as shown in Table 1. Nevertheless, long-lived species such as O$_3$ and H$_2$O$_2$ have effectively been quantified in DBD system by spectroscopic methods [90]. On the other hand, the powerful non-selective hydroxyl radical in aqueous plasma reactors has been measured using diverse chemical probes including phenol, dimethyl sulfoxide (DMSO), disodium salt of terephthalic acid (NaTA), terephthalic acid (TA) and 4-hydroxybenzoate (HDB) [136,273,274]. The products resulting from the reaction of OH with these chemical trapping agents are often measured using different methods [46].

Furthermore, plasma generated radicals in liquid phase namely, OH, superoxide anion (O_2), atomic oxygen ($O^.$) among others have been identified using advanced techniques such as electron paramagnetic resonance (EPR) spectroscopy [275,276] and related Spectrophotometric methods [277,278]. Indeed, a successful and comprehensive review on quantification of ROS mainly O_3, H_2O_2, $OH^.$, $O^.$ O_2^-, etc. in liquid plasma technologies was published by Mouele et al. [32]. The authors reported that O_3 and H_2O_2 could successfully be measured by indigo and per titanyl sulphate spectroscopic methods, respectively, while OH radical could specifically be measured by fluorescence spectrometry method using terephthalic acid as a probe. In total these measurement methods have been found effective for the determination of ROS in aqueous plasma actuators, however, the choice of a particular technique may depend on the availability and cost of the equipment.

4.13.1. Impact of solution pH and scavengers on the production of reactive species in DBD and DBD/catalysts configurations

Besides reactor configuration aspect, the efficiency of a DBD reactor also depends on the amount of reactive species produced. However, the presence of scavengers in DBD actuators could diminish their concentration resulting in low degradation efficacy of the targeted pollutants. A comprehensive study on the effect of both solution pH and scavenging of the production of reactive species mainly O_3, H_2O_2 and OH radicals in double cylindrical DBD configuration using distilled water as model solution was conducted by Mouele et al. [90]. The authors showed that the amount of ozone in both acidic and basic pH fluctuated during time on stream though the highest concentration of ozone 0.79 M was achieved in acidic pH 2.5. This suggested that O_3 was being formed and scavenged in the DCDBD reactor via different reaction paths. Its decomposition by UV radiation (at $\lambda \leq 310$ nm) leads to oxygen molecules and singlet atomic oxygen that further reacts with water molecules to generate OH radicals. The rearrangement of OH results in the formation of H_2O_2 follows an avalanche of chemical reaction chains as early sustained by Haugland [180] and Tang et al. [164]. Following these trends, and by considering the nucleophilic and electrophilic reactions of ozone, it can be inferred that the amount of O_3 in DBD systems could fluctuate in the presence or absence of catalyst. High amount of ozone can be produced at low pH values [164]. Unlike ozone, H_2O_2 in DBD reactors is abundantly produced in basic conditions as product from various chemical reactions. Hydrogen peroxide is often considered as one of the primary sources of $OH^.$ via dissociation reaction. Its high amount in DBD systems may result in improved concentration of OH. This latter being the major product of most advanced oxidation processes is non-selective and highly reactive towards aqueous chemical species. In this regard, Mouele et al. [90] showed that in the absence of buffer, OH resulting from countless reaction chains [164] are abundantly produced in the DBD system in basic conditions (pH $\geq$ 8.5) with a concentration range of 8.24–9.66 mg/L. However, the addition of small amounts of buffer solution (KH_2PO_4 + Na_2HPO_4, pH = 7.39) significantly reduced OH concentration in DBD reactor to the range of 0.97–1.27 mg/L at pH $\geq$ 8.5. This was ascribed to the reaction of phosphate anion scavengers, mostly $H_2PO_4^-$, HPO_4^- and PO_4^- from the buffer with OH radicals. Moreover, the authors demonstrated that the addition of 6.36 g of Na_2CO_3 in DBD reactor drastically decreased the amount of OH radicals from 0. 389 mg/L (without scavenger) to 0.001 mg/L (with scavenger). This noticeable decay was attributed to the scavenging reaction of carbonate/bicarbonate (CO_3^{2-}/HCO_3^-) with OH radicals and has been widely reported [279–283]. Therefore, these mitigations show that trace amounts of scavengers in DBD configurations can diminish the amount of active species and consequently affect the solution pH which in return may impact on the decomposition rate of water toxins.

5. Generation of reactive nitrogen species in DBD configurations

Besides the aspects highlighted above, the efficiency of DBD systems may also depend on the nature of the feed gas which in return influences operational parameters during optimisation processes. The common feed gases used in DBD advanced technologies include dry air, oxygen (O_2), and argon (Ar) and the impact of their composition on the removal efficiency of targeted pollutants has been evaluated by Wardenier et al. [161]. The authors reported that excellent decomposition of model toxins could be achieved with oxygen plasma followed by argon and air plasma. This classification is likely associated with the nature and different amounts of chemical species produced in each system at ambient conditions. During diagnostic studies of plasma induced by dielectric barrier discharge technologies using air as the feed gas, various reactive oxygen (ROS) apart from those reviewed above, reactive nitrogen species (RNS) deriving from air nitrogen have also been accounted. The production of RNS in air DBDs has been highlighted by various authors [28–30,93,191,284] and the common mechanisms for the formation of RNS have been summarised and are presented in Fig. 17.
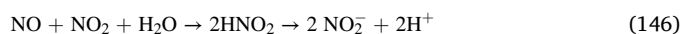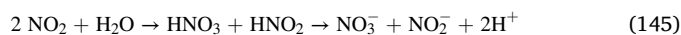
The efficacy of O_3 produced in DBDs at the feed gases was examined by Lukes et al. [285]. Lukes and colleagues proved that changing from oxygen to plasma air (N_2, O) resulted in the decrease of the amount of ozone due to its reaction with N_2 forming nitrogen oxide (NO) in the discharge zone as shown in Eqs. (140)–(143).

$$N_2 + e^- \rightarrow 2N^. + e^- \tag{140}$$

$$O_2 + e^- \rightarrow 2O^. + e^- \tag{141}$$

$$N^. + O_2 \rightarrow NO + O^. \tag{142}$$

$$O^. + O_2 + M \rightarrow O_3 + M \tag{143}$$

Next, Kogelschatz [98] sustained that NO that is significantly generated in air plasma reacts with O_3 forming nitrogen dioxide (NO_2) according to Eq. (144).

$$NO + O_3 \rightarrow NO_2 + O_2 \tag{144}$$

This indicates that the low performance of air plasma compared to that of O_2 plasma could be the consequence of reduced rates of formation of $OH^.$ and O_3. Even though literature claims that a significant amount of O_3 could be achieved/measured in the absence of N_2 species, the reduced amount of O_3 in DBD systems does not imply that O_3 directly interacts with pollutants but could indicate that O_3 undergoes side reactions with co-species due to its electrophilic and nucleophilic properties. For instance, in the presence of H_2O_2 in plasma-treated liquids, O_3 is quickly converted to OH radicals as earlier demonstrated in Eq. (34). This, therefore, implies that ozone is often absent in some DBD configurations or present in very minute concentrations. It should be recalled that the circulation and dissolution of gas phase chemical species into the plasma-treated effluent give rise to secondary oxidising agents (oxygen and nitrogen species) in the liquid which further affect the physicochemical properties of the DBD aqueous media mainly pH and conductivity of the solution being treated. Apart from hydrogen cations (H^+) that may likely result from water dissociation, nitrogen species (NO and NO_2) previously discussed are often responsible for the formation of nitrite (NO_2^-) and nitrate (NO_3^-) that induce the acidification of the air plasma-treated waters. Consequently, various studies have proved the presence of nitric (HNO_3) and nitrous (HNO_2) acids in air plasma treated solutions [223,286] resulting from aqueous NO_2^- and NO_3^- and the formation these acids has been reported in Lukes et al. [285] according to Eqs. (145) and (146).

$$2 NO_2 + H_2O \rightarrow HNO_3 + HNO_2 \rightarrow NO_3^- + NO_2^- + 2H^+ \tag{145}$$

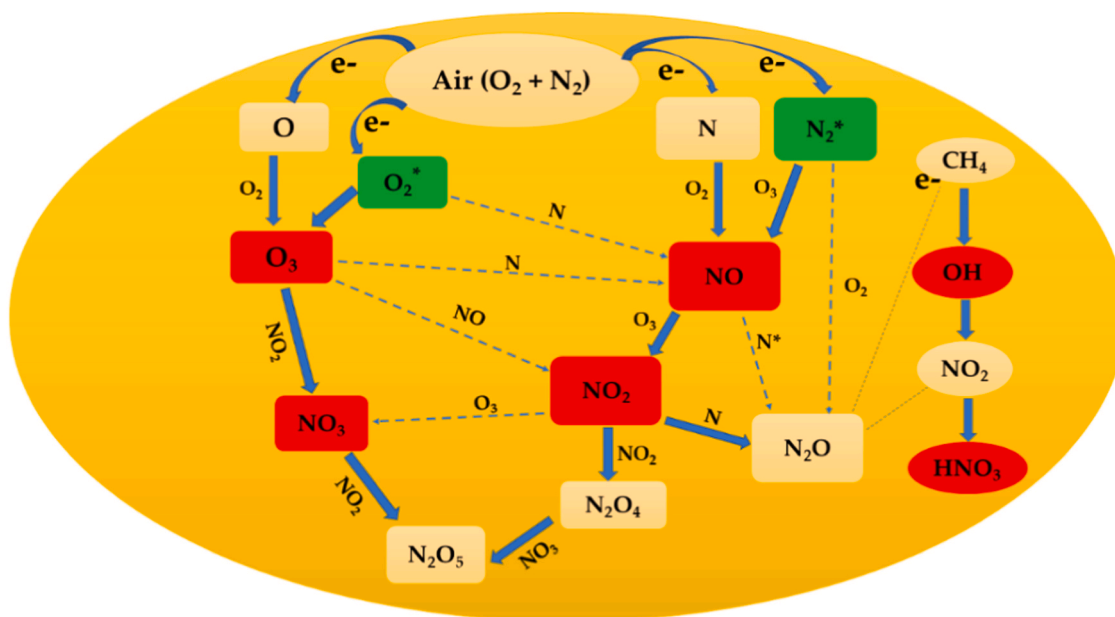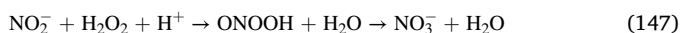$$NO + NO_2 + H_2O \rightarrow 2HNO_2 \rightarrow 2 NO_2^- + 2H^+ \tag{146}$$

Fig. 17. Plasma chemistry nitrogen-based impurities [6,102].

The acidity of DBD plasma treated solutions induced by nitrogen species is often dictated by nitrite and nitrate concentrations [195]. Wardenier et al. [161] emphasised that the concentration of nitrite remains in the DBD treated solution is often lower than that of nitrate due to sequential oxidation side reactions as shown in Eqs. (147)–(149).

$$NO_2^- + H_2O_2 + H^+ \rightarrow ONOOH + H_2O \rightarrow NO_3^- + H_2O \quad (147)$$

$$NO_2^- + O_3 \rightarrow NO_3^- + O_2 \quad (148)$$

$$NO_2^- + HO^. \rightarrow NO_2 + HO^- \quad (149)$$

Therefore, the reduced performance of air plasma encountered in literature could be ascribed to these two scenarios including O_3 quenching by NO and aqueous decomposition of nitrite to nitrate that is often one of the major by-products quantified in air plasma treated waters [195]. Thus, the abundance of nitrate in treated effluents has become an outstanding challenge in DBD processes that limit their application at the industrial level. This signifies that any amount of nitrates higher than 50 mg/L in surface and groundwater as permitted by the EU Nitrates Directive (91/676/EEC), may require further treatment for the removal of nitrates. This review demonstrates that nitrogen species in DBDs technologies are mostly involved in the generation of secondary species that induce acidification of water being treated instead of directly reacting with the targeted pollutants. This in return may impede their complete removal.

5.1. Quantification of reactive nitrogen species in DBD configurations

The determination of RNS in DBD systems has been shortly reported in the literature, though their formation in plasma systems may not only appear limiting to the efficiency of the reactor being employed but they may somehow contribute to improve deactivation/inactivation of bacteria from polluted water [286–288]. Likewise, their presence/formation in various plasma reactors are claimed to be stopped. Hence, it is important to determine their amount or concentration in the solutions being investigated. Wright et al. [289] claimed that pure oxygen (O_2) can be used to avoid the formation of RNS in DBD systems, however, the rise of temperature to about 150 °C could be a limiting factor, though this claim has not been widely reported in the literature. Schwartz et al. [290] outlined that N_2 often emits UVA, UVB and UVC while NO radiates in the UVA region and N_2 and N_2^+ in the residue. In

case O_2 impurities are present in the plasma zone, NO is likely to form leading to an intense generation of UVA radiations [291] which can subsequently be absorbed by O_3 if produced in the system as endorsed by Grebenshchikov et al. [292]. Indeed, FT-IR has been employed to ascertain the concentration of RNS in DBD systems whose exhausts that are operated with dry air (without liquid in the reactor vessel) and are connected to a gas cell (e.g., Pike Technologies Ltd.) with a varying path-length incorporated in a FTIR spectrometer (4700, Jasco Ltd, for example). In this regard, the concentrations of RNS are defined at different absorption wavenumbers. For instance, N_2O could be sensed at 2240 cm^{-1}, N_2O_5 at 750 cm^{-1}, HNO_3 at 890 cm^{-1}, and NO_2 at 1580 cm^{-1} according to Fitzsimmons et al. [293]. According to Sakiyama et al. [294], when FTIR and UV-absorption spectroscopies in combination with OES are used in DBD systems in the absence of liquid, the concentration of long species mainly H_2O_2, HNO_2, HNO_3 and NO_3 are often below the detection limit and their concentration could be deduced/estimated as a function of time until steady state is reached using computational method or numerical model via conversion of their amount into partial pressure using the ideal gas law. In this case, the DBD reactor is often flushed out with plasma effluent that replaces air and hence channelled through the FTIR column followed by analysis. Similar investigation on the determination of RNS in DBD configuration was also conducted by Pavlovich et al. [295] who quantified ozone and various RNS during chemical diagnostic of air plasma for surface disinfection. Focusing on the surface micro-discharge (SMD) of the induced air plasma, the authors quantitatively measured the plasma chemistry in gas-phase using infra-red spectroscopy (FTIR) employing small gas volumes. Their results revealed that O_3, NO, NO_2 and other NOx were present, and the antibacterial inactivation was more effective in RNS mode than in that of O_3. On the one hand, their outcomes implied that plasma chemistry should carefully be characterised during its application in surface cleansing or water/wastewater remediation. On the other hand, their results signified that, despite being considered as scavengers of ROS, RNS can also contribute to the detoxification of water contaminants. Besides, Abdelaziz et al. [296] designed a surface dielectric barrier discharge (SDBD) whose plasma source was directly incorporated into a chamber of a glass tube of 220 mm long and 24 mm inner diameter. The outlet of the glass tube connected to the FTIR that was linked to a gas cell with a path length of 3 cm was used for quantification of RNS produced in gas phase. The concentration of ozone

produced was measured by UV ozone monitor also referred to as O_3 analyzer. Various authors outlined that the concentration of O_3 and that of RNS species such as O_3, N_2O, N_2O_5, and NO_2 in SDBD at the applied conditions could be influenced by the amount of O_2 in the feed gas. While NO is often not detected in FTIR spectra perhaps into its rapid oxidation to NO_2 and NO_3 and further to N_2O_5 [296–298]; the increase of O_2 content in the system may result in an increase of O_3 concentration. On the other hand, the highly energised electrons and ROS and RNS generated in DBD reactors collide with O_2 and N_2 molecules to produce NxOy forming a chain of chemical reactions. The measurement of RNS in DBD technologies in gas phase using OES with or without FTIR or UV–vis has been extensively reported in the literature [287,299–301]. Furthermore, an advanced laser induced fluorescence (LIF) system assembled with a self-developed fluorescence telescope, an optimised and synchronised tunable pulsed laser with high precision, followed by a surface discharge generator and intensified Charge Coupled Device (iCCD) camera, and an oscilloscope has also been reported effective for the detection and measurement of RNS ($\sim$ ppb level) in DBD systems [298]. However, the authors claimed that the requirement of a pixel resolved spatial distribution and detection in the outer plasma zone could be problematic because of the small concentration of RNS (often at ppb level) and recurrent interference might limit its applicability. These investigations show that diagnosis of plasma chemistry focusing on the quantification of RNS in DBD configurations during post-discharge in gaseous state can successfully be achieved, however the determination of long-lived RNS species such as NO_2^-, NO_3^-, HNO_2 and HNO_3, etc. in liquid phase is still a challenging task. Nevertheless, nitrogen oxides including nitrate (NO_3^-), nitrite (NO_2^-), peroxynitrite ($ONOO^-$) have been identified in the aqueous phase mostly at low pH values [295]. During research studies conducted by Machala et al. [302], the concentrations of nitrites and nitrates in the solution being treated was determined using high performance liquid chromatography (HPLC) system with a 7 mm All sep A1 anion exchange column (10 cm $\times$ 4.6 mm) and an eluent consisting of 0.85 mmol L^{-1} $NaHCO_3$/0.9 mmol L^{-1} Na_2CO_3 at a flow rate of 1.2 mL min^{-1}. The samples withdrawn from DBD reactor were stabilised with a buffer solution (2 mmol L^{-1} Na_2HPO_4/KH_2PO_4 solution, pH 6.9) within a short time frame (3 min) prior to prevent the acidic decay of nitrites before being infused into the chromatography column. On the other hand, peroxynitrite concentration was measured via its reaction with 2, 7-dichlorodihydrofluorescein diacetate (DCFH-DA) resulting in highly fluorescent dichlorofluorescein (DCF) in the solution governed by ROS. The absorbance measurements were performed at 500 nm while sample fluorescence was depicted at excitation and emission wavelengths of 502 and 523 nm, correspondingly following previous DCFH-DA assay fluorescence reports [303,304]. Unlike nitrite and nitrate, the measurement of peroxynitrite fluorescence was achieved with a spectrophotometer. The acidic disintegration of peroxynitrite in samples withdrawn from the plasma reactor was stopped by addition of phosphate buffer (2 mmol L^{-1} Na_2HPO_4/KH_2PO_4 solution) within 5 min of withdrawal as in previous cases. Furthermore, the pH and conductivity probe was used to monitor/measure pH and conductivity of plasma treated water samples. Pavlovich et al. [305] investigated the correlation of ozone with antibacterial effects in air dielectric barrier discharge during treatment of water. In their work, the authors measured the principal long-lived nitrogen chemical species including nitrites (NO_2^-) and nitrates (NO_3^-) in DBD-treated aqueous solutions using UV–vis spectroscopy. But beforehand, UV absorbance scans of sodium nitrate and sodium nitrite used as standards were scanned in the wavelength range of 200–400 nm. Thereafter, the concentration of nitrate and nitrite in plasma-remediated samples was determined, in accordance with their previous work [306]. The measurement of nitrogen species mainly nitrous acid (HONO) and its conjugate base nitrite ion (NO_2^-) as well as nitroacidium (H_2ONO^+) by UV–vis spectroscopy was also conducted by Riordan et al. [307]. The determination of RNS concentration in DBD configurations or any other aqueous systems using diverse protocols has

extensively been outlined [298,299,308].

5.2. Removal of nitrous oxides from DBD configurations

Plasma systems driven by air (N_2, O_2) and pure nitrogen (N_2) gas-discharges produce diverse species including ROS and RNS. The accumulation of RNS, mostly nitrogen oxides (NOx) in the solution being treated by DBD configurations could be a potential limiting factor that can impede the complete degradation/mineralisation of targeted pollutants. Though Oehmigen et al. [299] and Naitali et al. [308] showed that NOx (NO + NO_2) enhanced antibacterial properties, they often behave as scavengers of oxygen (O_2) and ROS such as O_3 and $OH^.$ and hence diminish their amounts in DBD configurations and further decelerate the depollution process [275]. So far, literature presents little information of methods used to prevent the formation of RNS in air/N_2-DBD protocols. Nevertheless, Obradovic et al. [309] reported that the formation of NOx in DBD technologies could be stopped by introduction/injection of ammonia (NH_3) gas downstream from the DBD reactor (in the plasma exhaust/outlet in gas phase) at reasonable amount below the detection limit of Nessler's reagent. In the direct oxidation stage, NO is oxidised to HNO_2 mainly by O_3 and $OH^.$, HO_2 and $O^.$ radicals generated in the plasma zone of the DBD reactor. Atkinson et al. [310] highlighted that the oxidation reactions of NO are fast and effective. The second step involves the removal of NO_2 via oxidation to form HNO_3 and to NO_3 by O_3. Hence, during direct oxidation, the decrease of NOx concentration is due to oxidation of NO to HNO_2, and NO_2 to HNO_3. The indirect oxidation method on the other hand driven by the mixture of flue gas and ozonised air is diagnosed at about 40 cm downstream from the DBD actuator. In this region, the concentration of $O^.$, $OH^.$ and HO_2 radicals are insignificant because of their limited lifetimes. Therefore, NO in this region is effectively oxidised to NO_2 by its reaction with O_3 [311]. However, in the absence of the back reaction (NO_2 to NO_3), the slow diminution of NO_2 concentration is noticeably observed only when NO is totally oxidised. The secondary way to stop the formation of NOx species in DBD plasma reactors might require the use of N_2 free pure gases such as O_2 or Ar which directly result in the production of ROS adequate for direct removal of contaminants.

6. Measurement of temperature in DBD systems

Literature supports that non-thermal plasma induced by DBD often referred to as silent discharges are run at room temperature and are safe to operate [33]. However, the electron temperature above room temperature recorded during plasma initiated by air, N_2, Ar, He or their mixture could become a limiting factor in the utilisation of DBD configurations for water and wastewater remediation. Hence, the measurement/assessment of electron temperature during DBD experiments is a necessary step to define the safety of DBD technologies. The most common techniques used to determine gas temperature in DBD configurations include optical emission spectroscopy (OES) [312–315] and diode laser absorption spectroscopy (DLAS) [316,317]. Williamson et al. [318] determined gas temperature of the bulk in a 30%N_2/70%Ar DBD system using time resolved diode-laser absorption spectroscopy of metastable Ar 4s' [1/2]° and resolved plasma emission of N_2^+ 1st Negative and N_2 2nd Positive. The outcomes of their work showed that gas temperature of the low power DBD system run at pressures of 10, 30, and 100 Torr and pulse repetition rates of 0.5–30 kHz was in the range of 350–400 K (76.85–126.87 °C) and somewhat above room temperature. Similar investigations on the measurement of DBD plasma bulk temperature were outlined by Horvatic et al. [319]. These studies inferred that DBD systems with electron temperature over 300 K should carefully be operated, certainly in well adapted cooling systems to avoid any experimental obstacle.

7. Discussion of the review

In advanced oxidation processes (AOPs), the combination of UV light and other reactive oxygen species (ROS) such as O_3, H_2O_2 contribute towards the production of $OH^.$. The most common AOPs mainly O_3/UV, H_2O_2/UV, O_3/UV/H_2O_2, and their combination with catalysts have been found significant in the removal of organic pollutants and killing of bacteria [320]. The utilisation of these techniques by themselves may be time consuming and may involve a lot of wet chemistry but work more effectively in combination. Conversely, AOPs based on non-thermal plasma processes like dielectric barrier discharges (DBDs) generate all ROS previously mentioned at once with few or no chemical additives [1]. Apart from this, UV light is also produced in DBD systems, and the benefit of producing O_3, H_2O_2, $O^.$, O_2^-, $OH^.$, etc. render DBD actuators robust advanced oxidation technologies. This manuscript demonstrated that O_3, H_2O_2, $O^.$, O_2 are selective towards organic pollutants while $OH^.$ is non-selective. So, it is certain that contaminants that O_3, H_2O_2, $O^.$, O_2 cannot decompose in DBDs could be further oxidised and mineralised by $OH^.$ following various reaction steps previously discussed. This can be observed from various studies reported in the literature which mostly show the degradation of the carbon skeleton of the initial pollutants into secondary by-products [11,221,242]. Nevertheless only a few authors showed full mineralisation of the targeted compounds decomposed in DBD reactors [238,243,245]. Therefore, extended research still needs to be conducted so as to achieve mineralisation.

Several researchers attempted the degradation of pharmaceuticals using AOPs, but only a few showed their total conversion into CO_2, H_2O, and harmless entities [167,238,321]. However, investigation of Liu et al. [76] proved that the CBZ compound subjected to DBD system was broken down into various degradation intermediates; however, their mineralisation into water and inoffensive substances was not mentioned. Similar observations could also be made in studies conducted by Magureanu et al. [165,166] and Marković et al. [92]. Likewise, after observation of all studies reviewed in this text and those presented in Table 2, it can be noticed that pollutant concentration, pH, kinetics, and energy yield required in the process are very important parameters that influence the removal of these toxins. Nevertheless, most of the parameters in the decomposition of pollutants from water and wastewater were not fully examined. Therefore, complete optimisation of these factors is required to establish the degradation conditions of these contaminants. The pollutant concentration is a very crucial parameter because many researchers have shown that the decomposition of water impurities decreases with an increase of pollutant concentration [6,90,166]. This is probably due to the chemical stability of their molecular structures that are designed to resist oxidants' attacks. Apart from this, literature has also shown that toxicants such as pharmaceuticals have been decomposed in DBD systems at different pH values while some have been well removed in acidic, neutral, or basic media [322,323], the stability of these compounds may also slow down the rate of their degradation which usually leads to pseudo first order kinetics [158]. Moreover, this review shows that the addition of catalysts in DBD systems initiates catalytic ozonation and photocatalytic ozonation leading to the abundance of reactive species in the solution, which can successfully be quantified using various methods [32,296]. In the case of air or N_2 feed gases, the formation of RNS and their removal can be achieved according to [275]. The thermal stability of DBD system can also be controlled following Okada and Kijima [314] and Lin et al. [315]. Likewise, analysis of certain AOPs mentioned in this text shows that the use of UV and ozone generators requires a certain amount of energy to induce oxidation processes [324]. However, most papers on DBD technologies reviewed in this text (Table 2) did not investigate the energy consumption which is an essential parameter. Nevertheless, with lower energy yield G_{50} estimated in Table 2, DBD could also be used not only as an efficient energy saving method that produces UV, O_3, H_2O_2,$^.$ OH, etc. but as a promising novel technology for the oxidation of pollutants from water effluents [33,90]. In addition, the limited use of chemicals in DBD configurations is beneficial to avoid more toxicity of the effluents being treated as various studies have demonstrated that degradation metabolites are sometimes more toxic that the initial pollutants [11,12,325,326]. Likewise, the toxicity of the degradation by-products in the studies was not highlighted, showing that these studies omitted two criteria that are important in water and wastewater decontamination. To recall, the general issue claimed by most wastewater treatment plants (WWTPs) is the production of sludge and the appearance of emerging micropollutants in treated effluents which further limit their reusability for industrial purposes, distribution to recipients in need, and their discharge into the environment even though Bögner et al. [327] suggested an alternative sludge pre-treatment via ozone application for water reuse in aquaculture systems. Therefore, complete removal of pharmaceuticals in/from final treated water is mandatory in this regard. Perhaps OH production systems need to be run for a prolonged time to allow a series of chemical reactions to occur till the total degradation of the pollutants is achieved [165,167]. Else in case of co-reactions between the degradation by-products, extended/selected heterogeneous catalysts could be added to the treatment system to boost the generation of selective and non-selective oxidisers, hence achieve total conversion of the degradation by-products [328–333]. This further inferred that effective AOPs aiming at producing huge amounts of OH radicals should be employed for the decontamination of effluents in WWTPs. Therefore, AOPs induced by DBD appear are potent technologies that can be used as integrative stages to treat final effluents from WWTPs before being discharged into the environment. The combination of various species produced in DBD configurations could be a promising mixture that can be used to fully remove organic pollutants such as dyes and other types of pollutants from final effluents. However, understanding the degradation mechanisms of each oxidant toward pollutants is crucial either in DBD or in other treatment systems. The studies reviewed in this text and in Table 2 indicate that O_3 and $OH^.$ are the principal reactive species that largely contributed to the decomposition of water pollutants in DBD configurations followed by NO_x and H_2O_2 that act as major precursors of OH radicals.

All these excellent treatment methods developed in the literature show great removal efficiencies but only a few of them stipulate how the by-products formed and traced their behaviour in aqueous media. Based on these remarks, a few questions need to be asked: Do these high removal percentages meant that complete oxidation of organic pollutants from water was achieved? If yes, why are the world's communities still facing a global water scarcity while potent treatment methods have already been developed? These interrogations demonstrate that even though considerable numbers of treatment methods have been established; the critical behaviour of organic toxins in WWTPs is still pertinent and hence needs to be addressed. During water and wastewater treatment, it is often believed that the following aspects might occur: 1) the operational/running cost of these advanced treatments is often beyond the allocated budget of various treatment protocols and hence limits their applicability at the industrial level [334]. 2) The use of excessive chemicals often leads to toxic sludge and undesired by-products in the treated effluents [162]. 3) The generated by-products often interact to form complex chains which in turn may be more harmful than parent molecules [11]. Therefore, the treated effluents can neither be reused, distributed nor discharged into the environment safely. In fact, the challenge of completely removing toxins from water has become a recurrent phenomenon because the degradation intermediates of some pollutants are usually unknown. Therefore, it is recommended that these decomposition intermediates should be detected and quantified to predict their degradation mechanistic pathways and hence to facilitate their removal to achieve a total water treatment process. To some extent, the generated by-products may not necessarily be toxic; they could just be too complex to be removed from the treated water. Likewise, their consumption by water receivers could have long term effects which are still under investigation. One may also

think that only metabolites could be toxic. But tiny by-products such as amides may also be harmful [335,336]. At this point, advanced treatment techniques need to be established to meet water global demand. Such technologies should incorporate both oxidation and mineralisation of target pollutants from water matrices [100,167,238,333]. In addition to that, the technology should be applicable with reasonable costs to achieve global utilisation. Based on the DBD advantages previously highlighted in this text, their configurations are certainly capable to meet these requirements. Therefore, it is important to emphasise that scientists involved in water and wastewater treatment should investigate and understand the properties of oxidants such as O₃, OH, etc. in aqueous media. Not only their generation routes in the applied systems but their reaction mechanisms towards targeted pollutants should be considered [337,338]. The toxicity behaviour of the parent pollutants and by-products formed should be carefully investigated and reported to assess the effectiveness of the treatment method used [157]. Knowing the limitations of the treatment options could assist scientists to develop suitable DBD systems that achieve total oxidation and mineralisation of water contaminants. This may further contribute to relieve the global water crisis and the provision of fresh, clean, and water free from toxins.

On the other hand, hydroxyl radical (OH·) is the main targeted product of AOPs. OH· undoubtfully mineralises all types of contaminants, including bacteria and viruses [102]. Therefore, the efficiency of the DBD-AOP systems may depend on the density of OH· produced. But based on its non-selective property, OH· often reacts with its precursors or other scavengers that usually reduce its concentration in the treatment process [172,173]. This hence impacts the mineralisation of contaminants and their by-products and may further lead to unexpected outcomes.

Attri et al. [339] reported that when comparing various feed gases in DBD-driven plasma, O₂ plasma produces higher amounts of H₂O₂, O₃, and OH species, compared to other feed gases in plasma systems. Hence, we propose that assessment of the effect of feed gas on the decomposition efficiency of targeted pollutants should be considered as an important aspect for future plasma research projects. Although this review proves that DBD technologies are prospective and effective for water and wastewater purification, Hegeler and Akiyama [340] claimed that the revision of DBD configurations should be considered.

Conversely, Go et al. [341] appealed that the relatively long duration of voltage pulse in some DBD geometries could be responsible for energy loss of ions during acceleration; particularly the heating of the gas and thermal decomposition of generated ozone could limit DBDs application. Therefore, the authors suggest that traditional DBD needs cooling for dielectric materials and the mitigations to this claim were outlined by Lin et al. [315]. A few studies have shown that the use of streamer discharge by a short voltage pulse front (several ns) and higher pulse amplitude (tens-hundreds kV) significantly increases the production yield of ozone [342,343]. This was also endorsed by Beloplotov et al. [344] and Ripenko et al. [345] who have used such an approach for the decomposition of water pollutants.

Altogether, the combinations of various homogeneous AOPs such as UV/O₃, O₃/H₂O₂, UV/H₂O₂ and UV/O₃/H₂O₂ induced in DBD configurations have been proved to largely generate powerful non-selective hydroxyl radicals [182]. Though various conventional DBDs systems have been used to decompose organic pollutants from water and wastewater [33], cylindrical DBDs have not been widely used in the treatment of water effluents. Therefore, this review emphasises that double cylindrical DBD (DCDBD) due to its superior properties previously discussed, can be used as a promising technology for the removal of targeted pollutants. The DCDBD technique reviewed in this text is cheap, feasible, and environmentally benign. 1 eV is enough as input energy to induce the plasma discharge. Although some studies may claim that the scalability of DBD systems is challenging, DBD configurations present various advantages over other electrical discharges and hence need to be considered as promising means for the direct removal of water pollutants. Many methods that meet the requirements for low cost, accessible treatment often lack good efficiency for complete removal of toxins from water. This is the case with various traditional techniques that have been used in water purification processes [346]. Certainly, they can treat water and wastewater but not all contaminants are removed. So, further integrative, and competitive methods are needed to oxidise contaminants that escape water recovery plants or wastewater treatment plants (WWTPs). In this case, DBD configurations could be considered as a potent, efficient route for AOPs that may degrade and mineralise recalcitrant toxins. The reaction mechanisms of the species produced in DCDBD may favour the choice of reagents to be used but a better comprehension of non-thermal plasma properties and its application for water and wastewater treatment is needed. Herein we suggest some promising areas of experimental research related to O₃-based advanced oxidation technologies for water and wastewater recovery.

8. Conclusions and future perspectives

The need to develop effective water treatment methods has gained attention in environmental science. The numerous water treatment techniques developed in the past three decades, compete with one another but they failed to destroy toxic substances from water supplies.

This review demonstrates that ozone being one of the major oxidants is produced in DBD technologies via different reactions. Its electrophilic reaction occurs with organic pollutants comprising electron donor groups (—OH, —NH₂, etc.) and the nucleophilic reaction happens with compounds containing electron withdrawing groups (—COOH, NO₂, etc.). Its cycloaddition reaction on pollutants leads to the formation of epoxides which are further hydrolysed to simpler entities by ring opening. The indirect reaction of ozone in DBD geometries involves its disintegration and the formation of numerous reactive species including O·, O_2^-, HO₂, OH·, etc. which directly attack water contaminants that ozone cannot oxidise. The addition of catalysts in DBD systems may induce both catalytic ozonation and photocatalysis if the UV radiation produced in the DBD reactor is strong enough to activate the catalysts used. These two processes enhance the density of ROS in the bulk and hence speed up the decontamination of polluted water. However, optimisation of factors mainly solution pH, catalysts dose and pollutant concentration are mandatory to achieve maximum pollutants' removal. On the other hand, OH radical being the main targeted oxidant in DBD technologies as in any other AOPs, is non-selective, thus oxidises, and mineralises all types of pollutants. Its common reactions with pollutants in DBD reactors include hydrogen abstraction, radical addition, electron transfer, and radical combination. Moreover, hydrogen peroxide mostly acting as the primary precursor of OH, also disintegrates to yield other species such as O_2^-, HO₂, etc.

The comparison of DBD technologies based on the energy yield G₅₀ shows the superiority of DCDBD and suggests that DCDBD configuration can still be used as an efficient method for remediation of contaminated water. Nevertheless, the value of G₅₀ being < 50% indicates that DBD geometries are energy efficient technologies.

The review further suggests that DCDBD is an effective integrative water treatment advanced oxidation process that mineralises recalcitrant toxins when properly applied. Hence, the comprehension of reaction mechanisms of ROS, their promotors and limiting factors in DBDs may be a key to improving the degradation efficiencies of the existing DBD technologies and hence their implementation. Nonetheless, the following aspects focusing on the use of DBD technologies for water purification should be considered in future studies.

The energy efficiency of DBD configurations should be estimated by calculating the energy yield (G₅₀) required to decompose half of the pollutant initial concentration as mentioned by Mouele et al. [33] and Malik et al. [34]. The energy yield (G₅₀) is a crucial parameter and should be considered during remediation of wastewater by DBD technologies.

In case the total degradation of selected contaminants is not achieved

with DBD alone, catalysts can be incorporated not as powder but suspended on solid supports (such as stainless-steel mesh coated with corrosion resistant layers) to boost the production of O_3 and co-existing species and hence improve the performance of the DBD reactors. The catalyst supports such as stainless-steel mesh (SS) should be coated with anticorrosion layer to prevent corrosive deterioration of SS in oxidative harsh environments as indicated by Pana et al. [140] and Dinu et al. [347].

The performance of DBD reactor technologies can be enhanced by coating the catalyst on the inner side of the dielectric barrier (quartz) of the DBD configurations as demonstrated by Mouele et al. [348] in such a way that the UV generated can be used directly to induce photocatalysis process and hence increase the density of O_3 and other aqueous species. This in return may advance the total oxidation of targeted pollutants in short periods.

Funding

Author contributions

Declaration of Competing Interest

The authors declare that they have no known competing financial interests or personal relationships that could have appeared to influence the work reported in this paper.

Acknowledgements

References

[1] E.S.M. Mouele, J.O. Tijani, O.O. Fatoba, L.F. Petrik, Degradation of organic pollutants and microorganisms from wastewater using different dielectric barrier discharge configurations-a critical review, Environ. Sci. Pollut. Res. 22 (2015) 18345–18362, https://doi.org/10.1007/s11356-015-5386-6.

[2] S.B. Gupta. Investigation of a Physical Disinfection Process Based on Pulsed Underwater Corona Discharges (Ph.D. thesis), Forschungszentrum Karlsrhue, Karlshrue, Germany, 2007.

[3] Lenntech I, History of Ozone, 2016, p. 1.

[4] P. Bruggeman, C. Leys, Non-thermal plasmas in and in contact with liquids, J. Phys. D Appl. Phys. 42 (2009), 053001, https://doi.org/10.1088/0022-3727/42/5/053001 (28pp).

[5] S.G. Zimmermann. Enhanced Wastewater Treatment by Ozone and Ferrate: Kinetics, Transformation Products and Full-Scale Ozonation (Ph.D. thesis), ETH Zurich, Zurich, Switzerland, 2011 (Accessed 14 January 2011), https://www.research-collection.ethz.ch/bitstream/handle/20.500.11850/152880/eth-4295-02.pdf.

[6] E.S.M. Mouele. Water Treatment Using Electrohydraulic Discharge System (Masters (M.Sc.) thesis), University of the Western Cape, 2014 (Accessed 10 September 2020). http://etd.uwc.ac.za/xmlui/handle/11394/4330.

[7] M.J. Farré, M.I. Franch, S. Malato, J.A. Ayllón, J. Peral, X. Doménech, Degradation of some biorecalcitrant pesticides by homogeneous and heterogeneous photocatalytic ozonation, Chemosphere 58 (2005) 1127–1133, https://doi.org/10.1016/j.chemosphere.2004.09.064.

[8] A. Zhihui, Y. Peng, L. Xiaohua, Degradation of 4-chlorophenol by microwave irradiation enhanced advanced oxidation processes, Chemosphere 60 (2005) 824–827, https://doi.org/10.1016/j.chemosphere.2005.04.027.

[9] J. Wu, H. Doan, S. Upreti, Decolorization of aqueous textile reactive dye by ozone, Chem. Eng. J. 142 (2008) 156–160, https://doi.org/10.1016/j.cej.2007.11.019.

[10] J.O. Tijani, O.O. Fatoba, G. Madzivire, L.F. Petrik, A review of combined advanced oxidation technologies for the removal of organic pollutants from water, Water Air Soil Pollut. 225 (2014) 2102, https://doi.org/10.1007/s11270-014-2102-y.

[11] J.O. Tijani, M.E.S. Mouele, O.O. Fatoba, O.O. Babajide, L.F. Petrik, Degradation of bisphenol-A by dielectric barrier discharge system: influence of polyethylene glycol stabilized nano zero valent iron particles, Adv. Nat. Sci. Nanosci. Nanotechnol. 8 (2017), 035013, https://doi.org/10.1088/2043-6254/aa7714.

[12] J.O. Tijani, M.E.S. Mouele, T.C. Tottito, O.O. Fatoba, L.F. Petrik, Degradation of 2-nitrophenol by dielectric barrier discharge system: the influence of carbon doped TiO2 photocatalyst supported on stainless steel mesh, Plasma Chem. Plasma Process. 37 (2017) 1343–1373, https://doi.org/10.1007/s11090-017-9824-8.

[13] S. Yang, P. Wang, X. Yang, G. Wei, W. Zhang, L. Shan, A novel advanced oxidation process to degrade organic pollutants in wastewater: microwave-activated persulfate oxidation, J. Environ. Sci. 21 (2009) 1175–1180, https://doi.org/10.1016/s1001-0742(08)62399-2.

[14] M. Saracino, S.S. Emmi, A. Zanelli, Water Remediation 2.0: Advanced Oxidation Processes', La Chimica el'Industria, Anno XCVII (5), 2015, pp. 18–25, DOI: ⟨10.17374/CI.2015.97.5.18⟩.

[15] S. Ledakowicz, M. Solecka, R. Zylla, Biodegradation, decolourisation and detoxification of textile wastewater enhanced by advanced oxidation processes, J. Biotechnol. 89 (2001) 175–184, https://doi.org/10.1016/s0168-1656(01)00296-6.

[16] Adel Al-kdasi, Azni Idris, Katayon Saed, Chuah Teong Guan, Treatment of textile wastewater by advanced oxidation processes-a review, Glob. Nest Int. J. 6 (2004) 222–230.

[17] S.B. Abdelmelek, J. Greaves, K.P. Ishida, W.J. Cooper, W. Song, Removal of pharmaceutical and personal care products from reverse osmosis retentate using advanced oxidation processes, Environ. Sci. Technol. 45 (2011) 3665–3671, https://doi.org/10.1021/es104287n.

[18] S. Slang, K. Palka, M. Vlcek, Thermal dependence of photo-induced effects in spin-coated As 20 Ge 12.5 S 67.5 thin films, J. Non-Cryst. Solids 471 (2017) 415–420, https://doi.org/10.1016/j.jnoncrysol.2017.06.033.

[19] E. Guivarch, S. Trevin, C. Lahitte, M.A. Oturan, Degradation of azo dyes in water by Electro-Fenton process, Environ. Chem. Lett. 1 (2003) 38–44, https://doi.org/10.1007/s10311-002-0017-0.

[20] G. Li Puma, A. Bono, D. Krishnaiah, J.G. Collin, Preparation of titanium dioxide photocatalyst loaded onto activated carbon support using chemical vapor deposition: a review paper, J. Hazard. Mater. 157 (2008) 209–219, https://doi.org/10.1016/j.jhazmat.2008.01.040.

[21] K. Rajeshwar, M.E. Osugi, W. Chanmanee, C.R. Chenthamarakshan, M.V. B. Zanoni, P. Kajitvichyanukul, R. Krishnan-Ayer, Heterogeneous photocatalytic treatment of organic dyes in air and aqueous media, J. Photochem. Photobiol. C Photochem. Rev. 9 (2008) 171–192, https://doi.org/10.1016/j.jphotochemrev.2008.09.001.

[22] H.R. Ghatak, Advanced oxidation processes for the treatment of biorecalcitrant organics in wastewater, Crit. Rev. Environ. Sci. Technol. 44 (2014) 1167–1219, https://doi.org/10.1080/10643389.2013.763581.

[23] Saracino Michela, Advanced Oxidation Processes Based on Photocatalysis for the Degradation of Organic Contaminants in Water (Dissertation Ph.D. thesis), Alma Mater Studiorum Università di Bologna, Dottorato di ricerca in Chimica, 28 Ciclo, 2016, DOI: ⟨10.6092/unibo/amsdottorato/7545⟩.

[24] I. Keisuke, N.J. Naghashkar, M.G. El-Din, Degradation of aqueous pharmaceuticals by ozonation and advanced oxidation processes: a review, Ozone Sci. Eng. 28 (2006) 353–414.

[25] K. Maria, D. Mantzavinos, D. Kassinos, Removal of residual pharmaceuticals from aqueous systems by advanced oxidation processes review article, Environ. Int. 35 (2) (2009) 402–417, https://doi.org/10.1016/j.envint.2008.07.009.

[26] B. Halliwell, G.J.M.C. Utteridge. Free Radicals in Biology and Medicine, 4th ed., Oxford University Press, New York, 2007.

[27] W. Sang, J. Cui, L. Mei, Q. Zhang, Y.Y. Li, D. Li, W. Zhang, Z. Li, Degradation of liquid phase N, N-dimethylformamide by dielectric barrier discharge plasma: mechanism and degradation pathways, Chemosphere 236 (2019), 124401.

[28] Y. Liu, C. Wang, X. Shen, A. Zhang, S. Yan, X. Li, A.C. Miruka, S. Wu, Y. Guo, S. Ognier, Degradation of glucocorticoids in aqueous solution by dielectric barrier discharge: kinetics, mechanisms, and degradation pathways, Chem. Eng. J. 374 (2019) 412–428.

[29] J. Jose, L. Philip, Degradation of chlorobenzene in aqueous solution by pulsed power plasma: Mechanism and effect of operational parameters, J. Environ. Chem. Eng. 7 (2019), 103476.

[30] A.P.S. Crema, L.D.P. Borges, G.A. Micke, A.N. Debacher, Degradation of indigo carmine in water induced by non-thermal plasma, ozone, and hydrogen peroxide: a comparative study and by-product identification, Chemosphere 244 (2020), 125502.

[31] M. Lapertot, C. Pulgarín, P. Fernández-Ibáñez, M.I. Maldonado, L. Pérez-Estrada, I. Oller, W. Gernjak, S. Malato, Enhancing biodegradability of priority substances

(pesticides) by solar photo-Fenton, Water Res. 40 (5) (2006) 1086–1094, https://doi.org/10.1016/j.watres.2006.01.002.

[32] E.S. Massima Mouele, O.O. Fatoba, O. Babajide, K.O. Badmus, L.F. Petrik, Review of the methods for determination of reactive oxygen species and suggestion for their application in advanced oxidation induced by dielectric barrier discharges, Environ. Sci. Pollut. Res. 25 (10) (2018) 9265–9282, https://doi.org/10.1007/s11356-018-1392-9.

[33] E.S. Massima Mouele, J.O. Tijani, K.O. Badmus, O. Pereao, O. Babajide, C. Zhang, T. Shao, E. Sosnin, V. Tarasenko, O.O. Fatoba, Katri Laatikainen, Leslie F. Petrik, Removal of pharmaceutical residues from water and wastewater using dielectric barrier discharge methods—a review, Int. J. Environ. Res. Public Health 18 (2021) 1683, https://doi.org/10.3390/ijerph18041683.

[34] M.A. Malik, Water purification by plasmas: which reactors are most energy efficient? Plasma Chem. Plasma Process. 30 (1) (2010) 21–31, https://doi.org/10.1007/s11090-009-9202-2.

[35] S. Tang, D. Yuan, Y. Rao, M. Li, G. Shi, J. Gu, T. Zhang, Percarbonate promoted antibiotic decomposition in dielectric barrier discharge plasma, J. Hazard. Mater. 366 (2019) 669–676, https://doi.org/10.1016/j.jhazmat.2018.12.056.

[36] H. Denham, A Theory Based on Free Radicaland Radiation Chemistry, From the Donner Laboratory of Biophysics and Medical Physics, University of Califomia, Berkeley, 1956.

[37] W.P. Arnold, C.K. Mittal, S. Katsuki, F. Murad, Nitric oxide activates guanylate cyclase and increases guanosine 3′:5′-cyclic monophosphate levels in various tissue preparations, Proc. Natl. Acad. Sci. USA 74 (1977) 3203–3207, https://doi.org/10.1073/pnas.74.8.3203.

[38] Barry Halliwell, Free radicals, reactive oxygen species and human disease: a critical evaluation with special reference to atherosclerosis, Br. J. Exp. Pathol. 70 (6) (1989) 737–757.

[39] S.S. Shinde, C.H. Bhosale, K.Y. Rajpure, J.H. Lee, Remediation of wastewater: role of hydroxyl radicals, J. Photochem. Photobiol. B Biol. 141 (2014) 210–216, https://doi.org/10.1016/j.jphotobiol.2014.10.015.

[40] D.R. Crosley, C.J. Araps, M. Doyle-Eisele, J.D. McDonald, Gas-phase photolytic production of hydroxyl radicals in an ultraviolet purifier for air and surfaces, J. Air Waste Manag. Assoc. 67 (2) (2016) 231–240, https://doi.org/10.1080/10962247.2016.1229236.

[41] N. Carslaw, L. Fletcher, D. Heard, T. Ingham, H. Walker, Significant OH production under surface cleaning and air cleaning conditions: impact on indoor air quality, Indoor Air 27 (6) (2017) 1091–1100, https://doi.org/10.1111/ina.12394.

[42] J. Li, S Wang, Y. Li, Z. Jiang, T. Xu, Y. Zhang, Supercritical water oxidation and process enhancement of nitrogen-containing organics and ammonia, Water Res. 185 (2020), 116222, https://doi.org/10.1016/j.watres.2020.116222.

[43] N. Wei, D. Xu, B. Hao, S. Guo, Y. Guo, S. Wang, Chemical reactions of organic compounds in supercritical water gasification and oxidation, Water Res. 190 (2021), 116634, https://doi.org/10.1016/j.watres.2020.116634.

[44] M.A. Oturan, E. Brillas, Electrochemical advanced oxidation processes (EAOPs) for environmental applications, Port. Electrochim. Acta 25 (2007) 1–18.

[45] I. Sirés, E. Brillas, M.A. Oturan, M.A. Rodrigo, M. Panizza, Electrochemical advanced oxidation processes: today and tomorrow. A review, Environ. Sci. Pollut. Res. 21 (14) (2014) 8336–8367, https://doi.org/10.1007/s11356-014-2783-1.

[46] K.O. Badmus, J.O. Tijania, C.P. Eze, O.O. Fatoba, L.F. Petrik, Quantification of radicals generated in a sonicator, Anal. Bioanal. Chem. Res. 3 (1) (2016) 139–147.

[47] Y. Jing, B.P. Chaplin, Mechanistic study of the validity of using hydroxyl radical probes to characterize electrochemical advanced oxidation processes, Environ. Sci. Technol. 51 (4) (2017) 2355–2365, https://doi.org/10.1021/acs.est.6b05513.

[48] Q. Liu, E. Liu, J. Li, Y. Qiu, R. Chen, Rapid ultrasonic-microwave assisted synthesis of spindle-like Ag/ZnO nanostructures and their enhanced visible-light photocatalytic and antibacterial activities, Catal. Today J. Org. Chem. 84 (2019) 9984–9994, https://doi.org/10.1021/acs.joc.9b01125.

[49] B. Jiang, J. Zheng, S. Qiu, M. Wu, Q. Zhang, Z. Yan, Q. Xue, Review on electrical discharge plasma technology for wastewater remediation, Chem. Eng. J. 236 (2014) 348–368.

[50] Lenntech I, History of Ozone, 2016, p. 1.

[51] U.V. Gunten, Ozonation of drinking water: part I. Oxidation kinetics and product formation, Water Res. 37 (7) (2003) 1443–1467, https://doi.org/10.1016/S0043-1354(02) 00457-8.

[52] U.V. Gunten, M. Ramseier, Critical Review of Literature for Rate Constants for Reaction of Chemical Oxidants with Inorganic and Organic Pollutants, Area, Eawag, Swiss Federal Institute of Aquatic Science and Technology, 8600 Dübendorf, Switzerland, 2010.

[53] W. Gujer, U.V. Gunten, A stochastic model of an ozonation reactor, Water Res. 37 (7) (2003) 1667–1677, https://doi.org/10.1016/S0043-1354(02)00456-6.

[54] Lenntech II, Ozone Toxicology, 2016, p. 1.

[55] U.V. Gunten, J. Hoigné, Factors controlling the formation of bromate during ozonation of bromide-containing waters, Aqua 41 (5) (1992) 299–304.

[56] Y. Magara, M. Itoh, T. Morioka, Application of ozone to water treatment and power consumption of ozone generating systems, Prog. Nucl. Energy 29 (1995) 175–182, https://doi.org/10.1016/0149-1970(95)00041-h.

[57] A.S. Powar, A. Perwuelz, N. Behary, L. Hoang, T. Aussenac, Application of ozone treatment for the decolorization of the reactive-dyed fabrics in a pilot-scale process—optimization through response surface methodology, Sustainability 12 (2) (2020) 471, https://doi.org/10.3390/su12020471.

[58] C.A.L. Graça, R.B. Lima, M.F.R. Pereira, A.M.T. Silva, A. Ferreira, Intensification of the ozone-water mass transfer in an oscillatory flow reactor with innovative design of periodic constrictions: optimization and application in ozonation water treatment, Chem. Eng. J. 389 (2020), 124412, https://doi.org/10.1016/j.cej.2020.124412.

[59] C. Morrison, A. Atkinson, A. Zamyadi, F. Kibuye, M. McKie, S. Hogard, P. Mollica, S. Jasim, E.C. Wert, Critical review and research needs of ozone applications related to virus inactivation: potential implications for SARS-CoV-2, Ozone Sci. Eng. (2020) 1–19, https://doi.org/10.1080/01919512.2020.1839739.

[60] (a) Q. Wen, Q. Chen, An overview of ozone therapy for treating foot ulcers in patients with diabetes, Am. J. Med. Sci. 360 (2020) 112–119, https://doi.org/10.1016/j.amjms.2020.05.012;
(b) E. Ugazio, V. Tullio, A. Binello, S. Tagliapietra, F. Dosio, Ozonated oils as antimicrobial systems in topical applications. their characterization, current applications, and advances in improved delivery techniques, Molecules 25 (2) (2020) 334, https://doi.org/10.3390/molecules25020334.

[61] L. Petani, L. Koker, J. Herrmann, V. Hagenmeyer, U. Gengenbach, C. Pylatiuk, Recent developments in ozone sensor technology for medical applications, Micromachines 11 (6) (2020) 624, https://doi.org/10.3390/mi11060624.

[62] M.B. Figueiredo, E. Heeres, P.J. Deuss, Ozone mediated depolymerization and solvolysis of technical lignins at ambient conditions in ethanol, Sustain. Energy Fuels 4 (2020) 265–276, https://doi.org/10.1039/c9se00740g.

[63] L. Afsah-Hejri, P. Hajeb, R.J. Ehsani, Application of ozone for degradation of mycotoxins in food: a review, Compr. Rev. Food Sci. Food Saf. 19 (2020) 1777–1808, https://doi.org/10.1111/1541-4337.12594.

[64] G.D. Savi, T. Gomes, S.B. Canever, A.C. Feltrin, K.C. Piacentini, R. Scussel, D. Oliveira, R.A. Machado-de-Avila, M. Cargnin, E. Angioletto, Application of ozone on rice storage: a mathematical modeling of the ozone spread, effects in the decontamination of filamentous fungi and quality attributes, J. Stored Prod. Res. 87 (2020), 101605, https://doi.org/10.1016/j.jspr.(2020)101605.

[65] Qisen Xiang, Liumin Fan, Yunfei Li, Shanshan Dong, Ke Li, Yanhong Bai, A review on recent advances in plasma-activated water for food safety: current applications and future trends, Crit. Rev. Food Sci. Nutr. (2020) 1–20, https://doi.org/10.1080/10408398.2020.1852173.

[66] F. Lin, Z. Wang, Z. Zhang, Y. He, Y. Zhu, J. Shao, D. Yuan, G. Chen, K. Cen, Flue gas treatment with ozone oxidation: an overview on NO, organic pollutants, and mercury, Chem. Eng. J. 382 (2020) 123030.

[67] Y.-Y. Xin, L. Zhou, K.-k Ma, J. Lee, H.I.A. Qazi, H.-P. Lib, C.-Y. Bao, Y.-X. Zhou, Removal of bromoamine acid in dye wastewater by gas-liquid plasma: the role of ozone and hydroxyl radical, J. Water Process Eng. 37 (2020), 101457.

[68] B.M.B. Ribeiro, T.M. Fujimoto, B.G.M. Bricio, U.L.R. Doubek, E. Tomaz, Gas-phase aromatic compounds degradation by a partially TiO2 coated photoreactor assisted with ozone, Process Saf. Environ. Prot. 135 (2020) 265–272.

[69] Y.N. Colmenares, W. Correr, B.S. Lima, V.R. Mastelaro, The effect of morphology on the ozone-gas sensing properties of zinc oxide sputtered films, Thin Solid Films 703 (2020), 137975.

[70] H. Jiang, X. Xu, R. Zhang, J. Chen, Y. Wang, Y. Zhang, F. Yang, A novel combined treatment for pyridine waste gas using liquid absorption, catalytic ozonation and sulfur autotrophic denitrification (LA-CO-SAD), Chem. Eng. J. 400 (2020), 125997.

[71] H. Zheng, S. Kong, N. Chen, Z. Niu, Y. Zhang, S. Jiang, Y. Yan, S. Qi, Source apportionment of volatile organic compounds: implications to reactivity, ozone formation, and secondary organic aerosol potential, Atmos. Res. 249 (2021), 105344.

[72] S. Ge, S. Wang, Q. Xu, T. Ho, Characterization and sensitivity analysis on ozone pollution over the Beaumont-Port Arthur Area in Texas of USA through source apportionment technologies, Atmos. Res. 247 (2021), 105249.

[73] S.M. Thagard, K. Takashima, A. Mizuno, Chemistry of the positive and negative electrical discharges formed in liquid water and above a gas–liquid surface, Plasma Chem. Plasma Process. 29 (2009) 455–473.

[74] V. Nehra, A. Kumar, H. Dwivedi, Atmospheric non-thermal plasma sources, Int. J. Eng. 2 (2008) 53–68.

[75] K.R. Stalder, J. Woloszko, I.G. Brown, C.D. Smith, Repetitive plasma discharges in saline solutions, Appl. Phys. Lett. 79 (2001) 4503–4505, https://doi.org/10.1063/1.1429752.

[76] Y. Liu, S. Mei, D. Iya-Sou, S. Cavadias, S. Ognier, Carbamazepine removal from water by dielectric barrier discharge: comparison of ex situ and in situ discharge on water, Chem. Eng. Process. Process Intensif. 56 (2012) 10–18, https://doi.org/10.1016/j.cep.2012.03.003.

[77] S.P. Rong, Y.B. Sun, Z.H. Zhao, Degradation of sulfadiazine antibiotics by water falling film dielectric barrier discharge, Chin. Chem. Lett. 25 (1) (2014) 187–192, https://doi.org/10.1016/j.cclet.2013.11.003.

[78] J. Zeng, B. Yang, X. Wang, Z. Li, X. Zhang, L. Lei, Degradation of pharmaceutical contaminant ibuprofen in aqueous solution by cylindrical wetted-wall corona discharge, Chem. Eng. J. 267 (2015) 282–288.

[79] P. Ajo, S. Preis, T. Vornamo, M. Mänttäri, M. Kallioinen, M. Louhi-Kultanen, Hospital wastewater treatment with pilot-scale pulsed corona discharge for removal of pharmaceutical residues, J. Environ. Chem. Eng. 6 (2018) 1569–1577.

[80] R. Banaschik, P. Lukes, H. Jablonowski, M.U. Hammer, K.-D. Weltmann, J. F. Kolb, Potential of pulsed corona discharges generated in water for the degradation of persistent pharmaceutical residues, Water Res. 84 (2015) 127–135.

[81] H. Zhang, Q. Huang, Z. Ke, L. Yang, X. Wang, Z. Yu, Degradation of microcystin-LR in water by glow discharge plasma oxidation at the gas-solution interface and its safety evaluation, Water Res. 46 (2012) 6554–6562.

[82] A.R. Crofton, S.M. Hudson, K. Howard, T. Pender, A. Abdelgawad, D. Wolski, W. M. Kirsch, Formulation and characterization of a plasma sterilized, pharmaceutical grade chitosan powder, Carbohydr. Polym. 146 (2016) 420–426.

[83] R.B. Gadri, J.R. Roth, T.C. Montie, K. Kelly-Wintenberg, P.P.-Y. Tsai, D. J. Helfritch, P. Feldman, D.M. Sherman, F. Karakaya, Z. Chen, UTK Plasma Sterilization Team, Sterilization and plasma processing of room temperature surfaces with a one atmosphere uniform glow discharge plasma _OAUGDP/, Surf. Coat. Technol. 131 (2000) 528–542.

[84] S.K. Pankaj, C. Bueno-Ferrer, N.N. Misra, V. Milosavljevic, C.P. O'Donnell, P. Bourke, K.M. Keener, P.J. Cullen, Applications of cold plasma technology in food packaging, Trends Food Sci. Technol. 35 (2014) 5–17.

[85] B. Wang, X. Ding, Z. Zhao, Y. Duan, Method development for directly screening pesticide residues in foodstuffs using ambient microfabricated glow discharge plasma (MFGDP) desorption/ionization mass spectrometry, Int. J. Mass Spectrom. 377 (2015) 507–514.

[86] T. Liu, Z. Cui, Y. Liu, X. Bai, In-situ fabrication of ultrafine Pd supported on nitrogen-doped reduced graphene oxide via nitrogen glow discharge plasma for catalytic reduction of 4-Nitrophenol, Appl. Catal. A Gen. 588 (2019), 117278.

[87] R. Pelalak, R. Alizadeh, E. Ghareshabani, Enhanced heterogeneous catalytic ozonation of pharmaceutical pollutants using a novel nanostructure of iron-based mineral prepared via plasma technology: a comparative study, J. Hazard. Mater. 392 (2020), 122269.

[88] M. Momeni, M. Tabibiazar, S. Khorram, M. Zakerhamidi, M. Mohammadifar, H. Valizadeh, M. Ghorbani, Pectin modification assisted by nitrogen glow discharge plasma, Int. J. Biol. Macromol. 120 (2018) 2572–2578.

[89] M.M. Rashid, M. Chowdhury, M.R. Talukder, Textile wastewater treatment by underwater parallel-multi-tube air discharge plasma jet, J. Environ. Chem. Eng. 8 (2020), 104504.

[90] E.S.M. Mouele, J.O. Tijani, M. Masikini, O.O. Fatoba, C.P. Eze, C.T. Onwordi, M. T.Z. Myint, H.H. Kyaw, J. Al-Sabahi, M. Al-Abri, S. Dobretsov, K. Laatikainen, L. F. Petrik, Spectroscopic measurements of dissolved O3, H2O2 and OH radicals in double cylindrical dielectric barrier discharge technology: treatment of methylene blue dye simulated wastewater, Plasma 3 (2020) 59–91, https://doi. org/10.3390/plasma3020007.

[91] S. Martínez-Jarquín, R. Winkler, Low-temperature plasma (LTP) jets for mass spectrometry (MS): ion processes, instrumental set-ups, and application examples, Trends Anal. Chem. 89 (2017) 133–145.

[92] M. Marković, M. Jović, D. Stanković, V. Kovačević, G. Roglić, G. Gojgić-Cvijović, D. Manojlović, Application of non-thermal plasma reactor and Fenton reaction for degradation of ibuprofen, Sci. Total Environ. 505 (2015) 1148–1155.

[93] S. Tang, D. Yuan, Y. Rao, J. Zhang, Y. Qu, J. Gu, Evaluation of antibiotic oxytetracycline removal in water using a gas phase dielectric barrier discharge plasma, J. Environ. Manag. 226 (2018) 22–29.

[94] M. Ansari, A.H. Mahvi, M.H. Salmani, M. Sharifian, H. Fallahzadeh, M. H. Ehrampoush, Dielectric barrier discharge plasma combined with nano catalyst for aqueous amoxicillin removal: performance modeling, kinetics and optimization study, energy yield, degradation pathway, and toxicity, Sep. Purif. Technol. 251 (2020), 117270, https://doi.org/10.1016/j.seppur.2020.117270.

[95] H. Zeghioud, P. Nguyen-Tri, L. Khezami, A. Amrane, A.A. Assadi, Review on discharge plasma for water treatment: mechanism, reactor geometries, active species, and combined processes, J. Water Process Eng. 38 (2020), 101664.

[96] Q. Wang, T. Wang, G. Qu, T. Zhang, Q. Sun, X. Guo, High-efficient removal of tetrabromobisphenol A in aqueous by dielectric barrier discharge: performance and degradation pathways, Sep. Purif. Technol. 240 (2020), 116615.

[97] V. Valinčius, V. Grigaitienė, A. Tamošiūnas, Report on the Different Plasma Modules for Pollution Removal MO 03, 2012. ⟨http://www.plastep.eu/filead min/dateien/Outputs/Report_on_the_different_Plasma_Modules_for_Pollution_Re moval.pdf⟩. (Accessed 12 September 2020).

[98] U. Kogelschatz, Dielectric-barrier discharges: their history, discharge physics, and industrial applications, Plasma Chem. Plasma Process. 23 (1) (2003) 1–46, https://doi.org/10.1023/A:1022470901385.

[99] H. Krause, B. Schweiger, E. Prinz, J. Kim, U. Steinfeld, Degradation of persistent pharmaceuticals in aqueous solutions by a positive dielectric barrier discharge treatment, J. Electrost. 69 (4) (2011) 333–338.

[100] K.-S. Kim, C.-S. Yang, Y.S. Mok, Degradation of veterinary antibiotics by dielectric barrier discharge plasma, Chem. Eng. J. 219 (2013) 19–27.

[101] D. Lopez-Serna, R. Petrovic, M. Barcelo, Occurrence and distribution of transformation, multi-class pharmaceuticals and their active metabolites and products in the Ebro River basin (NE Spain), Sci. Total Environ. 440 (2012) 280–289.

[102] J.L. Lopez, Dielectric Barrier Discharge, Ozone Generation, and Their Applications, Complex Plasmas Summer Institute, 2008.

[103] U. Kogelschatz, B. Eliasson, W. Egli, Dielectric-barrier discharges. Principle and Applications, J. Phys. IV Proc., EDP Sciences, 07, C4, 1997, pp. C4-47–C4-66, ff10.1051/jp4:1997405ff. ffjpa-00255561f.

[104] Lenntech III, Ozone Generation, 2016, p. 1.

[105] W.T.M. Audenaert, M. Callewaert, I. Nopens, J. Cromphout, R. Vanhoucke, A. Dumoulin, P. Dejans, S.W.H. Van Hulle, Full-scale modelling of an ozone reactor for drinking water treatment, Chem. Eng. J. 157 (2–3) (2010) 551–557.

[106] U.V. Gunten, M. Elovitz, H.-P. Kaiser, Calibration of full-scale ozonation systems with conservative and reactive tracers, J. Water Supply Res. Technol. AQUA 48 (6) (1999) 250–256, https://doi.org/10.2166/aqua.1999.0027.

[107] Y.S. Mok, J.-O. Jo, H.-J. Lee, H.T. Ahn, J.T. Kim, Application of dielectric barrier discharge reactor immersed in wastewater to the oxidative degradation of organic contaminant, Plasma Chem. Plasma Process. 27 (2007) 51–64, https://doi.org/10.1007/s11090-006-9043-1.

[108] J. Hoigné, The chemistry of ozone in water. Process Technologies for Water Treatment Earlier Brown Boveri Symposia, Springer, Boston, MA, 1988, pp. 121–141, https://doi.org/10.1007/978-1-4684-8556-1_11.

[109] B. Bethi, S.H. Sonawane, B.A. Bhanvase, S.P. Gumfekar, Nanomaterials-based advanced oxidation processes for wastewater treatment: a review, Chem. Eng. Process Intensif. 109 (2016) 178–189, https://doi.org/10.1016/j. cep.2016.08.016.

[110] T.T. Dang, V.M. Do, V.T. Trinh, Nano-catalysts in ozone-based advanced oxidation processes for wastewater treatment, Curr. Pollut. Rep. 6 (2020) 217–229, https://doi.org/10.1007/s40726-020-00147-3.

[111] M. Ansari, A. Hossein Mahvi, M. Hossein Salmani, M. Sharifian, H. Fallahzadeh, M. Hassan Ehrampoush, Dielectric barrier discharge plasma combined with nano catalyst for aqueous amoxicillin removal: performance modeling, kinetics and optimization study, energy yield, degradation pathway, and toxicity, Sep. Purif. Technol. 251 (2020) 117270, https://doi.org/10.1016/j.seppur.2020.117270.

[112] N. Sobana, K. Selvam, M. Swaminathan, Optimization of photocatalytic degradation conditions of direct red 23 using nano-Ag doped TiO2, Sep. Purif. Technol. 62 (2008) 648–653, https://doi.org/10.1016/j.seppur.2008.03.002.

[113] P.-F. Biard, B. Werghi, I. Soutrel, R. Orhand, A. Couvert, A. Denicourt-Nowicki, A. Roucoux, Efficient catalytic ozonation by ruthenium nanoparticles supported on SiO2 or TiO2: towards the use of a nonwoven fiber paper as original support, Chem. Eng. J. 289 (2016) 374–381, https://doi.org/10.1016/j.cej.2015.12.051.

[114] S.-W. Cheng, Y.-H. Li, C.-S. Yuan, P.Y. Tsai, H.Z. Shen, C.H. Hung, An innovative advanced oxidation technology for effective decomposition of formaldehyde by combining Iron modified nano-TiO2 (Fe/TiO2) photocatalytic degradation with ozone oxidation, Aerosol Air Qual. Res. 18 (2018) 3220–3233, https://doi.org/10.4209/aaqr.2018.05.0156.

[115] S. Shokrollahzadeh, M. Abassi, M. Ranjbar, A new nano-ZnO/perlite as an efficient catalyst for catalytic ozonation of azo dye, Environ. Eng. Res. 24 (2018) 513–520, https://doi.org/10.4491/eer.2018.322.

[116] M.W. Lekota, K.M. Dimpe, P.N. Nomngongo, MgO-ZnO/carbon nanofiber nanocomposite as an adsorbent for ultrasound-assisted dispersive solid-phase microextraction of carbamazepine from wastewater prior to high-performance liquid chromatographic detection, J. Anal. Sci. Technol. 10 (25) (2019) 1–12, https://doi.org/10.1186/s40543-019-0185-1.

[117] T.H.Y. Duong, T.N. Nguyen, H.T. Oanh, T.A.D. Thi, L.N.T. Giang, H.T. Phuong, N. Tuan Anh, B.M. Nguyen, V.T. Quang, G.T. Le, T.V. Nguyen, Mechanisms of disposal of acid and alkali in rabbit duodenum, Am. J. Physiol. 229 (1975) 1641, https://doi.org/10.1155/2019/4376429, 1–1648.

[118] G. Asgari, A. Seidmohammadi, A. Esrafili, J. Faradmal, M. Noori Sepehr, M. Jafarinia, The catalytic ozonation of diazinon using nano-MgO-CNT-Gr as a new heterogenous catalyst: the optimization of effective factors by response surface methodology, RSC Adv. 10 (2020) 7718–7731, https://doi.org/10.1039/C9RA10095D.

[119] Y. Huang, J. Jiang, L. Ma, Y. Wang, M. Liang, Z. Zhang, L. Li, Iron foam combined ozonation for enhanced treatment of pharmaceutical wastewater, Environ. Res. 183 (2020) 109205, https://doi.org/10.1016/j.envres.2020.109205.

[120] Y. Guo, L. Yang, X. Cheng, X. Wang, The application and reaction mechanism of catalytic ozonation in water treatment, J. Environ. Anal. Toxicol. 2 (2012) 1–6, https://doi.org/10.4172/2161-0525.1000150.

[121] S. Khuntia, M.K. Sinha, P. Singh, Theoretical and experimental investigation of the mechanism of the catalytic ozonation process by using a manganese-based catalyst, Environ. Technol. (2019) 1–8, https://doi.org/10.1080/09593330.2019.1640800.

[122] B. Wang, H. Zhang, F. Wang, X. Xiong, K. Tian, Y. Sun, T. Yu, Application of heterogeneous catalytic ozonation for refractory organics in wastewater, Catalysts 9 (241) (2019) 1–43, https://doi.org/10.3390/catal9030241.

[123] J. Wang, X. Quan, S. Chen, H. Yu, Y. Chen, Performing homogeneous catalytic ozonation using heterogeneous Mn2+−bonded oxidized carbon nanotubes by self-driven pH variation induced reversible desorption and adsorption of Mn2+, Environ. Sci. Nano 6 (2019) 1932–1940, https://doi.org/10.1039/C9EN00204A.

[124] N. Savage, M.S. Diallo, Nanomaterials and water purification: opportunities and challenges, J. Nanopart. Res. 7 (2005) 331–342, https://doi.org/10.1007/s11051-005-7523-5.

[125] M.T. Amin, A.A. Alazba, U. Manzoor, A review of removal of pollutants from water/wastewater using different types of nanomaterials, Adv. Mater. Sci. Eng. 2014 (2014) 1–24. ⟨https://www.hindawi.com/journals/amse/2014/825910/⟩.

[126] B. Legube, Catalytic ozonation: a promising advanced oxidation technology for water treatment, Catal. Today 53 (1999) 61–72, https://doi.org/10.1016/S0920-5861(99)00103-0.

[127] X. Li, J. Ma, H. He, Recent advances in catalytic decomposition of ozone, J. Environ. Sci. 94 (2020) 14–31, https://doi.org/10.1016/j.jes.2020.03.058 (China).

[128] S.N. Malik, P.C. Ghosh, A.N. Vaidya, S.N. Mudliar, Hybrid ozonation process for industrial wastewater treatment: principles and applications: a review, J. Water Process Eng. 35 (2020) 101193, https://doi.org/10.1016/j.jwpe.2020.101193.

[129] N.B. McGuinness, M. Ziółek, A. Whelan, H. John, C. Zhao, G. Zhang, D. Dionysiou Dionysios, Byrne J. Anthony, S.C. Pillai, Nanotechnology solutions for global water challenges. Water Challenges and Solutions on a Global Scale, 2015, pp. 375–411, https://doi.org/10.1021/bk-2015-1206.ch018.

[130] B. Kasprzyk-Hordern, M. Ziółek, J. Nawrocki, Catalytic ozonation and methods of enhancing molecular ozone reactions in water treatment, Appl. Catal. B Environ. 46 (2003) 639–669, https://doi.org/10.1016/S0926-3373(03)00326-6.

[131] L. Zhao, Z. Sun, J. Ma, H. Liu, Enhancement mechanism of heterogeneous catalytic ozonation by cordierite-supported copper for the degradation of

nitrobenzene in aqueous solution, Environ. Sci. Technol. 43 (2009) 2047–2053, https://doi.org/10.1021/es803125h.

[132] G. Moussavi, A. khavanin, R. Alizadeh, The integration of ozonation catalyzed with MgO nanocrystals and the biodegradation for the removal of phenol from saline wastewater, Appl. Catal. B Environ. 97 (2010) 160–167, https://doi.org/10.1016/j.apcatb.2010.03.036.

[133] B. Wang, X. Xiong, H. Ren, Z. Huang, Preparation of MgO nanocrystals and catalytic mechanism on phenol ozonation, RSC Adv. 7 (69) (2017) 43464–43473, https://doi.org/10.1039/c7ra07553g.

[134] A. Alinejad, H. Akbari, M. Ghaderpoori, A.K. Jeihooni, A. Adibzadeh, Catalytic ozonation process using a MgO nano-catalyst to degrade methotrexate from aqueous solutions and cytotoxicity studies in human lung epithelial cells (A549) after treatment, RSC Adv. 9 (15) (2019) 8204–8214, https://doi.org/10.1039/c9ra00320g.

[135] S.S. Sable, K.J. Shah, P.-C. Chiang, S.-L. Lo, Catalytic oxidative degradation of phenol using iron oxide promoted sulfonated-ZrO2 by advanced oxidation processes (AOPs), J. Taiwan Inst. Chem. Eng. 91 (2018) 434–440, https://doi.org/10.1016/j.jtice.2018.06.030.

[136] J. Ma, X. Li, C. Zhang, Q. Ma, H. He, Novel CeMnaOx catalyst for highly efficient catalytic decomposition of ozone, Appl. Catal. B Environ. 264 (2020), 118498, https://doi.org/10.1016/j.apcatb.2019.118498.

[137] Niu, T. Wei, Q. Li, G. Zhang, G. Xian, Z. Long, Z. Ren, Ce-based catalysts used in advanced oxidation processes for organic wastewater treatment: a review, J. Environ. Sci. 96 (2020) 109–116, https://doi.org/10.1016/j.jes.2020.04.033.

[138] V.V. Patil, P.R. Gogate, A.P. Bhat, P.K. Ghosh, Treatment of laundry wastewater containing residual surfactants using combined approaches based on ozone, catalyst, and cavitation, Sep. Purif. Technol. 239 (2020), 116594, https://doi.org/10.1016/j.seppur.2020.116594.

[139] Qi.C. Guo, X. Xu, B. Gao, Q. Yue, B. Jiang, Z. Qian, C. Wang, Y. Zhang, Co/Fe and Co/Al layered double oxides ozone catalyst for the deep degradation of aniline: preparation, characterization, and kinetic model, Sci. Total Environ. 715 (2020), 136982, https://doi.org/10.1016/j.scitotenv.2020.136982.

[140] I. Pana, V. Braic, M. Dinu, E.S.M. Mouele, A.C. Parau, L.F. Petrik, M. Braic, In vitro corrosion of titanium nitride and oxynitride-based biocompatible coatings deposited on stainless steel, Coatings 10 (8) (2020) 710, https://doi.org/10.3390/coatings10080710.

[141] J. Ma, M. Sui, T. Zhang, C. Guan, Effect of pH on MnOx/GAC catalyzed ozonation for degradation of nitrobenzene, Water Res. 39 (2005) 779–786, https://doi.org/10.1016/j.watres.2004.11.020.

[142] M.-O. Buffle, J. Schumacher, S. Meylan, M. Jekel, U. von Gunten, Ozonation and advanced oxidation of wastewater: effect of O3 dose, pH, DOM and HO.-scavengers on ozone decomposition and HO. generation, Ozone Sci. Eng. 28 (2006) 247–259, https://doi.org/10.1080/01919510600718825.

[143] M.S. Elovitz, U. von Gunten, H.-P. Kaiser, Hydroxyl radical/ozone ratios during ozonation processes. II. The effect of temperature, pH, alkalinity, and DOM properties, Ozone Sci. Eng. 22 (2000) 123–150, https://doi.org/10.1080/01919510008547216.

[144] A.M. Amat, A. Arques, M.a. Miranda, R. Vincente, S. Seguí, Degradation of two commercial anionic surfactants by means of ozone and/or UV irradiation, Environ. Eng. Sci. 24 (2007) 790–794, https://doi.org/10.1089/ees.2006.0030.

[145] A.J. Barik, P.R. Gogate, Degradation of 4-chloro 2-aminophenol using combined strategies based on ultrasound, photolysis, and ozone, Ultrason. Sonochem. 28 (2016) 90–99, https://doi.org/10.1016/j.ultsonch.2015.07.001.

[146] A.J. Barik, P.R. Gogate, Degradation of 2,4-dichlorophenol using combined approach based on ultrasound, ozone, and catalyst, Ultrason. Sonochem. 36 (2017) 517–526, https://doi.org/10.1016/j.ultsonch.2016.08.017.

[147] J. Sanz, J.I. Lombraña, A.M. De Luis, F. Varona, UV/H2O2 chemical oxidation for high loaded effluents: a degradation kinetic study of las surfactant wastewaters, Environ. Technol. 24 (2003) 903–911, https://doi.org/10.1080/09593330309385627.

[148] R.C. Martins, A.M. Silva, S. Castro-Silva, P. Garção-Nunes, R.M. Quinta-Ferreira, Advanced oxidation processes for treatment of effluents from a detergent industry, Environ. Technol. 32 (2011) 1031–1041.

[149] G. Boczkaj, A. Fernandes, Wastewater treatment by means of advanced oxidation processes at basic pH conditions: a review, Chem. Eng. J. 320 (2017) 608–633, https://doi.org/10.1016/j.cej.2017.03.084.

[150] F.J. Beltrán, J.F. García-Araya, P.M. Álvarez, Sodium dodecylbenzene sulfonate removal from water and wastewater. 1. Kinetics of decomposition by ozonation, Ind. Eng. Chem. Res. 39 (2000) 2214–2220, https://doi.org/10.1021/ie990721a.

[151] X.-J. Wang, Y. Song, J.-S. Mai, Combined Fenton oxidation and aerobic biological processes for treating a surfactant wastewater containing abundant sulfate, J. Hazard. Mater. 160 (2008) 344–348, https://doi.org/10.1016/j.jhazmat.2008.02.117.

[152] H. Zangeneh, A.A.L. Zinatizadeh, M. Feizy, A comparative study on the performance of different advanced oxidation processes (UV/O3/H2O2) treating linear alkyl benzene (LAB) production plant's wastewater, J. Ind. Eng. Chem. 20 (2014) 1453–1461, https://doi.org/10.1016/j.jiec.2013.07.031.

[153] T.E. Agustina, H.M. Ang, V.K. Vareek, A review of synergistic effect of photocatalysis and ozonation on wastewater treatment, J. Photochem. Photobiol. C 6 (2005) 264–273, https://doi.org/10.1016/j.jphotochemrev.2005.12.003.

[154] U. Kogelschatz, Fundamentals and Applications of Dielectric-Barrier Discharges, 2000.

[155] J. Jo, Y.S. Mok, In-situ production of ozone and ultraviolet light using a barrier discharge reactor for wastewater treatment, J. Zhejiang Univ. Sci. A 10 (9) (2009) 1359–1366.

[156] Y.S. Mok, J.-O. Jo, J.C. Whitehead, Degradation of an azo dye Orange II using a gas phase dielectric barrier discharge reactor submerged in water, Chem. Eng. J. 142 (1) (2008) 56–64, https://doi.org/10.1016/j.cej.2007.11.012.

[157] M. Tichonovas, E. Krugly, V. Racys, R. Hippler, V. Kauneliene, I. Stasiulaitiene, D. Martuzevicius, Degradation of various textile dyes as wastewater pollutants under dielectric barrier discharge plasma treatment, Chem. Eng. J. 229 (2013) 9–19, https://doi.org/10.1016/j.cej.2013.05.095.

[158] P.M.K. Reddy, S. Mahammadunnisa, C. Subrahmanyam, Catalytic non-thermal plasma reactor for mineralization of endosulfan in aqueous medium: a green approach for the treatment of pesticide contaminated water, Chem. Eng. J. 238 (2014) 157–163, https://doi.org/10.1016/j.cej.2013.08.087.

[159] N. Wardenier, P. Vanraes, A. Nikiforov, S.W.H. Van Hulle, C. Leys, Removal of micropollutants from water in a continuous-flow electrical discharge reactor, J. Hazard. Mater. 362 (2019) 238–245, https://doi.org/10.1016/j.jhazmat.2018.08.095.

[160] N. Wardenier, Z. Liu, A. Nikiforov, S.W.H. Van Hulle, C. Leys, Micropollutant elimination by O3, UV and plasma-based AOPs: an evaluation of treatment and energy costs, Chemosphere 234 (2019) 715–724, https://doi.org/10.1016/j.chemosphere.2019.06.033.

[161] N. Wardenier, Y. Gorbanev, I. Van Moer, A. Nikiforov, S.W.H. Van Hulle, P. Surmont, F. Lynen, C. Leys, A. Bogaerts, P. Vanraes, Removal of alachlor in water by non-thermal plasma: reactive species and pathways in batch and continuous process, Water Res. 161 (2019) 549–559, https://doi.org/10.1016/j.watres.2019.06.022.

[162] S. Rong, Y. Sun, Z. Zhao, H. Wang, Dielectric barrier discharge induced degradation of diclofenac in aqueous solution, Water Sci. Technol. 69 (1) (2014) 76–83, https://doi.org/10.2166/wst.2013.554.

[163] X. Tao, C. Yang, Z. Wei, L. Huang, J. Chen, W. Cong, R. Xie, D. Xu, Synergy between Fenton process and DBD for methyl orange degradation, Mater. Res. Bull. 120 (2019), 110581, https://doi.org/10.1016/j.materresbull.2019.110581.

[164] S. Tang, D. Yuan, Y. Rao, M. Li, G. Shi, J. Gu, T. Zhang, Percarbonate promoted antibiotic decomposition in dielectric barrier discharge plasma, J. Hazard. Mater. 366 (2019) 669–676.

[165] M. Magureanu, D. Piroi, N.B. Mandache, V. David, A. Medvedovici, V. I. Parvulescu, Degradation of pharmaceutical compound pentoxifylline in water by non-thermal plasma treatment, Water Res. 44 (2010) 3445–3453.

[166] M. Magureanu, D. Piroi, N.B. Mandache, V. David, A. Medvedovici, C. Bradu, V. I. Parvulescu, Degradation of antibiotics in water by non-thermal plasma treatment, Water Res. 45 (2011) 3407–3416.

[167] K.S. Kim, S.K. Kam, Y.S. Mok, Elucidation of the degradation pathways of sulfonamide antibiotics in a dielectric barrier discharge plasma system, Chem. Eng. J. 271 (2015) 31–42.

[168] P. Vanraes, G. Willems, N. Daels, S.W.H. Van Hulle, K. De Clerck, P. Surmont, F. Lynen, Z. Vandamme, J. Van Durme, A. Nikiforov, C. Leys, Decomposition of atrazine traces in water by combination of non-thermal electrical discharge and adsorption on nanofiber membrane, Water Res. 72 (2015) 361–371.

[169] M.A. Malik, A. Ghaffar, S.A. Malik, Water purification by electrical discharges, Plasma Sources Sci. Technol. 10 (2001) 82–91, https://doi.org/10.1088/0963-0252/10/1/311.

[170] G. Okolongo, Advanced Oxidative Water Treatment Process Using an Electrohydraulic Prototype Design Case Study Results Conclusions & Scopes, 2011, pp. 1–8.

[171] M. Magureanu, D. Dobrin, N.B. Mandache, C. Bradu, A. Medvedovici, V. I. Parvulescu, The mechanism of plasma destruction of enalapril and related metabolites in water, Plasma Process. Polym. 10 (2013) 459–468, https://doi.org/10.1002/ppap.201200146.

[172] B.R. Locke, M. Sato, P. Sunka, M.R. Hoffmann, J.S. Chang, Electrohydraulic discharge and nonthermal plasma for water treatment, Ind. Eng. Chem. Res. 45 (2006) 882–905, https://doi.org/10.1021/ie050981u.

[173] P.K. Panicker. Ionization of Air by Corona Discharge, University of Texas at Arlington, 2003. Master of Science in Aerospace Engineering.

[174] G.V. Buxton, C.L. Greenstock, W.P. Helman, A.B. Ross, Critical review of rate constants for reactions of hydrated electrons, hydrogen atoms and hydroxyl radicals (·OH/·O−) in aqueous solution, J. Phys. Chem. Ref. Data 17 (2) (1988) 513–886, https://doi.org/10.1063/1.555805.

[175] W.H. Glaze, Reaction products of ozone: a review, Environ. Health Perspect. 69 (1986) 151–157.

[176] H. Biinger, Ullmann's Encyclopedia of Industrial Chemistry, Vol. B 1: Fundamentals of Chemical Engineering, VCH, Weinheim – New York – Basel – Cambridge 1990, XV, 833 S., 490 Abb. u. 114 Tab., geb., DM 530, Chemie Ing. Tech., 63, 1991, pp. 830–830. (https://doi.org/10.1002/cite.330630809).

[177] R.E. Kirk, D.F. Othmer, Encyclopedia of Chemical Technology, 4th ed., Ozone, Wiley-Interscience, London, ISBN 0-471-52686-X, 1996, pp. 953–994.

[178] D.R. Lide, Handbook of chemistry and physics, 79th ed., Solubility of Selected Gases in Water, Chemical Rubber Co, Cleveland (OH), ISBN, 8(89), 1999, pp. 8–86.

[179] R. Atkinson, Kinetics and mechanisms of the gas-phase reactions of the hydroxyl radical with organic compounds under atmospheric conditions, Chem. Rev. 85 (1985) 69–201.

[180] R.P. Haugland, Handbook of fluorescence probes, 6th ed., Molecular Probes, Eugene (OR), 1996.

[181] M.D. Gurol, R. Vatistas, Oxidation of phenolic compounds by ozone and ozone + u.v. radiation: a comparative study, Water Res. 21 (8) (1987) 895–900, https://doi.org/10.1016/S0043-1354(87)80006-4.

[182] W.F.L.M. Hoeben, Pulsed Corona-Induced Degradation of Organic Materials in Water, Technische Universiteit Eindhoven, Eindhoven, 2000, Proefschrift-ISBN 90386-15493 NUGI 812.

[183] M. Dors, Plasma Water Treatment, Centre for Plasma and Laser Engineering, The Szewalski Institute of Fluid-Flow Machinery Polish Academy of Sciences Gdaosk, Poland, 2007. ⟨http://www.plastep.eu/fileadmin/dateien/Events/2011/11 0725_Summer_School/Plasma_water_treatment.pdf⟩.

[184] P.J. Bruggeman, M.J. Kushner, B.R. Locke, J.G.E. Gardeniers, W.G. Graham, D. B. Graves, R.C.H.M. Hofman-Caris, Plasma–liquid interactions: a review and roadmap, Plasma Sources Sci. Technol. 25 (2016), 053002 (59pp).

[185] J.E. Foster, Plasma-based water purification: challenges and prospects for the future, Phys. Plasmas 24 (5) (2017), 055501, https://doi.org/10.1063/1.4977921.

[186] A.G. Wilson, Ozone: a versatile oxidizing agent in academic syntheses and industrial processes, Synlett Spotlight 262 (1) (2009) 155–156, https://doi.org/10.1055/s-0028-1083138.

[187] J. Rivera-Utrilla, M. Sánchez-Polo, C.A. Zaror, Degradation of naphthalene sulfonic acids by oxidation with ozone in aqueous phase, Phys. Chem. Chem. Phys. 4 (2002) 1129–1134, https://doi.org/10.1039/B108194B.

[188] V. Yargeau, C. Leclair, Impact of operating conditions on decomposition of antibiotics during ozonation: a review, Ozone Sci. Eng. 30 (2008) 175–188, https://doi.org/10.1080/01919510701878387.

[189] J. Madureira, E. Ceriani, N. Pinhao, E. Marotta, R. Melo, S.C. Verde, C. Paradisi, F. M.A. Margaça, Oxidation of clofibric acid in aqueous solution using a non-thermal plasma discharge or gamma radiation, Chemosphere 187 (2017) 395–403.

[190] S. Tang, D. Yuan, Y. Rao, N. Li, J. Qi, T. Cheng, Z. Sun, J. Gu, H. Huang, Persulfate activation in gas phase surface discharge plasma for synergetic removal of antibiotic in water, Chem. Eng. J. 337 (2018) 446–454.

[191] Y. Liu, H. Zhang, J. Sun, J. Liu, X. Shen, J. Zhan, A. Zhang, S. Ognier, S. Cavadias, P. Li, Degradation of aniline in aqueous solution using non-thermal plasma generated in microbubbles, Chem. Eng. J. 345 (2018) 679–687.

[192] W. Sang, J. Cui, Y. Feng, L. Mei, Q. Zhang, D. Li, W. Zhang, Degradation of aniline in aqueous solution by dielectric barrier discharge plasma: mechanism and degradation pathways, Chemosphere 223 (2019) 416–424.

[193] M. Magureanu, N.B. Mandache, V.I. Parvulescu, Degradation of pharmaceutical compounds in water by non-thermal plasma treatment, Water Res. 81 (2015) 124–136.

[194] G. Iervolino, V. Vaiano, V. Palma, Enhanced removal of water pollutants by dielectric barrier discharge nonthermal plasma reactor, Sep. Purif. Technol. 215 (2019) 155–162.

[195] X.-Y. Pan, X.-C. Qiao, Influences of nitrite on paracetamol degradation in dielectric barrier discharge reactor, Ecotoxicol. Environ. Saf. 180 (2019) 610–615.

[196] O.V. Alekseeva, S.D. Razumovskii, Kinetics of phenol oxidation with ozone in a thin layer on a solid surface, Kinet. Catal. 47 (2006) 533–536, https://doi.org/10.1134/S0023158406040082.

[197] R.F. Dantas, M. Canterino, R. Marotta, C. Sans, S. Esplugas, R. Andreozzi, Bezafibrate removal by means of ozonation: primary intermediates, kinetics, and toxicity assessment, Water Res. 41 (12) (2007) 2525–2532, https://doi.org/10.1016/j.watres.2007.03.011.

[198] R. Munter, S. Preis, S. Kamenev, E. Siirde, Methodology of ozone introduction into water and wastewater treatment, Ozone Sci. Eng. 15 (1993) 149–165, https://doi.org/10.1080/01919519308552265.

[199] A. Pintar, G. Berčič, M. Besson, P. Gallezot, Catalytic wet-air oxidation of industrial effluents: total mineralization of organics and lumped kinetic modelling, Appl. Catal. B Environ. 47 (2004) 143–152, https://doi.org/10.1016/j.apcatb.2003.08.005.

[200] Y. Du, M. Qiu, Comparative study of advanced oxidation for textile wastewater, Desalin. Water Treat. 51 (31–33) (2013) 5954–5958, https://doi.org/10.1080/19443994.2012.763051.

[201] U. Hübner, U.V. Gunten, M. Jekel, Evaluation of the persistence of transformation products from ozonation of trace organic compounds – a critical review, Water Res. 68 (2015) 150–170.

[202] Y. Chen, L. Sun, Z. Yu, L. Wang, G. Xiang, S. Wan, Synergistic degradation performance, and mechanism of 17β-estradiol by dielectric barrier discharge non-thermal plasma combined with Pt–TiO2, Sep. Purif. Technol. 152 (2015) 46–54.

[203] A. Khataee, R. Honarnezhad, M. Fathinia, Degradation of sodium isopropyl xanthate from aqueous solution using sonocatalytic process in the presence of chalcocite nanoparticles: insights into the degradation mechanism and phytotoxicity impacts, J. Environ. Manag. 211 (2018) 225–237, https://doi.org/10.1016/j.jenvman.2018.01.054.

[204] S.P. Ghuge, A.K. Saroha, Catalytic ozonation for the treatment of synthetic and industrial effluents – application of mesoporous materials: a review, J. Environ. Manag. 211 (2018) 83–102, https://doi.org/10.1016/j.jenvman.2018.01.052.

[205] J. Gu, X. Fan, X. Liu, S. Li, Z. Wang, S. Tang, D. Yuan, Mesoporous manganese oxide with large specific surface area for high-performance asymmetric supercapacitor with enhanced cycling stability, Chem. Eng. J. 324 (2017) 35–43, https://doi.org/10.1016/j.cej.2017.05.014.

[206] R.M. Sellers, Spectrophotometric determination of hydrogen-peroxide using potassium titanium (Iv) oxalate, Analyst 105 (1980) 950–954, https://doi.org/10.1039/an9800500950.

[207] T.C. Wang, G.Z. Qu, X.Q. Yin, Q.H. Sun, D.L. Liang, X.T. Guo, H.Z. Jia, Dimethyl phthalate elimination from micro-polluted source water by surface discharge plasma: performance, active species roles and mechanisms, J. Hazard. Mater. 357 (2018) 279–288, https://doi.org/10.1016/j.jhazmat.2018.06.014.

[208] M. Deborde, S. Rabouan, P. Mazellier, J.-P. Duguet, B. Legube, Oxidation of bisphenol A by ozone in aqueous solution, Water Res. 42 (16) (2008) 4299–4308, https://doi.org/10.1016/j.watres.2008.07.015.

[209] A. Colombo, G. Cappelletti, S. Ardizzone, I. Biraghi, C.L. Bianchi, D. Meroni, C. Pirola, F. Spadavecchia, A endocrine disruptor complete degradation using TiO2 photocatalysis with ozone, Environ. Chem. Lett. 10 (1) (2011) 55–60, https://doi.org/10.1007/s10311-011-0328-0.

[210] K.S. Tay, N.A. Rahman, M.R.B. Abas, Degradation of bisphenol A by ozonation: rate constants, influence of inorganic anions, and by-products, Maejo Int. J. Sci. Technol. 6 (01) (2012) 77–94.

[211] J.C.C. Da Silva, J.A. Reis Teodoro, R.J. de, C.F. Afonso, S.F. Aquino, R. Augusti, Photodegradation of bisphenol A in aqueous medium: monitoring and identification of by-products by liquid chromatography coupled to high-resolution mass spectrometry, Rapid Commun. Mass Spectrom. 28 (9) (2014) 987–994, https://doi.org/10.1002/rcm.6863.

[212] Lenntech IV, Ozone Reaction Mechanisms, 2016, p. 1.

[213] P.A. Mikheyev, A.V. Demyanov, I.V. Kochetov, A.A. Sludnova, A.P. Torbin, A. M. Mebel, V.N. Azyazov, Ozone and oxygen atoms production in a dielectric barrier discharge in pure oxygen and O2/CH4 mixtures. Modeling and experiment, Plasma Sources Sci. Technol. 29 (1) (2020) 1–17.

[214] K.H. Baek, Y.S. Heo, J.Y. Park, T. Kang, Y.E. Lee, J. Lim, S.B. Kim, C. Jo, Inactivation of Salmonella typhimurium by non-thermal plasma bubbles: exploring the key reactive species and the influence of organic matter, Foods 9 (11) (2020) 1689, https://doi.org/10.3390/foods9111689.

[215] T. Wang, G. Qu, J. Ren, Q. Yan, Q. Sun, D. Liang, S. Hu, Evaluation of the potentials of humic acid removal in water by gas phase surface discharge plasma, Water Res. 89 (2016) 28–38.

[216] K.H.H. Aziz, H. Miessner, S. Mueller, A. Mahyar, D. Kalass, D. Moeller, I. Khorshid, M.A.M. Rashid, Comparative study on 2,4-dichlorophenoxyacetic acid and 2,4-dichlorophenol removal from aqueous solutions via ozonation, photocatalysis and non-thermal plasma using a planar falling film reactor, J. Hazard. Mater. 343 (2018) 107–115.

[217] F. Judée, S. Simon, C. Bailly, T. Dufour, Plasma-activation of tap water using DBD for agronomy applications: identification and quantification of long lifetime chemical species and production/consumption mechanisms, Water Res. 133 (2018) 47–59.

[218] K. Wang, J. Pang, L. Li, S. Zhou, Y. Li, T. Zhang, Synthesis of hydrophobic carbon nanotubes/reduced graphene oxide composite films by flashlight irradiation, Front. Chem. Sci. Eng. 12 (2018) 376–382.

[219] C. Wang, S. Sun, L. Zhang, J. Yin, T. Jiao, L. Zhang, Y. Xu, J. Zhou, Q. Peng, Facile preparation, and catalytic performance characterization of AuNPs-loaded hierarchical electrospun composite fibers by solvent vapor annealing treatment, Colloids Surf. A Physicochem. Eng. Asp. 561 (2019) 283–291.

[220] P.R. Gogate, A.B. Pandit, A review of imperative technologies for wastewater treatment I: oxidation technologies at ambient conditions, Adv. Environ. Res. 8 (3–4) (2004) 501–551.

[221] J. Staehelin, Hoigne, Decomposition of ozone in water in the presence of organic solutes acting as promoters and inhibitors of radical chain reactions, Environ. Sci. Technol. 19 (12) (1985) 1206–1213, https://doi.org/10.1021/es00142a012.

[222] R. Munter, Advance oxidation processes – current status and prospects, Proc. Estonian Acad. Sci. Chem. 50 (2) (2001) 59–80.

[223] S.G. Bratsch, Standard electrode potentials and temperature coefficients in water at 298.15 K, J. Phys. Chem. Ref. Data 18 (1) (1989) 1–21, https://doi.org/10.1063/1.555839.

[224] O. Legrini, E. Oliveros, A.M. Braun, Photochemical processes for water treatment, Chem. Rev. 93 (2) (1993) 671–698.

[225] O. Carp, C.L. Huisman, A. Reller, Photoinduced reactivity of titanium dioxide, Prog. Solid State Chem. 32 (1–2) (2004) 33–177, https://doi.org/10.1016/j.progsolidstchem.2004.08.001.

[226] R. Gilmour, M. Ray, Water Treatment Using Advanced Oxidation Processes: Application Perspectives, 2012. Available at: ⟨https://ir.lib.uwo.ca/etdhttps://ir.lib.uwo.ca/etd/836⟩.

[227] D. Chen, M. Sivakumar, A.K. Ray, Heterogeneous photocatalysis in environmental remediation, Asia-Pac. J. Chem. Eng. 8 (5–6) (2000) 505–550, https://doi.org/10.1017/CBO9781107415324.004.

[228] E.S.M. Mouele, M. Dinu, F. Cummings, O.O. Fatoba, M.T.Z. Myint, H.H. Kyaw, A. C. Parau, A. Vladescu, M.G. Francesconi, S. Pescetelli, A. Di Carlo, A. Agresti, M. Al-Abri, S. Dobretsov, M. Braic, L.F. Petrik, Effect of calcination time on the physicochemical properties and photocatalytic performance of carbon and nitrogen co-doped TiO2 nanoparticles, Catalysts 10 (8) (2020) 847, https://doi.org/10.3390/catal10080847.

[229] W.K. Lafi, Z. Al-Qodah, Combined advanced oxidation and biological treatment processes for the removal of pesticides from aqueous solutions, J. Hazard. Mater. 137 (1) (2006) 489–497, https://doi.org/10.1016/j.jhazmat.2006.02.02.

[230] S. Babić, M. Zrnčić, D. Ljubas, L. Ćurković, I. Škorić, Photolytic and thin TiO2 film assisted photocatalytic degradation of sulfamethazine in aqueous solution, Environ. Sci. Pollut. Res. 22 (15) (2015) 11372–11386, https://doi.org/10.1007/s11356-015-4338-5.

[231] P. Nyamukamba, L. Tichagwa, J.C. Ngila, L. Petrik, Plasmonic metal decorated titanium dioxide thin films for enhanced photodegradation of organic contaminants, J. Photochem. Photobiol. A Chem. 343 (2017) 85–95, https://doi.org/10.1016/j.jphotochem.2017.04.014.

[232] P. Nyamukamba, L. Tichagwa, S. Mamphweli, L. Petrik, Silver/carbon codoped titanium dioxide photocatalyst for improved dye degradation under visible light, Int. J. Photoenergy 2017 (2017) 1–9, https://doi.org/10.1155/2017/3079276.

[233] J. Ren, J. Li, L. Lv, J. Wang, Degradation of caffeic acid by dielectric barrier discharge plasma combined with Ce doped CoOOH catalyst, J. Hazard. Mater. 402 (2021), 123772, https://doi.org/10.1016/j.jhazmat.2020.123772.

[234] X. Yan, C. Yi, Y. Wang, W. Cao, D. Mao, Q. Ou, P. Shen, H. Wang, Multi-catalysis of nano-zinc oxide for bisphenol A degradation in a dielectric barrier discharge plasma system: effect and mechanism, Sep. Purif. Technol. 231 (2020), 115897, https://doi.org/10.1016/j.seppur.2019.115897.

[235] J. Cheng, D. Wang, B. Wang, H. Ning, Y. Zhang, Y. Li, J. An, P. Gao, Plasma-catalytic degradation of ciprofloxacin in aqueous solution over different MnO2 nanocrystals in a dielectric barrier discharge system, Chemosphere 253 (2020), 126595, https://doi.org/10.1016/j.chemosphere.2020.126595.

[236] S. Li, H. Chen, X. Wang, X. Dong, Y. Huang, D. Guo, Catalytic degradation of clothianidin with graphene/TiO2 using a dielectric barrier discharge (DBD) plasma system, Environ. Sci. Pollut. Res. 27 (2020) 29599–29611, https://doi.org/10.1007/s11356-020-09303-0.

[237] W. Haixia, F. Jiawei, C. Weigang, Y. Chenwei, Dielectric barrier discharge-coupled Fe-based zeolite to remove ammonia nitrogen and phenol pollutants from water, Sep. Purif. Technol. 243 (2020), 116344, https://doi.org/10.1016/j.seppur.2019.116344.

[238] D. He, Y. Sun, L. Xin, J. Feng, Aqueous tetracycline degradation by non-thermal plasma combined with nano-TiO2, Chem. Eng. J. 258 (2014) 18–25.

[239] F.J. Beltrán, J.M. Encinar, M.A. Alonso, Nitroaromatic hydrocarbon ozonation in water: 2. Combined ozonation with hydrogen peroxide or UV radiation, Ind. Eng. Chem. Res. 37 (1998) 32–40, https://doi.org/10.1021/ie9704253.

[240] F.J. Beltrán, A. Aguinaco, J.F. García-Araya, A. Oropesa, Ozone and photocatalytic processes to remove the antibiotic sulfamethoxazole from water, Water Res. 42 (14) (2008) 3799–3808.

[241] O.L. Li, J.S. Chang, Y. Guo, Pulsed arc electrohydraulic discharge characteristics and plasma parameters of sludge-water, in: Proceedings of the IEEE Conference on Electrical Insulation and Dielectric Phenomena, 2009, pp. 331–334, doi: ⟨10.1109/ceidp.2009.5377847⟩.

[242] G. Zhang, Y. Sun, C. Zhang, Z. Yu, Decomposition of acetaminophen in water by a gas phase dielectric barrier discharge plasma combined with TiO2-rGO nanocomposite: mechanism and degradation pathway, J. Hazard. Mater. 323 (2017) 719–729, https://doi.org/10.1016/j.jhazmat.2016.10.008.

[243] K.H.H. Aziz, H. Miessner, S. Mueller, D. Kalass, D. Moeller, I. Khorshid, M.A. M. Rashid, Degradation of pharmaceutical diclofenac and ibuprofen in aqueous solution, a direct comparison of ozonation, photocatalysis, and non-thermal plasma, Chem. Eng. J. 313 (2017) 1033–1041.

[244] L. Xin, Y. Sun, J. Feng, J. Wang, D. He, Degradation of triclosan in aqueous solution by dielectric barrier discharge plasma combined with activated carbon fibers, Chemosphere 144 (2016) 855–863, https://doi.org/10.1016/j.chemosphere.2015.09.054.

[245] J. Wang, Y. Sun, J. Feng, L. Xin, J. Ma, Degradation of triclocarban in water by dielectric barrier discharge plasma combined with TiO2/activated carbon fibers: effect of operating parameters and byproducts identification, Chem. Eng. J. 300 (2016) 36–46, https://doi.org/10.1016/j.cej.2016.04.041.

[246] P.M.K. Reddy, S.K. Mahammadunnisa, C.H. Subrahmanyam, Mineralization of aqueous organic pollutants using a catalytic plasma reactor, Indian J. Chem. Sect. A Inorg. Phys. Theor. Anal. Chem. 53 (2014) 499–503.

[247] L. Xin, Y. Sun, J. Feng, Ag3PO4/TiO2-assisted degradation of malachite green in aqueous solution treated by dielectric barrier discharge plasma, Chem. Technol. Biotechnol. 91 (2016) 2131–2142, https://doi.org/10.1002/jctb.4840.

[248] J. Chen, J. Feng, S. Lu, Z. Shen, Y. Du, L. Peng, P. Nian, S. Yuan, A. Zhang, Non-thermal plasma and Fe2+ activated persulfate ignited degradation of aqueous crystal violet: degradation mechanism and artificial neural network modeling, Sep. Purif. Technol. 191 (2018) 75–85, https://doi.org/10.1016/j.seppur.2017.09.016.

[249] P. Nian, L. Peng, J. Feng, X. Han, B. Cui, S. Lu, J. Zhang, Q. Liu, A. Zhang, Aqueous methylparaben degradation by dielectric barrier discharge induced non-thermal plasma combined with ZnO-rGO nanosheets, Sep. Purif. Technol. 211 (2019) 832–842, https://doi.org/10.1016/j.seppur.2018.10.048.

[250] M. Ansari, M. Sharifian, M.H. Ehrampoush, A.H. Mahvi, M.H. Salmani, H. Fallahzadeh, Dielectric barrier discharge plasma with photocatalysts as a hybrid emerging technology for degradation of synthetic organic compounds in aqueous environments: a critical review, Chemosphere 263 (2021), 128065, https://doi.org/10.1016/j.chemosphere.2020.128065.

[251] P.S. Baily, Academic Press, ISBN6-12-073101-0, 39-I, 1978, pp. 111–113.

[252] L.W. Gassie, J.D. Englehardt, Advanced oxidation and disinfection processes for onsite net-zero greywater reuse: a review, Water Res. 125 (15) (2017) 384–399.

[253] S. Giannakis, S. Rtimi, C. Pulgarin, Light-assisted advanced oxidation processes for the elimination of chemical and microbiological pollution of wastewaters in developed and developing countries, Molecules 22 (2017) 1070, https://doi.org/10.3390/molecules22071070.

[254] S. Giannakis, S. Liu, A. Carratalà, S. Rtimi, M. Bensimon, C. Pulgarin, Effect of Fe (II)/Fe (III) species, pH, irradiance and bacterial presence on viral inactivation in wastewater by the photo-Fenton process: kinetic modeling and mechanistic interpretation, Appl. Catal. B Environ. 204 (2017) 156–166.

[255] S. Giannakis, Analogies and differences among bacterial and viral disinfection by the photo-Fenton process at neutral pH: a mini review, Environ. Sci. Pollut. Res. 25 (2018) 27676–27692.

[256] S. Giannakis, B. Androulaki, C. Comninellis, C. Pulgarin, Wastewater and urine treatment by UVC-based advanced oxidation processes: implications from the interactions of bacteria, viruses, and chemical contaminants, Chem. Eng. J. 343 (2018) 270–282.

[257] X.M. Pan, M.N. Schuchmann, C. Von Sonntag, Oxidation of benzene by the OH radical. A product and pulse radiolysis study in oxygenated aqueous solution, J. Chem. Soc. Perkin Trans. 2 (1993) 289–297, https://doi.org/10.1039/p29930000289.

[258] H. Mätzing, Chemical kinetics of flue gas cleaning by irradiation with electrons, in: I. Prigogine, Stuart A. Rice (Eds.), Advances in Chemical Physics, John Wiley & Sons Ltd., 2007, pp. 315–402, https://doi.org/10.1002/9780470141298.ch4.

[259] C. von Sonntag, H.-P. Schuchmann, Elucidation of peroxyl radical reactions in aqueous solution using radiation chemistry techniques, Angew. Chem. 103 (1991) 1255–1279, https://doi.org/10.1002/ange.19911031006.

[260] N. Getoff, Radiation- and photo induced degradation of pollutants in water. A comparative study, Int. J. Radiat. Appl. Instrum. Part C Radiat. Phys. Chem. 37 (5–6) (1991) 673–680.

[261] T.A. Ternes, M. Meisenheimer, D. McDowell, F. Sacher, H.-J. Brauch, B. Haist-Gulde, G. Preuss, U. Wilme, N. Zulei-Seibert, Removal of pharmaceuticals during drinking water treatment, Environ. Sci. Technol. 36 (17) (2002) 3855–3863.

[262] T. Moeller. Inorganic Chemistry, 6th ed., Wiley, New York, 1957. LCCC Nr. 52-7487.

[263] Ullmann Encyclopedia of Industrial Chemistry, 5th ed., Ozone, Volume A18, Verlag Chemie, Einheim, Germany, 1991, pp. 349–357, ISBN 3-527-20118-1.

[264] D.F. Kirk, R.E. Othmer, Encyclopedia of Chemical Technology. Ozone, 4th ed., Wiley-Interscience, London, UK, 1996, pp. 953–994. ISBN 0-471-52686-X.

[265] M. Sahni, B.R. Locke, Quantification of hydroxyl radicals produced in aqueous phase pulsed electrical discharge reactors, Ind. Eng. Chem. Res. 45 (17) (2006) 5819–5825, https://doi.org/10.1021/ie0601504.

[266] Q. Huang, C. Fang, Degradation of 3,3′,4,4′-tetrachlorobiphenyl (PCB77) by dielectric barrier discharge (DBD) non-thermal plasma: degradation mechanism and toxicity evaluation, Sci. Total Environ. 739 (2020), 139926, https://doi.org/10.1016/j.scitotenv.2020.139926.

[267] S. Patai (Ed.), The Chemistry of the Hydroxyl Group, Interscience Publishers, New York, 1971 (Accessed 11 September 2020), ⟨https://agris.fao.org/agris-search/search.do?recordID=US201300472202⟩.

[268] V.V. Kovačević, B.P. Dojčinović, M. Jović, G.M. Roglić, B.M. Obradović, M. M. Kuraica, Measurement of reactive species generated by dielectric barrier discharge in direct contact with water in different atmospheres, J. Phys. D Appl. Phys. 50 (15) (2017), 155205, https://doi.org/10.1088/1361-6463/aa5fde.

[269] S. Ma, K. Kim, S. Chun, S.Y. Moon, Y. Hong, Plasma-assisted advanced oxidation process by a multi-hole dielectric barrier discharge in water and its application to wastewater treatment, Chemosphere 243 (2020) 125377, https://doi.org/10.1016/j.chemosphere.2019.125377.

[270] Z. Xu, C. Cheng, J. Shen, Y. Lan, S. Hu, W. Han, P.K. Chu, In vitro antimicrobial effects and mechanisms of direct current air-liquid discharge plasma on planktonic Staphylococcus aureus and Escherichia coli in liquids, Bioelectrochemistry 121 (2018) 125–134.

[271] J. Ren, N. Jiang, K. Shang, N. Lu, J. Li, Y. Wu, Synergistic degradation of trans-ferulic acid by water falling film DBD plasma coupled with cobalt oxyhydroxide: performance and mechanisms, Chem. Eng. J. 372 (2019) 321–331.

[272] K.H.H. Aziz, A. Mahyar, H. Miessner, S. Mueller, D. Kalass, D. Moeller, I. Khorshid, M.A.M. Rashid, Application of a planar falling film reactor for decomposition and mineralization of methylene blue in the aqueous media via ozonation, Fenton, photocatalysis and non-thermal plasma: a comparative study, Process Saf. Environ. Prot. 113 (2018) 319–329.

[273] Q. Tang, W. Jiang, Y. Cheng, S. Lin, T.M. Lim, J. Xiong, Generation of reactive species by gas-phase dielectric barrier discharges, Ind. Eng. Chem. Res. 50 (17) (2011) 9839–9846, https://doi.org/10.1021/ie200039w.

[274] X. Chen, W. Bian, X. Song, D. Liu, J. Zhang, Degradation of 4-chlorophenol in a dielectric barrier discharge system, Sep. Purif. Technol. 120 (2013) 102–109, https://doi.org/10.1016/j.seppur.2013.09.029.

[275] H. Wu, P. Sun, H. Feng, H. Zhou, R. Wang, Y. Liang, J. Lu, W. Zhu, J. Zhang, J. Fang, Reactive oxygen species in a non-thermal plasma microjet and water system: generation, conversion, and contributions to bacteria inactivation—an analysis by electron spin resonance spectroscopy, Plasma Process. Polym. 9 (2012) 417–424.

[276] H. Tresp, M.U. Hammer, J. Winter, K.-D. Weltmann, S. Reuter, Quantitative detection of plasma-generated radicals in liquids by electron paramagnetic resonance spectroscopy, J. Phys. D Appl. Phys. 46 (2013), 435401.

[277] S.-A. Cheng, W.-K. Fung, K.-Y. Chan, P.K. Shen, Optimizing electron spin resonance detection of hydroxyl radical in water, Chemosphere 52 (10) (2003) 1797–1805, https://doi.org/10.1016/s0045-6535(03)00369-2.

[278] Q. Wang, F. Ding, N. Zhu, H. Li, P. He, Y. Fang, Determination of hydroxyl radical by capillary zone electrophoresis with amperometric detection, J. Chromatogr. A 1016 (1) (2003) 123–128, https://doi.org/10.1016/s0021-9673(03)01294-9.

[279] S. Sahin, S. Demir, C. Güer, Simultaneous UV–vis spectrophotometric determination of disperse dyes in textile wastewater by partial least squares and principal component regression, Dyes Pigment. 73 (2007) 368–376.

[280] L. Qifu, N. Guohua, J. Yiman, W. Zhaojun, J. Song, L. Kefu, Special type of plasma dielectric barrier discharge reactor for direct ozonization of water and degradation of organic pollution, J. Phys. D Appl. Phys. 41 (2008), 085207.

[281] J. Tschirch, R. Dillert, D. Bahnemann, B. Proft, A. Biedermann, B. Goer, Photodegradation of methylene blue in water, a standard method to determine the activity of photocatalytic coatings? Res. Chem. Intermed. 34 (2008) 381–392.

[282] K.W. Mano, H. Hayashi, M. Yamada, S. Takahashi, N. Takada, H. Kanda, M. Goto, Atmospheric-pressure pulsed discharge plasma in capillary slug flow system for dye decomposition, Chem. Eng. Process. Process Intensif. 135 (2019) 133–140.

[283] J. Wang, Q. Qian, Q. Chen, X. Liu, Y. Luo, H. Xue, Z. Li, Significant role of carbonate radicals in tetracycline hydrochloride degradation based on solar light-

driven TiO2-seashell composites: removal and transformation pathways, Chin. J. Catal. 41 (2020) 1511–1521.

[284] A. Fahmy, A. El-Zomrawy, A.M. Saeed, A.Z. Sayed, M.A.E. El-Arab, H.A. Shehata, Modelling and optimizing Acid Orange 142 degradation in aqueous solution by non-thermal plasma, Chemosphere 210 (2018) 102–109.

[285] P. Lukes, M. Clupek, V. Babicky, V. Janda, P. Sunka, Generation of ozone by pulsed corona discharge over water surface in hybrid gas–liquid electrical discharge reactor, J. Phys. D Appl. Phys. 38 (2005) 409–416.

[286] K. Oehmigen, M. Hähnel, R. Brandenburg, Ch. Wilke, K.-D. Weltmann, Th. von Woedtke, The role of acidification for antimicrobial activity of atmospheric pressure plasma in liquids, Plasma Process. Polym. 7 (3–4) (2010) 250–257, https://doi.org/10.1002/ppap.200900077 (Special Issue: Plasma Medicine).

[287] M. Laroussi, Low temperature plasma-based sterilization: overview and state-of-the-art, Plasma Process. Polym. 2 (5) (2005) 391–400, https://doi.org/10.1002/ppap.200400078.

[288] P. Lukes, E. Dolezalova, I. Sisrova, M. Clupek, Aqueous-phase chemistry and bactericidal effects from an air discharge plasma in contact with water: evidence for the formation of peroxynitrite through a pseudo-second-order post-discharge reaction of H2O2 and HNO2, Plasma Sources Sci. Technol. 23 (3) (2014), 015019 (15pp).

[289] A. Wright, M. Taglioli, F. Montazersadgh, A. Shaw, F. Iza, H.C.H. Bandulasena, Microbubble-enhanced DBD plasma reactor: design, characterisation and modelling, Chem. Eng. Res. Des. 144 (2019) 159–173.

[290] A.J. Schwartz, Y. Cheung, J. Jevtic, V. Pikelja, A. Menon, S.J. Ray, G.M. Hieftje, New inductively coupled plasma for atomic spectrometry: the microwave-sustained, inductively coupled, atmospheric-pressure plasma (MICAP), J. Anal. Spectrom. 31 (2016) 440–449, https://doi.org/10.1039/C5JA00418G.

[291] A.V. Pipa, M. Schmidt, K. Becker, Ultraviolet (UV) emissions from a unipolar submicrosecond pulsed dielectric barrier discharge (DBD) in He-Air mixtures, J. Phys. Conf. Ser. 86 (2007) 1–14, https://doi.org/10.1088/1742-6596/86/1/012014.

[292] S.Y. Grebenshchikov, Z.-W. Qu, H. Zhu, R. Schinke, New theoretical investigations of the photodissociation of ozone in the Hartley, Huggins, Chappuis, and Wulf bands, Phys. Chem. Chem. Phys. 9 (2007) 2044–2064, https://doi.org/10.1039/b701020f.

[293] C. Fitzsimmons, J.T. Shawcross, J.C. Whitehead, Plasma-assisted synthesis of N2O5 from NO2 in air at atmospheric pressure using a dielectric pellet bed reactor, J. Phys. D Appl. Phys. 32 (1999) 1136–1141, https://doi.org/10.1088/0022-3727/32/10/310.

[294] Y. Sakiyama, D.B. Graves, H.-W. Chang, T. Shimizu, G.E. Morfill, Plasma chemistry model of surface microdischarge in humid air and dynamics of reactive neutral species, J. Phys. D Appl. Phys. 45 (2012), 425201, https://doi.org/10.1088/0022-3727/45/42/425201.

[295] M.J. Pavlovich, D.S. Clark, D.B. Graves, Quantification of air plasma chemistry for surface disinfection, Plasma Sources Sci. Technol. 23 (2014), 065036, https://doi.org/10.1088/0963-0252/23/6/065036 (10pp).

[296] A.A. Abdelaziz, T. Ishijima, N. Osawa, T. Seto, Quantitative analysis of ozone and nitrogen oxides produced by a low power miniaturized surface dielectric barrier discharge: effect of oxygen content and humidity level, Plasma Chem. Plasma Process. 39 (2019) 165–185, https://doi.org/10.1007/s11090-018-9942-y.

[297] V. Cooray, M. Rahman, Efciencies for production of NOx and O3 by streamer discharges in air at atmospheric pressure, J. Electrostat. 63 (2005) 977–983.

[298] Liang Gao, Chun-Lei Feng, Zhi-Wei Wang, Hongbin Ding, High sensitive and high temporal and spatial resolved image of reactive species in atmospheric pressure surface discharge reactor by laser induced fluorescence, Rev. Sci. Instrum. 88 (2017), 053107.

[299] K. Oehmigen, J. Winter, M. Hähnel, C. Wilke, R. Brandenburg, K.-D. Weltmann, T. von Woedtke, Estimation of possible mechanisms of Escherichia coli inactivation by plasma treated sodium chloride solution, Plasma Process. Polym. 8 (10) (2011) 904–913, https://doi.org/10.1002/ppap.201000099.

[300] J. Pregent, L. Vandsburger, V. Blanchard, P. Blanchet, B. Riedl, A. Sarkissian, L. Stafford, Determination of active species in the modification of hardwood samples in the flowing afterglow of N2 dielectric barrier discharges open to ambient air, Cellulose 22 (2015) 811–827, https://doi.org/10.1007/s10570-014-0496-8.

[301] R.K. Gangwar, O. Levasseur, N. Naudé, N. Gherardi, F. Massines, J. Margot, L. Stafford, Determination of the electron temperature in plane-to-plane He dielectric barrier discharges at atmospheric pressure, Plasma Sources Sci. Technol. 25 (2016), 015011, https://doi.org/10.1088/0963-0252/25/1/015011 (9pp).

[302] Z. Machala, B. Tarabova, K. Hensel, E. Spetlikova, L. Sikurova, P. Lukes, Formation of ROS and RNS in water electro-sprayed through transient spark discharge in air and their bactericidal effects, Plasma Process. Polym. 10 (2013) 649–659, https://doi.org/10.1002/ppap.201200113.

[303] H. Possel, H. Noack, W. Augustin, G. Keilhoff, G. Wolf, 2,7-Dihydrodichlorofluorescein diacetate as a fluorescent marker for peroxynitrite formation, FEBS Lett. 416 (2) (1997) 175–178, https://doi.org/10.1016/s0014-5793(97)01197-6.

[304] J.P. Crow, Dichlorodihydrofluorescein and dihydrorhodamine 123 are sensitive indicators of peroxynitritein vitro: implications for intracellular measurement of reactive nitrogen and oxygen species, Nitric Oxide 1 (2) (1997) 145–157, https://doi.org/10.1006/niox.1996.0113.

[305] M.J. Pavlovich, H.-W. Chang, Y. Sakiyama, D.S. Clark, D.B. Graves, Ozone correlates with antibacterial effects from indirect air dielectric barrier discharge treatment of water, J. Phys. D Appl. Phys. 46 (14) (2013), 145202, https://doi.org/10.1088/0022-3727/46/14/145202.

[306] M.J. Traylor, M.J. Pavlovich, S. Karim, P. Hait, Y. Sakiyama, D.S. Clark, D.B. Graves, Long-term antibacterial efficacy of air plasma-activated water, J. Phys. D Appl. Phys. 44 (2011), 472001, https://doi.org/10.1088/0022-3727/44/47/472001 (4pp).

[307] E. Riordan, N. Minogue, D. Healy, P. O'Driscol, J.R. Sodeau, Spectroscopic and optimization modeling study of nitrous acid in aqueous solution, J. Phys. Chem. A 109 (5) (2005) 779–786, https://doi.org/10.1021/jp040269v.

[308] M. Naitali, G. Kamgang-Youbi, J.-M. Herry, M.-N. Bellon-Fontaine, J.-L. Brisset, Combined effects of long-living chemical species during microbial inactivation using atmospheric plasma-treated water, Appl. Environ. Microbiol. 76 (22) (2010) 7662–7664, https://doi.org/10.1128/aem.01615-10.

[309] B.M. Obradović, G.B. Sretenović, M.M. Kuraica, A dual-use of DBD plasma for simultaneous NOx and SO2 removal from coal-combustion flue gas, J. Hazard. Mater. 185 (2011) 1280–1286.

[310] D.L. Atkinson, R.A. Baulch, J.N. Cox, R.F. Crowley, R.G. Hampson, M.E. Hynes, M.J. Jenkin, J. Troe Rossi, Evaluated kinetic and photochemical data for atmospheric chemistry: volume I – gas phase reactions of Ox, HOx, NOx and SOx species, Atmos. Chem. Phys. 4 (2004) 1461–1738.

[311] E.A. Filimonova, R.H. Amirov, H.T. Kim, I.H. Park, Comparative modeling of NOx and SO2 removal from pollutant gases using pulsed-corona and silent discharges, J. Phys. D Appl. Phys. 33 (2000) 1716–1727.

[312] M. Touzeau, M. Vialle, A. Zellagui, G. Gousset, M. Lefebvre, M. Pealat, Spectroscopic temperature measurements in oxygen discharges, J. Phys. D Appl. Phys. 24 (1) (1991) 41–47, https://doi.org/10.1088/0022-3727/24/1/008.

[313] A. Chelouah, E. Marode, G. Hartmann, S. Achat, A new method for temperature evaluation in a nitrogen discharge, J. Phys. D Appl. Phys. 27 (5) (1994) 940–945, https://doi.org/10.1088/0022-3727/27/5/010.

[314] A. Okada, K. Kijima, Measurement of C2 rotational temperature in Ar-SiH4-CH4 inductively coupled plasma flame with Abel inversion, J. Phys. D Appl. Phys. 35 (17) (2002) 2126–2132, https://doi.org/10.1088/0022-3727/35/17/308.

[315] K.-M. Lin, S.-Y. Chuang, W.-Y. Guo, C.-H. Cheng, C.-C. Ou, Thermal characterization of a single microdischarge in atmospheric pressure air dielectric barrier discharges, Plasma Sources Sci. Technol. 29 (2020), 075002, https://doi.org/10.1088/1361-6595/ab8e4b (18pp).

[316] C. Penache, M. Miclea, A. Brauning-Demian, O. Hohn, S. Schossler, T. Jahnke, K. Niemax, H. Schmidt-Bocking, Characterization of a high-pressure microdischarge using diode laser atomic absorption spectroscopy, Plasma Sources Sci. Technol. 11 (2002) 476–483.

[317] A.H. Timmermans, M.J. van de Sande, J.J.A.M. van der Mullen, Plasma characterization of an atmospheric microwave plasma torch using diode laser absorption studies of the argon 4s3P2state, Plasma Sources Sci. Technol. 12 (3) (2003) 324–334, https://doi.org/10.1088/0963-0252/12/3/305.

[318] J.M. Williamson, P. Bletzinger, B.N. Ganguly, Gas temperature determination in a N2/Ar dielectric barrier discharge by diode-laser absorption spectroscopy and resolved plasma emission, J. Phys. D Appl. Phys. 37 (2004) 1658–1663.

[319] V. Horvatic, A. Michels, N. Ahlmann, G. Jestel, C. Vadla, J. Franzke, Time-resolved line emission spectroscopy and the electrical currents in the plasma jet generated by dielectric barrier discharge for soft ionization, Spectrochim. Acta Part B 113 (2015) 152–157.

[320] U.V. Gunten, Oxidation processes in water treatment: are we on track? Environ. Sci. Technol. 52 (9) (2018) 5062–5075.

[321] S. Krishna, E. Ceriani, E. Marotta, A. Giardina, P. Špatenka, C. Paradisi, Products and mechanism of verapamil removal in water by air non-thermal plasma treatment, Chem. Eng. J. 292 (2016) 35–41.

[322] E.S. Elmolla, M. Chaudhuri, Degradation of the antibiotics amoxicillin, ampicillin and cloxacillin in aqueous solution by the photo-Fenton process, J. Hazard. Mater. 172 (2–3) (2009) 1476–1481, https://doi.org/10.1016/j.jhazmat.2009.08.015.

[323] D. Dimitrakopoulou, I. Rethemiotaki, Z. Frontistis, N.P. Xekoukoulotakis, D. Venieri, D. Mantzavinos, Degradation, mineralization and antibiotic inactivation of amoxicillin by UV-A/TiO2 photocatalysis, J. Environ. Manag. 98 (2012) 168–174, https://doi.org/10.1016/j.jenvman.2012.01.010.

[324] S. Sikarwar, R. Jain, Nano photo catalytic degradation of the pharmaceutical agent balsalazide under UV slurry photo reactor, Water Air Soil Pollut. 226 (2015) 277, https://doi.org/10.1007/s11270-015-2531-2.

[325] A.L. Giraldo-Aguirre, E.D. Erazo-Erazo, O.A. Flórez-Acosta, E.A. Serna-Galvis, R.A. Torres-Palma, TiO2 photocatalysis applied to the degradation and antimicrobial activity removal of oxacillin: evaluation of matrix components, experimental parameters, degradation pathways and identification of organics by-products, J. Photochem. Photobiol. A Chem. 311 (2015) 95–103, https://doi.org/10.1016/j.jphotochem.2015.06.021.

[326] I. Tantis, L. Bousiakou, Z. Frontistis, D. Mantzavinos, I. Konstaninou, M. Antonopoulou, G.-A. Karikas, P. Lianos, Photocatalytic and photoelectrocatalytic degradation of the drug omeprazole on nanocrystalline titania films in alkaline media: effect of applied electrical bias on degradation and transformation products, J. Hazard. Mater. 294 (2015) 57–63, https://doi.org/10.1016/j.jhazmat.2015.03.042.

[327] D. Bögner, F. Schmachtl, B. Mayr, C.P. Franz, S. Strieben, G. Jaehne, K. Lorkowski, M.J. Slater, Sludge pre-treatment through ozone application: alternative sludge reuse possibilities for recirculating aquaculture system optimization, Ozone Sci. Eng. 41 (2) (2019) 105–117, https://doi.org/10.1080/01919512.2018.1510765.

[328] A.G. Bubnov, E.Yu. Burova, V.I. Grinevich, V.V. Rybkin, J.-K. Kim, H.-S. Choi, Comparative actions of NiO and TiO2 catalysts on the destruction of phenol and its derivatives in a dielectric barrier discharge, Plasma Chem. Plasma Process. 27 (2007) 177–187, https://doi.org/10.1007/s11090-007-9052-8.

[329] G.Z. Qu, N. Lu, J. Li, Y. Wu, G.F. Li, D. Li, Simulataneous pentachlorophenol decomposition and granular activated carbon regeneration assisted by dielectric barrier discharge plasma, J. Hazard. Mater. 172 (2009) 472–478, https://doi.org/10.1016/j.jhazmat.2009.07.035.

[330] B.P. Dojcinovic, G.M. Roglic, B.M. Obradovic, M.M. Kuraica, M.M. Kostic, J. Nešic, D.D. Manojlovic, Decolorization of reactive textile dyes using water falling film dielectric barrier discharge, J. Hazard. Mater. 192 (2) (2011) 763–771.

[331] P.M.K. Reddy, C. Subrahmanyam, Green approach for wastewater treatment-degradation and mineralization of aqueous organic pollutants by discharge plasma, Ind. Eng. Chem. Res. 51 (2012) 11097–11103, https://doi.org/10.1021/ie301122p.

[332] M.R. Ghezzar, S. Ognier, S. Cavadias, F. Abdelmalek, A. Addou, DBDplate-TiO2 treatment of Yellow Tartrazine azo dye solution in falling film, Sep. Purif. Technol. 104 (2013) 250–255.

[333] I. Sirés, E. Brillas, Remediation of water pollution caused by pharmaceutical residues based on electrochemical separation and degradation technologies: a review, Environ. Int. 40 (2012) 212–229, https://doi.org/10.1016/j.envint.2011.07.012.

[334] A.P. Hills, N. Mokhtar, N.M. Byrne, Assessment of physical activity and energy expenditure: an overview of objective measures: review article, Front. Nutr. 1 (2014) 1–16, https://doi.org/10.3389/fnut.2014.00005.

[335] B. Jarungwit, S. Techkarnjanaruk, R. Honda, S. Angthong, N. Boonapatcharoen, S. Muenmee, P. Prachanurak, Use of aged sludge bioaugmentation in two-stage activated sludge system to enhance the biodegradation of toxic organic compounds in high strength wastewater, Chemosphere 202 (2018) 208–217.

[336] N. Nakada, H. Shinohara, A. Murata, K. Kiri, S. Managaki, N. Sato, H. Takada, Removal of selected pharmaceuticals and personal care products (PPCPs) and endocrine-disrupting chemicals (EDCs) during sand filtration and ozonation at a municipal sewage treatment plant, Water Res. 41 (19) (2007) 4373–4382, https://doi.org/10.1016/j.watres.2007.06.038.

[337] Y. Qi, Ozonation of water and waste water: a practical guide to understanding ozone and its applications, Int. J. Environ. Stud. 67 (2010) 795–796, https://doi.org/10.1080/00207233.2010.517628.

[338] B.L. Loeb, Forty years of advances in ozone technology a review of ozone: science & engineering, Ozone Sci. Eng. 40 (2018) 3–20, https://doi.org/10.1080/01919512.2017.1383129.

[339] P. Attri, F. Tochikubo, J.H. Park, E.H. Choi, K. Koga, M. Shiratani, Impact of Gamma rays and DBD plasma treatments on wastewater treatment, Sci. Rep. 8 (2018) 1–11, https://doi.org/10.1038/s41598-018-21001-z.

[340] F. Hegeler, H. Akiyama, Spatial and temporal distributions of ozone after a wire-to-plate streamer discharge, IEEE Trans. Plasma Sci. 25 (1997) 1158–1165, https://doi.org/10.1109/27.649640.

[341] T. Go, Y. Tanaka, N. Yamazaki, S. Mukaigawa, K. Takaki, T. Fujiwara, Dependence of initial oxygen concentration on ozone yield using inductive energy storage system pulsed power generator, IEEJ Trans. Fundam. Mater. 129 (2009) 477–482, https://doi.org/10.1541/ieejfms.129.477.

[342] T. Matsumoto, D. Wang, T. Namihira, S. Katsuki, Akiyama, Performances of nanosecond pulsed discharge, in: Acta Physica Polonica A, Proceedings of the 2nd Euro-Asian Pulsed Power Conference, Vilnius, Lithuania, 115(6), 2009, pp. 22–26.

[343] T. Huiskamp, W.F.L.M. Hoeben, F.J.C.M. Beckers, E.J.M. Van Heesch, A.J.M. Pemen, Subnanosecond transient plasma for atmospheric plasma processing experiments: application to ozone generation and NO removal, J. Phys. D Appl. Phys. 50 (2017), 405201, https://doi.org/10.1088/1361-6463/aa8617.

[344] D.V. Beloplotov, M.I. Lomaev, V.F. Tarasenko, D.A. Sorokin, Positive streamers in a point-to-plane gap filled with air and nitrogen at low and high voltages, J. Phys. Conf. Ser. (2018) 12025, https://doi.org/10.1088/1742-6596/1094/1/012025.

[345] V.S. Ripenko, M.V. Erofeev, V.F. Tarasenko, Atmospheric pressure diffuse discharge treatment of aqueous solution of methylenum coeruleum, J. Phys. Conf. Ser. (2019) 12123, https://doi.org/10.1088/1742-6596/1393/1/012123.

[346] C.D. Swartz, B. Genthe, J. Chamier, L.F. Petrik, J.O. Tijani, A. Adeleye, C.J. Coomans, A. Ohlin, D. Falk, J.G. Menge, Emerging Contaminants in Wastewater Treated for Direct Potable Re-Use: The Human Health Risk Priorities in South Africa, Volume I: A Concise Research Report; Volume II: A Prioritization Framework for Monitoring Contaminants of Emerging Concern in Reclaimed Water for Potable Use; Volume III: Occurrence, Fate, Removal and Health Risk Assessment of Chemicals Of Emerging Concern In Reclaimed Water For Potable Reuse. Report to The Water Research Commission: Project No. K5/2369 Final report in press, 2017.

[347] M. Dinu, E. Mouele, A. Parau, A. Vladescu, L. Petrik, M. Braic, Enhancement of the corrosion resistance of 304 stainless steel by Cr–N and Cr(N,O) coatings, Coatings 8 (4) (2018) 132, https://doi.org/10.3390/coatings8040132.

[348] E.S.M. Mouele, S. Ngqoloda, S. Pescetelli, A. Di Carlo, M. Dinu, A. Vladescu, A.C. Parau, A. Agresti, M. Braic, C.J. Arendse, L.F. Petrik, Spin coating immobilisation of C-N-TiO2 co-doped nano catalyst on glass and application for photocatalysis or as electron transporting layer for perovskite solar cells, Coatings 10 (2020) 1029, https://doi.org/10.3390/coatings10111029.